

**UCLA**

**UCLA Electronic Theses and Dissertations**

**Title**

In Vitro Generation of Adaptive Immunity from Hematopoietic Stem Cells

**Permalink**

<https://escholarship.org/uc/item/7qx121wd>

**Author**

Seet, Christopher

**Publication Date**

2018

Peer reviewed|Thesis/dissertation

UNIVERSITY OF CALIFORNIA

Los Angeles

***In Vitro* Generation of Adaptive Immunity from Hematopoietic Stem Cells**

A dissertation submitted in partial satisfaction of the requirement for the degree of  
Doctor of Philosophy in Cellular & Molecular Pathology

by

Christopher SY Seet

2018

© Copyright by  
Christopher SY Seet  
2018

ABSTRACT OF THE DISSERTATION

***In Vitro* Generation of Adaptive Immunity from Hematopoietic Stem Cells**

by

Christopher SY Seet

Doctor of Philosophy in Cellular & Molecular Pathology

University of California, Los Angeles, 2018

Professor Gay M. Crooks, Chair

The engagement of a dendritic cell with a T cell expressing a cognate T cell receptor is the defining event in the initiation of adaptive immunity against pathogens and cancer cells. The ability to understand, manipulate, and engineer T cell and dendritic cell anti-tumor immune responses is reshaping our approach to cancer therapy.

This dissertation presents research exploring two parallel avenues for enhancing anti-tumor adaptive immunity through the *in vitro* development of T cells and cDC1 dendritic cells from human hematopoietic stem and progenitor cells. While dealing with two distantly related hematopoietic lineages and their emergence from primitive progenitor cells, the common theme uniting these projects is the opportunity to more effectively engineer adaptive immunity through an improved understanding of these earliest stages of immune cell development.



The dissertation of Christopher SY Seet is approved.

Kenneth A. Dorshkind

Dinesh Subba Rao

John M. Timmerman

Gay M. Crooks, Committee Chair

University of California, Los Angeles

2018

This dissertation is dedicated to  
my parents, Drs. Julia Ying and Geoffrey Seet,  
my wife, Dr. Emily Leung Seet,  
and sons, Liam and Aidan Seet

## TABLE OF CONTENTS

	Abstract	ii
	List of figures	vi-vii
	Acknowledgements	viii-ix
	Vita	x-xi
Chapter 1	Introduction	1-21
Chapter 2	Generation of Mature T Cells from Human Hematopoietic Stem/Progenitor Cells in Artificial Thymic Organoids	22-72
Chapter 3	Regulation of Human cDC1 (CLEC9A+) Dendritic Cell Differentiation by Notch Signaling	73-106

## LIST OF FIGURES

### Chapter 1

Figure 1-1	Human T cell development	3
Figure 1-2	Endogenous DC subsets aligned across species	11
Figure 1-3	The cancer-immunity cycle	14

### Chapter 2

Figure 2-1	Human T cell development in the ATO system	26
Figure 2-2	Comparison of T cell differentiation between the ATO and OP9-DL1 systems	29
Figure 2-3	Comparison of ATO and thymic T cell differentiation and maturation	31
Figure 2-4	T cell differentiation in ATOs from different HSPC sources and subsets	33
Figure 2-5	Generation of TCR diversity and functional T cells in ATOs	34
Figure 2-6	Generation of antigen-specific T cells from TCR-engineered HSPCs in ATOs	37
Supplementary Figure 2-1	ATOs form solid tissue-like structures	56
Supplementary Figure 2-2	The effect of cell number on T cell differentiation in ATOs	57
Supplementary Figure 2-3	T cell differentiation in ATOs is independent of B27 lot and stromal cell irradiation	58
Supplementary Figure 2-4	Enhanced T cell positive selection and maturation in ATOs compared with OP9-DL1 monolayer co-cultures	59
Supplementary Figure 2-5	Enhanced positive selection in ATOs requires 3D structure and optimal cell line and culture medium	60
Supplementary Figure 2-6	Recapitulation of thymopoiesis and naive T cell phenotype in ATOs	61
Supplementary Figure 2-7	Generation of T cells from multiple HSPC sources and subsets	63
Supplementary Figure 2-8	TCR diversity and functional validation of ATO-derived CD4+ T cells	64
Supplementary Figure 2-9	Differentiation and allelic exclusion of TCR-engineered T cells in ATOs	65

## Chapter 3

Figure 3-1	Notch ligand promotes cDC1 output from HSPCs at the expense of monocyte, cDC2, and pDC output	77
Figure 3-2	Notch ligand induced cDC1 differentiation is conserved across alternative Notch ligands and different HSPC sources	78
Figure 3-3	The effect of DLL1 on cDC1 differentiation is Notch-dependent and cell intrinsic	79
Figure 3-4	Notch signaling acts on DC-specific progenitors to direct cDC1 differentiation and suppress alternative lineage fates	80
Figure 3-5	Notch signaling induces a cDC1 transcriptional program in multipotent MDPs prior to cDC1 differentiation	81
Figure 3-6	Notch-induced cDC1 express surface markers consistent with cDC1 identity	83
Figure 3-7	Notch-induced cDC1 express a gene signature of endogenous cDC1 regardless of HSPC origin	84
Figure 3-8	Notch-induced cDC1 respond to TLR 3/8 agonists, express costimulatory and lymph node homing molecules, and undergo chemotaxis in response to CCL21	86
Figure 3-9	Notch-induced cDC1 potently activate naïve allogeneic T cells and autologous antigen-specific T cells	87
Figure 3-10	Notch-induced cDC1 cross-present antigen from necrotic cells to activate autologous antigen-specific T cells	88
Figure 3-11	Notch-induced cDC1 prime <i>de novo</i> CD8+ T cell responses to tumor-associated antigens	89

## ACKNOWLEDGEMENTS

I would like to thank my mentor, Dr. Gay Crooks, who through her expertise and generosity made possible the work presented here. Dr. Crooks has been a true mentor and advocate in every respect, allowing me the freedom to explore my ideas while providing guidance and direction when it's needed most. Moreover, through her example, she has taught me the value of optimism, appreciating the joy in science, and creating the bright, interpersonal environment in which science, teamwork, and collaboration flourishes.

I thank my Committee, Drs. Ken Dorshkind, Dinesh Rao, and John Timmerman for their collective wisdom and scientific input throughout this work. I thank Dr. Owen Witte for his generous mentorship, both scientifically and with regard to my career development. I thank Drs. Mitchell Wong and Linda Demer for overseeing my PhD studies through the UCLA STAR Program, and for their continued career guidance.

Being part of the Crooks Lab has been an incredible experience, characterized by scientific and intellectual collaboration, openness, friendship, good food, and generosity of spirit. In particular, I thank Dr. Amélie Montel-Hagen, with whom I was fortunate to collaborate with on many projects, most significantly the ATO work (Chapter 2), which was an ideal combining of our skills and ideas in something that evolved from a fun and interesting diversion to a scientifically rewarding experience. I thank Suwen Li, a graduate student in Pharmacology, whose skill, dedication, and good humor working on the dendritic cell project (Chapter 3) made it possible. I thank Judy Zhu, our lab manager, for being a pillar of the lab, assisting with every aspect of our work, while also being a source of moral support for all. Brent Chick, Howard Chen, Shawn Lopez, and Rebecca Chan provided invaluable technical assistance. In addition to those above, I thank Dr. Stephanie de Barros, Dr. Vanessa

Bundy, Patrick Chang, Victoria Sun, and Dr. Steven Tsai for their conversations, collegiality, and friendship; and similarly recent alumni of the lab: Dr. Julia Chin, Edward He, Shundi Ge, Dr. William Kim, Kenneth Kim, Dr. Lisa Kohn, Runfeng Miao, and Dr. Salemez Sandoval.

This work would not have been possible without the many friends and collaborators with whom I have had the privilege of working. Drs. Owen Witte, Don Kohn, Toni Ribas, David Baltimore, and Lili Yang have been invaluable collaborators and supporters of our T cell work from its inception. From UCLA, Caltech, and CHLA, I have been fortunate to count Drs. Michael Bethune, Aaron Cooper, Eric Gschweng, Alok Joglekar, Jocelyn Kim, Caroline Kuo, Satiro de Oliveira, Chintan Parekh, and Drake Smith as collaborators and friends. I thank members of the Witte lab, in particular Jami Witte and Xiao-Hua Li for their collaboration on further work not presented here. I also thank Dr. Mary Sehl for her collaboration on our clinical sample collection protocol.

I thank the staff of the BSCRC Flow Cytometry core: Jessica Scholes, Felicia Codrea, and Jeff Calimlim for going above and beyond to make our work possible. I thank Dr. David Casero for his outstanding collaboration in all our bioinformatics analysis.

I would like to mention several groups that I consider to have been of particular importance to my training and career development: The Broad Stem Cell Research Center at UCLA, the UCLA STAR program, the CTSI KL2 program, and the Engineering Immunity Consortium. I also thank my funding sources: UCLA CTSI, the Broad Stem Cell Research Institute at UCLA, and Tower Cancer Research Foundation.

Finally, I would like to thank my wife, Dr. Emily Seet, for her support, patience, and encouragement throughout my training; and my parents Drs. Julia Ying and Geoff Seet for fostering in me a love of nature and science as a young child, and encouraging me to follow my interests, wherever they led.

## VITA

### EDUCATION & TRAINING

- B.A., Biological Science, University of Chicago, Chicago, IL 1999-2002
- M.D. (Honors), University of Sydney, Sydney, Australia 2004-2007
- Internship/Residency in Internal Medicine, Loyola University Medical Center, Maywood, IL 2008-2011
- Fellowship in Hematology/Oncology 2011-2014  
University of California Los Angeles, Los Angeles, CA

### POSITIONS HELD

- Research Technologist, Department of Pathology 2002-2004  
University of Chicago, Chicago, IL, PI: Barbara Kee, Ph.D.
- Honors Research Scholar 2005-2007  
Centenary Institute of Cancer Medicine and Cell Biology  
University of Sydney, Sydney, Australia, PI: Antony Basten, MBBS FRACP
- Intern and Resident in Internal Medicine 2008-2011  
Loyola University Medical Center, Maywood, IL
- Resident Research Scholar, Cardinal Bernadin Cancer Center 2009-2011  
Loyola University Medical Center, Maywood, IL, PI: Jiwang Zhang, MD PhD
- Fellow, Division of Hematology-Oncology 2011-2014  
David Geffen School of Medicine at UCLA
- Fellow, Special Training in Advanced Research (STAR) Program 2014-2016  
David Geffen School of Medicine at UCLA, PI: Gay M. Crooks, MBBS
- Health Sciences Clinical Instructor 2016-present  
Division of Hematology-Oncology, Department of Medicine  
David Geffen School of Medicine at UCLA

### PROFESSIONAL ACTIVITIES

- Member, American Society of Hematology 2011-present
- Member, American Society of Clinical Oncology 2011-present

### HONORS AND SPECIAL AWARDS

- G.S. Caird Scholarship in the Basic and Clinical Sciences 2005  
Faculty of Medicine, University of Sydney
- Jan Coppel Memorial Prize for Cancer Medicine 2007  
Faculty of Medicine, University of Sydney
- Resident Research Scholarship, Department of Medicine 2009  
Loyola University Medical Center
- First Place, Research Day Abstract Competition 2011  
Department of Medicine, Loyola University Medical Center
- Fellow Teaching Award Nominee, Department of Medicine 2012  
David Geffen School of Medicine at UCLA
- NIH T32 Hematology Training Grant 2013-2016
- Tower Cancer Research Foundation Career Development Award 2015  
Young Investigator Award at Immunology LA 2015  
American Association of Immunologists
- Research Innovator Award, Department of Medicine, UCLA 2015
- 3<sup>rd</sup> Place, Department of Medicine Poster Competition, UCLA 2016
- BSCRC Clinical Fellowship 2016  
Eli & Edythe Broad Center for Regenerative Medicine, UCLA
- 1<sup>st</sup> Place, Department of Medicine Poster Competition, UCLA 2017
- UCLA Clinical and Translational Science Institute (CTSI) Core Voucher Award 2017
- UCLA Department of Medicine Grand Rounds (invited seminar) 2017
- BSCRC Clinical Fellowship 2017  
Eli & Edythe Broad Center for Regenerative Medicine, UCLA
- NIH/CTSI KL2 Translational Science Award 2017



## RESEARCH GRANTS AND FELLOWSHIPS RECEIVED

- STAR Program, David Geffen School of Medicine at UCLA 7/2012-present
- NIH T32HL066992 Hematology Training Grant 7/2013-6/2016
- Tower Cancer Research Foundation, Career Development Award 6/2015-6/2016
- Broad Stem Cell Research Center at UCLA, Clinical Fellowship 7/2016-6/2017
- UCLA CTSI Core Voucher Award 7/2017-1/2018
- Broad Stem Cell Research Center at UCLA, Clinical Fellowship 7/2017-6/2018
- NIH/CTSI KL2TR001882 Translational Science Award 7/2017-6/2018

## SELECTED PRESENTATIONS

1. **Seet C.S.**, Miao R., Chin C., He C., Zhu Y., Chan R., Crooks G.M. *Identification of a human clonogenic monocyte/macrophage progenitor in fetal and adult hematopoiesis*. Poster presentation, American Association of Immunologists (ASH) Annual Meeting, 2015.
2. **Seet C.S.**, He C., Bethune M.T., Li S., Chick B., Gschweng E.H., Zhu Y., Kim K., Kohn D.B., Baltimore D., Montel-Hagen A., Crooks G.M. *Artificial Thymic Organoids Permit Allelic Exclusion and Efficient Generation of Naïve TCR-Engineered T cells from Human Hematopoietic Stem Cells In Vitro*, Poster presentation, American Society of Hematology (ASH) 45<sup>th</sup> Annual Meeting, San Diego, CA, Dec. 5, 2016
3. **Seet C.S.**, Department of Medicine Grand Rounds, David Geffen School of Medicine at UCLA, Invited seminar, *Immunotherapy for Hematologic Malignancies: Clinical and Scientific Advances*, UCLA, August 23, 2017
4. Montel-Hagen, A.\*, **Seet C.S.\* (\*Co-first authors)**, Li, S., Chick, B., Chang, P., Zhu, Y., He, C., Lopez, S., Crooks, G.M., *In Vitro Generation of Human Pluripotent Stem Cell-Derived T Cells for Immunotherapy*, Oral presentation, American Society of Hematology (ASH) 59<sup>th</sup> Annual Meeting, Atlanta, GA, Dec. 11, 2017
5. **Seet C.S.**, Li, S., Chick, B., Casero, D., Gschweng, E.H., Zhu, Y., Miao, R., Montel-Hagen, A., Kohn, D.B., Sehl, M., Crooks, G.M., *Notch Signaling Promotes the Differentiation of Human CLEC9A+ Dendritic Cells from Hematopoietic Stem and Progenitor Cells*, Oral presentation, American Society of Hematology (ASH) 59<sup>th</sup> Annual Meeting, Atlanta, GA, Dec. 11, 2017

## SELECTED PUBLICATIONS

1. **Seet C.S.**, Brumbaugh R. L., Kee B. L. *Early B Cell Factor Promoted B-Lymphopoiesis with Reduced Interleukin-7 Responsiveness in the Absence of E2A*. Journal of Experimental Medicine, 2004, Jun 21;199(12):1689-700.
2. Zhang J.\*, **Seet C.S.\* (\*co-first authors)**, Sun C., Li J., You D., Volk A., Breslin P., Li X., Wei W., Qian Z., Zeleznik-Le, N.J., Zhang Z., Zhang J. *p27kip1 maintain a subset of leukemia stem cells in the quiescent state in murine MLL-leukemia*. Molecular Oncology, 2013, Dec;7(6):1069-82.
3. Kohn L. A., **Seet C.S.**, Scholes J. Codrea F. Chan R., Zaidi-Merchant S., Zhu Y. De Oliveira S., Kapoor N., Shah A., Abdel-Azim H., Kohn D.B., Crooks G.M. *Human lymphoid development in the absence of common  $\gamma$ -chain receptor signaling*, J Immunol. 2014, Jun 1;192(11):5050-8.
4. Berent-Maoz B., Montecino-Rodriguez E., Flice M., Casero D, **Seet C.S.**, Crooks G. M., Lowry W., Dorshkind K. *The Expansion of Thymopoiesis in Neonatal Mice is Dependent on Expression of High mobility group A2 protein (Hmga2)*, PLOS One, 2015, May 1;10(5):e0125414.
5. **Seet C.S.**, Crooks G.M., Chapter 74: Lymphopoiesis, *Williams Hematology*, 9<sup>th</sup> Edition, Kaushansky K. et al. (Editor), McGraw-Hill Education, Dec. 2015.
6. Casero D., Sandoval S., **Seet C.S.**, Scholes J., Zhu Y., Ha V., Parekh C, Crooks G.M. *Long non-coding RNA profiling of human lymphoid progenitor cells reveals transcriptional divergence of B cell and T cell lineages*. Nature Immunology, 2015, Dec;16(12):1282-91.
7. **Seet C.S.**, He C., Bethune M.T., Li S., Chick B., Gschweng E.H., Zhu Y., Kim K., Kohn D.B., Baltimore D., Montel-Hagen A., Crooks G.M. *Generation of mature T cells from human hematopoietic stem and progenitor cells in artificial thymic organoids*. Nature Methods, 2017 May;14(5):521-530.

## PATENTS

1. UCLA-P144WO: A Method For Generating Human Dendritic Cells For Immunotherapy, Non-provisional patent application, May, 2016. **Seet, C.S.** / Crooks, G.M.
2. UCLA.P0014WO: Methods Of Generating T-Cells From Stem Cells And Immunotherapeutic Methods Using The T-Cells, Non-provisional patent application, Oct., 2016. **Seet, C.S.** / Montel-Hagen, A. / Crooks, G.M.

## CHAPTER 1

### PART I: HUMAN T CELL DEVELOPMENT FROM HEMATOPOIETIC STEM AND PROGENITOR CELLS

#### Human T cell development in the thymus

T lymphocytes are the critical effectors of anti-tumor and antiviral adaptive immunity. After birth, steady-state T cells originate from hematopoietic stem cells (HSCs) resident in the adult bone marrow via a series of CD34+ lineage-restricted progenitors, but, unlike other hematopoietic lineages, undergo lineage commitment and differentiation in the thymus, an organ specialized in function to foster T cell development and shape the T cell repertoire.

The earliest stages of thymopoiesis are thought to begin with emigration to the thymus of circulating multipotent progenitor cells (“thymus seeding progenitors” or TSP), the identity of which are unclear<sup>1</sup>. Within the bone marrow, our group identified a candidate CD34+ lymphoid-primed multipotent progenitor phenotype expressing the thymic-homing molecules CCR7 and CD62L with T-lineage transcriptional priming and prominent *in vitro* T cell potential<sup>2</sup>; however, circulating progenitors including a common lymphoid progenitor expressing CD10 and negative for CD24 present further candidate thymic-seeding progenitor populations<sup>3</sup>. Within the thymus itself, the hematopoietic stem and progenitor (HSPC) compartment contrasts markedly with that of the bone marrow in that the majority of cells are T-lineage committed progenitor (pro-T) cells, marked by expression of the T cell associated marker CD7<sup>4</sup>. However, our group previously identified a small population of

CD34+CD7<sup>-</sup> cells within the postnatal thymus that in *in vitro* assays retained erythroid, myeloid, and lymphoid potential, reminiscent of a bone marrow-like multipotent progenitor<sup>4</sup>, which we term an “early thymic progenitor” (ETP) based on its most primitive differentiation state. The CD34+CD7<sup>+</sup> pro-T cell population could in turn be further subdivided based on expression of CD1a, with CD1a<sup>-</sup> pro-T cells retaining myeloid and lymphoid potential, and CD1a<sup>+</sup> pro-T cells lymphoid-restricted<sup>4, 5</sup>.

In the thymus, ETPs encounter a microenvironment that will ultimately enforce T cell commitment and suppress alternative lineage fates. Among the earliest signals encountered in the thymus are those from the Notch ligand DLL4 expressed by cortical thymic epithelial cells (cTECs) and the cytokine interleukin-7 (IL-7)<sup>6, 7, 8</sup>. These and other factors are thought to enforce T-lineage transcriptional priming and the step-wise loss of myeloerythroid, B cell, and eventually NK cell potential. Inputs from Notch, cytokine signaling, and stromal cell interactions regulate both temporally segregated and combinatorial expression of a dynamic transcription factor network required for programming T cell commitment and, eventually, differentiation<sup>9</sup>. The complexity of transcriptional regulation of early T cell differentiation may indeed reflect the spatiotemporal complexity of the intrathymic migration of developing thymocytes, which is thought play a key role in T cell differentiation<sup>10, 11</sup>. Pro-T cells programmed by cTEC-expressed DLL4 likely transit through the thymic cortex where they progress to CD34<sup>-</sup>CD4<sup>-</sup>CD8<sup>-</sup> (double negative; DN) precursors, followed by upregulation of CD4 (CD4 immature single positive; CD4ISP). During this DN-CD4ISP window, somatic rearrangement of the TCR V $\beta$  loci occurs, resulting in generation of V $\beta$  diversity and expression (in combination with the pre-TCR $\alpha$  surrogate light chain) of a pre-T cell receptor (pre-TCR)<sup>12</sup>. Competent pre-TCR signaling licenses T cell precursors to

expand and proceed to become CD4+CD8+ (double positive; DP) precursors, a process known as  $\beta$ -selection)<sup>13, 14, 15</sup> (Fig. 1).

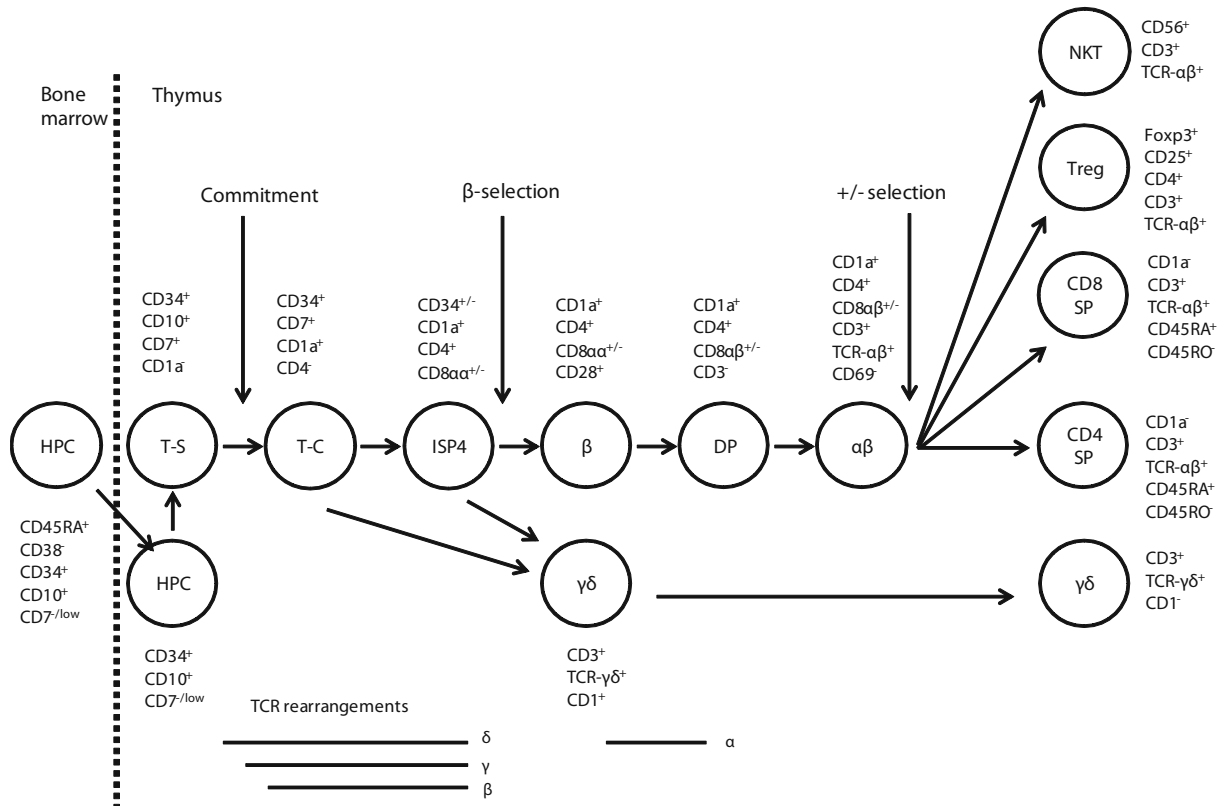


**Fig. 1-1: Human T cell development.** Key progenitor and precursor stages are shown, together with their characteristic surface markers. The approximate stages at which T cell commitment and selection checkpoints occur are shown. (Adapted from Van de Walle, Davids & Taghon, 2016)<sup>5</sup>

Productive rearrangement of TCR Va loci the DP stage results in expression of an  $\alpha\beta$  TCR (TCR $\alpha\beta$ ) on the cell surface, in a pentameric complex with CD3 chains. Low affinity interactions of a TCR $\alpha\beta$ <sup>+</sup> T cell precursor with a peptide-MHC (pMHC) complex, likely presented by TECs, licenses DP cells to mature to either CD8 single positive (CD8SP) or CD4 single positive (CD4SP) T cells depending on recognition of MHC class I or class II complexes, respectively, through a process known as positive selection<sup>11, 15, 16</sup>. High affinity interaction with pMHC antigens presented by medullary TECs and/or thymic dendritic cells (DCs) are

interpreted as self-reactivity and may result in one of several tolerogenic fates collectively termed central tolerance, including apoptosis (clonal deletion) or diversion to intraepithelial lymphocyte (IEL) or regulatory T cell (Treg) lineages<sup>15, 17, 18, 19</sup>. T cells that escape central tolerance mechanisms undergo thymic egress and form the peripheral naïve T cell repertoire.

Relevant to the work presented in Chapter 2, the transition between thymic T cell precursors and peripheral-like naïve T cells in the thymus can be tracked by specific changes in surface marker expression. After undergoing positive selection, DP markers including CD45RO and CD1a are downregulated, and naïve T cell markers including CD45RA, CD27, CD62L, and CCR7 are upregulated on the most mature thymic T cell subsets prior to thymic egress<sup>20, 21</sup>. This shift in surface marker expression does not coincide with the DP-to-SP transition however, and DP-like “immature naïve” CD8SP and CD4SP T cells which are CD1a+CD45RO+CD45RA<sup>-</sup> exist in the thymus prior to maturation to “mature naïve” T cells<sup>22, 23</sup>. Interestingly, this CD45RO/CD45RA switch is subsequently reversed in the periphery when a naïve T cell (CD45RA<sup>+</sup>) engages its cognate antigen and transitions to an effector/memory phenotype (CD45RO<sup>+</sup>)<sup>21</sup>.

### ***In vitro* generation of human T cells from hematopoietic stem and progenitor cells**

The ability to model thymopoiesis *in vitro* has permitted unprecedented advancement in our understanding of the molecular regulation of T cell development, however these advances have predominantly been confined to the mouse system. The earliest efforts at modeling T cell differentiation *in vitro* were fetal thymic organ cultures (FTOCs), consisting of T cell-depleted thymic fragments from fetal/neonatal mice seeded with mouse hematopoietic stem and progenitor cells (HSPCs)<sup>24</sup>. These cultures were also shown to foster

the differentiation of HSPCs to mature T cells. A variation of this, reaggregated thymic organ cultures (RTOCs), consisting of primary mouse thymic stroma reaggregated with HSPCs allowed for manipulation of the stromal microenvironment, however both FTOCs and RTOCs in general exhibited low efficiency, high experimental variability, and logistical difficulty in obtaining the requisite primary thymic tissue from large numbers of mice. Furthermore, human HSPCs seeded in mouse or human FTOCs and RTOCs developed into mature T cells at low efficiency<sup>25, 26</sup>.

A major advance in the field was the discovery that a mouse bone marrow stromal cell line (OP9) transduced with a murine Notch ligand (*Dll1* or *Dll4*) was sufficient to support T cell commitment and differentiation from mouse HSPCs in the presence of IL-7 and FLT3 ligand (FLT3L)<sup>27</sup>. The so-called OP9-DL1 system in general supported the differentiation of mouse HSPCs to the DP stage, as well as limited maturation to mature CD8SP T cells with relatively suppressed CD4SP differentiation, possibly due to the strength of Notch signaling and/or the relative paucity of MHC class II presentation in the system. Importantly, the OP9-DL1 system also supported T lineage commitment and early T cell differentiation from human cord blood (CB) CD34<sup>+</sup> HSPCs<sup>28, 29, 30, 31</sup>. T cell differentiation of CB HSPCs on OP9-DL1 was characterized by acquisition of pro-T cell phenotypes (characterized in the OP9-DL1 system as CD34<sup>+</sup>CD7<sup>+</sup>CD5<sup>-</sup> or CD5<sup>+</sup> cells<sup>32</sup>) followed by thymic-like transit through CD34<sup>-</sup>DN, CD4ISP, and DP stages. Notably, acquisition of TCR $\alpha\beta$ /CD3 surface expression was low in the OP9-DL1 system, as was the development of mature bona fide CD8SP or CD4SP T cells co-expressing TCR $\alpha\beta$ /CD3<sup>24, 28, 30, 31</sup>. This suggests that positive selection of human T cell precursors is relatively impaired in the OP9-DL1 system. This impairment could not be overcome by ectopic stromal expression of human MHC-I molecules, or by introduction in HSPCs of a fully rearranged TCR transgene<sup>28, 33</sup>, indicating that factors in addition to MHC-

I expression and TCR competency are required for positive selection of human T cells. Indeed, the generation of positively selected mature human T cells from HSPCs in immunodeficient mice, as well as in FTOCs (albeit with low efficiency)<sup>24</sup> suggests that the xenogeneic nature of OP9-DL1 is not in and of itself limiting the positive selection of human T cells. Interestingly, the highest frequencies of CD3+CD8SP T cells achievable in the OP9-DL1 system (around 2% of total cells) were from CD34+ cells isolated from the human postnatal thymus<sup>28, 33</sup>, consisting primarily of pro-T cells, and suggesting the further possibility that microenvironmental cues delivered at the pro-T cell stage or earlier may in some way contribute to positive selection potential, however this remains speculative.

### ***In vitro* generation of engineered human T cells from hematopoietic stem and progenitor cells**

Introduction of a fully rearranged TCR into mature peripheral blood T cells imparts the antigen specificity of that TCR to the recipient cell<sup>34</sup>. Extending on this, *in vivo* and *in vitro* experiments using TCR-transgenic mice or murine HSPCs, respectively, have shown that ectopic expression of a TCR in HSPCs permits the development of antigen-specific T cells expressing that TCR<sup>35, 36, 37</sup>. Importantly, as the exogenous TCR is prematurely expressed on the surface of T cell precursors upon induction of endogenous CD3 expression (as early as the DN stage in mice), the requirement for TCR rearrangement and beta-selection is functionally bypassed, and rearrangement of both endogenous TCR V $\beta$  loci suppressed through the physiological process of allelic exclusion<sup>38, 39, 40</sup>.

The generation of human TCR-engineered T cells from HPSCs has been more challenging. Studies in immunodeficient mice capable of engrafting human HSPCs have confirmed the ability of TCR-transduced CD34+ HSPCs to give rise to mature, antigen-

specific T cells with suppression of endogenous TCR expression<sup>38, 39, 40, 41</sup>. Similarly, the OP9-DL1 system supported T-lineage commitment and early T cell differentiation of TCR-transduced HSPCs, however consistent with impaired positive selection in this system, generation of mature CD8+ TCR-engineered T cells was impaired, typically representing only 0–2% of cultures, with the highest efficiencies achieved using postnatal thymic CD34+ cells<sup>33, 42, 43</sup>. Nevertheless, these studies point to several novel properties of *in vitro* antigen-specific T cell differentiation, in particular the suppression of TCR V $\beta$  rearrangement and thus endogenous TCR expression.

### **Significance for cancer immunotherapy**

The finding that the antigen reactivity of large numbers of peripheral blood T cells can be “redirected” by transduction of an antigen-specific TCR has led to the development of clinically significant new adoptive immunotherapies for cancer. Both TCR and chimeric antigen receptor (CAR)-transduced T cells have demonstrated efficacy in a variety of advanced malignancies, in some cases with unprecedented responses<sup>44</sup>. Despite their efficacy, current therapeutic strategies have several key limitations. First, most approaches require the use of autologous T cells given the risk of graft-versus-host disease (GVHD) mediated by allogeneic donor T cells; thus TCR- or CAR-T cell therapies are likely to come with costly individualized manufacturing processes, and furthermore exclude those patients with an insufficient quantity or quality of peripheral blood T cells. Second, TCR mispairing may occur when transduced TCR  $\alpha$  and  $\beta$  chains heterodimerize with preexisting endogenous TCR chains, possibly reducing tumor specificity or introducing novel, potentially autoimmune reactivities; although newer strategies to enforce heterodimerization of transduced TCR



chains may obviate this risk. Finally, the activation and expansion of T cells that is required for both transduction with a retroviral or lentiviral vector and expansion to therapeutic numbers may result in exhaustion and diminished *in vivo* efficacy and persistence of adoptive transferred T cells.

The *in vitro* generation of antigen receptor-engineered T cells from HSPCs (or, ultimately, from self-renewing pluripotent stem cells) offers several compelling potential solutions to these challenges<sup>45</sup>. Gene editing in stem cells can be used to introduce stable genetic changes in progeny T cells to impart therapeutically favorable characteristics, for example disruption of MHC expression for universal engraftment, or disruption of inhibitory co-receptors such as PD-1 to potentiate efficacy in immunosuppressive tumor microenvironments. Second, as the differentiation state of peripheral blood CD8+ T cells is associated with *in vivo* efficacy<sup>46, 47</sup>, the ability to generate naïve, antigen-specific T cells *in vitro* which can in theory mount both effector and memory T cell responses *in vivo* may lead to improvements in efficacy and persistence of adoptively transferred T cells. Finally, mitigation of GVHD risk through disruption of endogenous TCR expression either through stem cell gene editing or TCR-induced V $\beta$  allelic exclusion, as discussed above, may present a path forward for the production of allogeneic but non-alloreactive “off-the-shelf” T cells therapies.

In Chapter 2, I describe our work developing an *in vitro* platform for the differentiation of mature TCR-engineered T cells from HSPCs. This system offers the advantages of *in vitro* T cell differentiation discussed above, and improves on the state of the art by facilitating efficient positive selection and maturation of functional human T cells *in vitro*. This platform may permit the development of standardized, efficient, and scalable approaches to the *de novo* generation of engineered T cells for cancer immunotherapy.

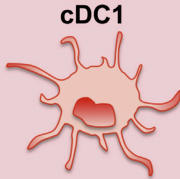
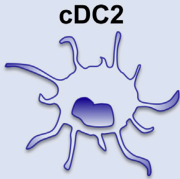

## PART II: HUMAN DENDRITIC CELL DEVELOPMENT FROM HEMATOPOIETIC STEM AND PROGENITOR CELLS

### Human dendritic cell subsets

Dendritic cells (DC) are the key antigen presenting cells underlying activation of adaptive T cell immunity. DCs provide the critical link between the innate sensing of danger signals and extracellular antigens in the periphery, and activation of naïve T cells within secondary lymphoid organs such as the lymph nodes and spleen. In humans and mice, multiple activated cell types including B cells, monocytes, and macrophages are capable of presenting peptide epitopes to T cells in the context of MHC-I or MHC-II molecules, however DCs are specialized for T cell engagement and activation through their expression of T cell costimulatory ligands and cytokines; their trafficking through secondary lymphoid organs; and their ability to take up and present to T cells antigens obtained from the microenvironment—a process known as cross-presentation.

The DC network in humans closely parallels that in mice, and can be organized into two main classes: “myeloid” or “conventional” DCs (cDC) and plasmacytoid DCs, based on historical assumptions that cDC but not pDC are related to the myeloid lineage. In mice, cDCs fall into at least two subsets based on expression of CD8 $\alpha$  or CD11b, which have been termed cDC1 and cDC2, respectively<sup>48, 49</sup>. Mouse cDC1 in turn can be classified as lymphoid organ resident or tissue-resident based on the absence or presence of the surface marker CD103, respectively<sup>50</sup>. While the physiologic roles played by each DC subset in adaptive immunity remains unclear, cDC1 in particular have been shown to be crucial players in initiating T cell adaptive immune responses to viruses and cancer<sup>50</sup>.

While cDC and pDC subsets have been studied in detail in mice, their identification in humans occurred only recently. Detailed studies of peripheral blood mononuclear cells (PBMCs) revealed specific circulating cell types correlating with mouse cDC1, cDC2, and pDC subsets<sup>48, 51, 52</sup>. These endogenous human DCs are contained within the lineage marker negative ( $\text{lin}^-$ ) HLA-DR<sup>+</sup> compartment. Within this population, cDC1 can be identified using one or more of the markers CD141 (BDCA-3), CLEC9A<sup>+</sup>, CADM1 (Necl-2), or XCR-1; whereas cDC2 in humans are identified as negative for cDC1 markers and positive for expression of CD1c (BDCA-1) and myeloid-associated markers such as CD11b, SIRP $\alpha$ , and CD115<sup>48, 53</sup>. pDC in turn can be identified by high surface expression of the IL-3 receptor CD123 and the pDC-specific marker CD303 (BDCA-2)<sup>48</sup> (Fig. 2). These phenotypic definitions have stood up remarkably well in later studies which have categorized human blood DC heterogeneity using single cell RNA-seq or mass cytometry methods<sup>49, 53, 54</sup>. These high-resolution data sets have furthermore allowed unbiased alignment of putative human cDC1, cDC2, and pDC populations with their validated counterparts in mice based on gene expression data, further confirming their identity.

	<b>cDC1</b> 	<b>cDC2</b> 	<b>pDC</b> 
<b>MOUSE</b>			
<b>common name</b>	<b>CD8<math>\alpha</math><sup>+</sup> cDC (LT)</b> <b>CD103<sup>+</sup> cDC (NLT)</b>	<b>CD4<sup>+</sup> CD11b<sup>+</sup> cDC (LT)</b> <b>CD11b<sup>+</sup> cDC (NLT)</b>	<b>SiglecH<sup>+</sup> BST2<sup>+</sup> pDC</b>
<b>other markers</b>	<i>TLR3<sup>+</sup> CADM1<sup>+</sup> XCR1<sup>+</sup></i> <i>CLEC9A<sup>+</sup> FLT3<sup>+</sup> CD205<sup>+</sup></i>	<i>SIRP<math>\alpha</math><sup>+</sup> CD11c<sup>+</sup></i> <i>FLT3<sup>+</sup></i>	<i>B220<sup>+</sup></i> <i>TLR7<sup>hi</sup> TLR9<sup>hi</sup></i>
<b>HUMAN</b>			
<b>common name</b>	<b>CD141<sup>+</sup>/hi cDC</b>	<b>CD1c<sup>+</sup> cDC</b>	<b>CD123<sup>+</sup> pDC</b>
<b>other markers</b>	<i>TLR3<sup>+</sup> CADM1<sup>+</sup> XCR1<sup>+</sup> FLT3<sup>+</sup></i> <i>CLEC9A<sup>+</sup> CD162<sup>hi</sup> CD205<sup>hi</sup></i>	<i>SIRP<math>\alpha</math><sup>+</sup> CD11b<sup>lo/+</sup></i> <i>FLT3<sup>+</sup> CD11c<sup>+</sup></i>	<i>CD303<sup>+</sup> CD304<sup>+</sup></i> <i>TLR7<sup>hi</sup> TLR9<sup>hi</sup></i>
<b>MACAQUE</b>			
<b>common name</b>	<b>XCR1<sup>+</sup> CADM1<sup>+</sup> cDC</b>	<b>CD1c<sup>+</sup> cDC</b>	<b>CD123<sup>+</sup> pDC</b>
<b>other markers</b>	<i>TLR3<sup>+</sup> CLEC9A<sup>+(RNA)</sup></i> <i>CD162<sup>hi</sup> CD205<sup>hi</sup></i>	<i>CD11c<sup>lo/-</sup> MHCII<sup>hi</sup></i>	<i>CD303<sup>+</sup></i> <i>TLR7<sup>hi</sup> TLR9<sup>hi</sup></i>
<b>SHEEP</b>			
<b>common name</b>	<b>SIRP<math>\alpha</math><sup>+</sup> CD26<sup>+</sup> cDC</b>	<b>SIRP<math>\alpha</math><sup>+</sup> CD26<sup>-</sup> cDC</b>	<b>CD45RB<sup>+</sup> pDC</b>
<b>other markers</b>	<i>TLR3<sup>+</sup> CADM1<sup>+</sup> CLEC9A<sup>+(RNA)</sup></i> <i>CD1b<sup>+</sup> CD205<sup>hi</sup></i>	<i>CD11c<sup>+</sup></i>	<i>TLR7<sup>hi</sup> TLR9<sup>hi</sup></i>
<b>PIG</b>			
<b>common name</b>	<b>SIRP<math>\alpha</math><sup>+</sup> CADM1<sup>+</sup> cDC</b>	<b>SIRP<math>\alpha</math><sup>+</sup> cDC</b>	<b>CD4<sup>hi</sup> SIRP<math>\alpha</math><sup>lo</sup> pDC</b>
<b>other markers</b>	<i>FLT3<sup>+</sup></i>	<i>CD11c<sup>+</sup> FLT3<sup>+</sup></i>	<i>MHCII<sup>+</sup> FLT3<sup>+</sup></i> <i>TLR7<sup>hi</sup> TLR9<sup>hi</sup></i>
<b>Conserved phenotype</b>	<i>TLR3<sup>+</sup> CADM1<sup>+</sup></i> <i>XCR1<sup>+</sup> CLEC9A<sup>+</sup></i>	<i>MHCII<sup>hi</sup> SIRP<math>\alpha</math><sup>+</sup></i>	<i>TLR7<sup>hi</sup> TLR9<sup>hi</sup></i>
<b>functions</b>	Ag cross-presentation to CD8 <sup>+</sup> T cells Th1 polarization TLR3-induced IFN- $\alpha$ production	Ag presentation to CD4 <sup>+</sup> T cells Th2 and Th17 polarization	TLR7/9-induced IFN- $\alpha$ / $\beta$ and IFN- $\lambda$ production

**Fig. 1-2: Endogenous DC subsets aligned across species.** Table showing validated surface markers and conserved functions. (Adapted from Dutertre et al., 2014)<sup>48</sup>

Relevant to the work presented in Chapter 3, human cDC1 have been the subject of multiple studies confirming their functional homology to cross-presenting CD8 $\alpha$ <sup>+</sup> (and CD103<sup>+</sup>) mouse cDC1. These studies have demonstrated their ability to prime T cell responses and cross-present viral and tumor-associated antigens acquired from extracellular sources to cytotoxic T cells<sup>50, 55, 56, 57, 58</sup>. These findings are significant in that prior to the discovery of endogenous human DCs, much of the work on dendritic cell function over the past 20 years has used monocyte-derived DCs (MoDC), which likely represent a DC-like activated monocyte state, and which lack many physiologic DC functions required for the competent priming of T cell responses *in vivo*<sup>59, 60</sup>. Thus, the

recognition of bona fide human cDC1 has both ushered in a greater understanding of the cellular requirements for initiating endogenous anti-tumor and antiviral immune responses, and elicited excitement at the possibility of their use in cancer immunotherapy, either as cellular vaccines or vaccine targets<sup>60</sup>.

### **Human dendritic cell development**

Early work characterizing DC differentiation from human bone marrow hematopoietic stem and progenitor cells (HSPCs) yielded unclear findings, particularly with regard to the myeloid versus lymphoid origins of human DCs. In retrospect, many such studies reported DC potential either based the ability to generate cells positive for HLA-DR, CD1a, and CD11c (markers also expressed on activated monocytes and MoDC), or directly by their ability to give rise to MoDC in permissive conditions, suggesting that early investigations of DC lineage potential in human hematopoietic progenitors were most likely confounded by monocytic/MoDC potential.

Subsequent to the characterization of specific human cDC and pDC markers, it was found that all three DC subsets form a specific hematopoietic lineage that diverges from lymphoid and myeloid lineages early during bone marrow hematopoiesis<sup>61, 62</sup>. Within the CD34+ bone marrow HSPC compartment, cDC1 specification based on transcriptional priming may occur as early as the hematopoietic stem cell stage<sup>63</sup>; however steady-state terminal differentiation appears to progress from at least a granulocyte-monocyte progenitor (GMP) through step-wise lineage restriction to a monocyte-DC progenitor (MDP) and finally a common DC progenitor (CDP) capable of generating cDC1, cDC2, and pDCs<sup>62</sup>. These and other recent studies identified FLT3L and GM-CSF as cytokines supportive of pan-DC

differentiation from DC progenitors<sup>64</sup>, however specific molecular cues regulating DC lineage fate decisions—particularly between the DC and monocyte fates, and later between the cDC1, cDC2, and pDC fates—remain unknown.

### ***In vitro* differentiation of human dendritic cells**

The ability to differentiate DCs *in vitro* is of importance not only for the experimental study of DC ontogeny and function, but also for potential generation of engineered DCs for immunotherapy.

As discussed, MoDC have been used as the surrogate DC-like cell for the majority of experimental and clinical studies of DC function. Enrichment of monocytes from PBMCs by either plastic adherence or CD14-bead selection, followed by culture in GM-CSF and IL-4 and “maturation” with pro-inflammatory stimuli (including IFN $\gamma$ , TNF $\alpha$ , and LPS) consistently yields large numbers of MoDC<sup>65</sup>, but are devoid of endogenous-type cDC or pDC subsets.

The generation of cDC1, cDC2, and pDC from HSPCs *in vitro* has not been extensively studied, likely due to their relatively recent characterization and the unknown molecular requirements for development. That being said, several recent studies have described methods for generating these three DC subsets *in vitro* from human CD34+ HSPCs, using both stromal support and stromal free cultures, and typically incorporating FLT3L and GM-CSF<sup>63, 66, 67, 68</sup>. However, these systems invariably showed mixed populations of predominantly myeloid cells with cDC1, cDC2, and pDCs present at low frequencies. While useful for modeling DC differentiation, an improved understanding of specific molecular signals regulating DC development is required before clinically relevant *in vitro* DC generation can take place.

## Significance for cancer immunotherapy

The discovery that tumors induce endogenous T cell responses has led to a paradigm shift in cancer therapy, which encompasses checkpoint blockade strategies and adoptive T cell therapies. These strategies target specific aspects of what has been described as the “cancer-immunity cycle”<sup>69</sup> (Fig. 3). This concept serves as a useful framework for understanding the formation of endogenous anti-tumor immunity through the uptake by DCs of necrotic cell antigens in the periphery; their migration to lymph nodes, and cross-presentation of acquired antigens to naïve T cells; and the migration of primed T cells back to the periphery where cytotoxicity may reinitiate the generation of tumor cell antigens. This framework also serves as a way to visualize the many points at which T cell immunity may be suppressed through adaptive immune evasion, and consequently points of therapeutic opportunity.

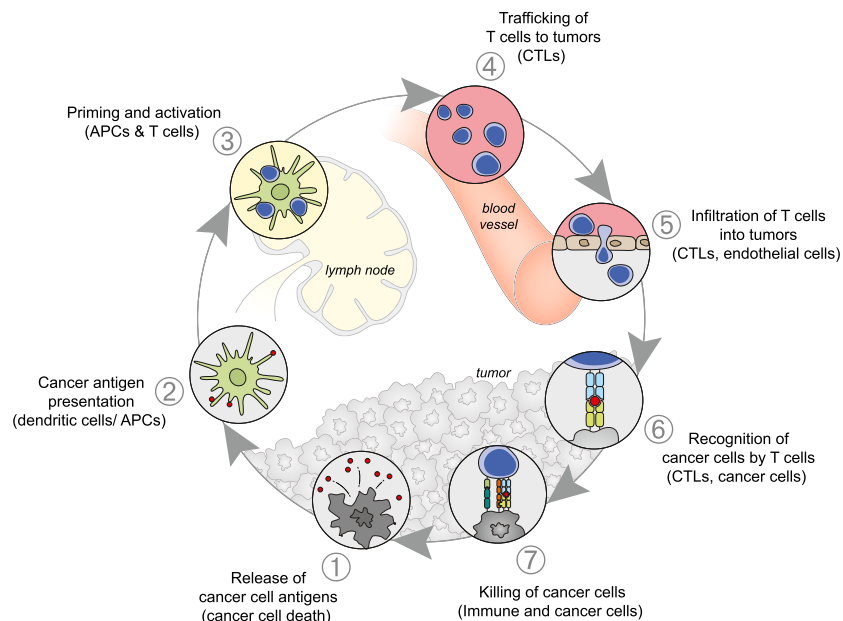


**Fig. 1-3: The cancer-immunity cycle.** Each stage of the generation and propagation of the endogenous anti-tumor immune response is susceptible to inhibition (adaptive immune evasion) or conversely to therapeutic intervention. Abbreviations: APCs, antigen presenting cells; CTLs, cytotoxic T lymphocytes. (Adapted from Chen & Mellman, 2013)<sup>69</sup>

One such opportunity is the enhancement of T cell priming in the lymph nodes through “DC vaccine” strategies. Over many years, these have taken the form of peptide, protein, and DNA vaccines, as well as adoptive cell therapies using autologous MoDC pulsed or transfected with putative tumor-associated antigens. While supported from evidence in mice, clinical efficacy of DC vaccines has been disappointing<sup>70</sup>. While multiple factors may underlie the lack of *in vivo* anti-tumor efficacy in the clinical setting (including adaptive immune evasion distal to T cell priming), one possibility is that the immunologic properties of MoDC are insufficient for *in vivo* efficacy. Specifically, MoDC are relatively poor at homing to lymph nodes, due to low expression of homing molecules such as CCR7; and under normal circumstances are inefficient at cross-presenting extracellular antigens, instead requiring short-lived *in vitro* pulsing or transfection with putative antigens. Furthermore, the *in vivo* stability of the MoDC phenotype is unknown.

Given these challenges to the therapeutic use of MoDC therapies, attention has turned to the use of endogenous-type DCs, either through *in vivo* targeting or adoptive cell therapy. Based on its described function, the cDC1 subset in particular has been proposed as the most likely candidate for initiating and sustaining endogenous anti-tumor adaptive immunity, however their rarity in the blood (approximately 0.03% of PBMCs<sup>55</sup>) has thus far precluded pre-clinical or clinical testing.

In Chapter 3, I describe the characterization of specific microenvironmental signals which in combination positively regulate the differentiation of human cDC1, effectively permitting their directed differentiation from HSPCs in clinically relevant cell numbers. It is my hope that this improved understanding of cDC1 differentiation may permit the engineering of anti-tumor T cell immune responses through the development of next-generation cDC1-based adoptive cell therapies.



## REFERENCES

1. Zlotoff, D.A., Schwarz, B.A. & Bhandoola, A. The long road to the thymus: the generation, mobilization, and circulation of T-cell progenitors in mouse and man. *Seminars in Immunopathology* **30**, 371 (2008).
2. Kohn, L.A. *et al.* Lymphoid priming in human bone marrow begins before expression of CD10 with upregulation of L-selectin. *Nature immunology* **13**, 963 (2012).
3. Six, E.M. *et al.* A human postnatal lymphoid progenitor capable of circulating and seeding the thymus. *The Journal of experimental medicine* **204**, 3085-3093 (2007).
4. Hao, Q.L. *et al.* Human intrathymic lineage commitment is marked by differential CD7 expression: identification of CD7<sup>+</sup> lympho-myeloid thymic progenitors. *Blood* **111**, 1318-1326 (2008).
5. Van de Walle, I., Davids, K. & Taghon, T. Characterization and Isolation of Human T Cell Progenitors. *Methods in molecular biology (Clifton, N.J.)* **1323**, 221-237 (2016).
6. Koch, U. *et al.* Delta-like 4 is the essential, nonredundant ligand for Notch1 during thymic T cell lineage commitment. *The Journal of experimental medicine* **205**, 2515-2523 (2008).
7. Shah, D.K. & Zuniga-Pflucker, J.C. An overview of the intrathymic intricacies of T cell development. *Journal of immunology (Baltimore, Md. : 1950)* **192**, 4017-4023 (2014).
8. Taghon, T., Waegemans, E. & Van de Walle, I. Notch signaling during human T cell development. *Current topics in microbiology and immunology* **360**, 75-97 (2012).
9. Rothenberg, E.V., Ungerback, J. & Champhekar, A. Forging T-Lymphocyte Identity: Intersecting Networks of Transcriptional Control. *Advances in immunology* **129**, 109-174 (2016).
10. Halkias, J., Melichar, H.J., Taylor, K.T. & Robey, E.A. Tracking migration during human T cell development. *Cellular and molecular life sciences : CMLS* **71**, 3101-3117 (2014).
11. Kurd, N. & Robey, E.A. T-cell selection in the thymus: a spatial and temporal perspective. *Immunological reviews* **271**, 114-126 (2016).
12. Biro, J. *et al.* Regulation of T cell receptor (TCR) beta gene expression by CD3 complex signaling in immature thymocytes: implications for TCRbeta allelic exclusion. *Proceedings of the National Academy of Sciences of the United States of America* **96**, 3882-3887 (1999).

13. Ciofani, M. *et al.* Obligatory role for cooperative signaling by pre-TCR and Notch during thymocyte differentiation. *Journal of immunology (Baltimore, Md. : 1950)* **172**, 5230-5239 (2004).
14. Xu, Y., Davidson, L., Alt, F.W. & Baltimore, D. Function of the pre-T-cell receptor alpha chain in T-cell development and allelic exclusion at the T-cell receptor beta locus. *Proceedings of the National Academy of Sciences of the United States of America* **93**, 2169-2173 (1996).
15. Carpenter, A.C. & Bosselut, R. Decision checkpoints in the thymus. *Nature immunology* **11**, 666-673 (2010).
16. Moran, A.E. & Hogquist, K.A. T-cell receptor affinity in thymic development. *Immunology* **135**, 261-267 (2012).
17. Perry, J.S.A. *et al.* Distinct contributions of Aire and antigen-presenting-cell subsets to the generation of self-tolerance in the thymus. *Immunity* **41**, 414-426 (2014).
18. Stritesky, G.L., Jameson, S.C. & Hogquist, K.A. Selection of self-reactive T cells in the thymus. *Annual review of immunology* **30**, 95-114 (2012).
19. Lambolez, F., Kronenberg, M. & Cheroutre, H. Thymic differentiation of TCR alpha beta(+) CD8 alpha alpha(+) IELs. *Immunological reviews* **215**, 178-188 (2007).
20. Bofill, M. *et al.* Immature CD45RA(low)RO(low) T cells in the human cord blood. I. Antecedents of CD45RA+ unprimed T cells. *Journal of immunology (Baltimore, Md. : 1950)* **152**, 5613-5623 (1994).
21. Appay, V., van Lier, R.A., Sallusto, F. & Roederer, M. Phenotype and function of human T lymphocyte subsets: consensus and issues. *Cytometry. Part A : the journal of the International Society for Analytical Cytology* **73**, 975-983 (2008).
22. Vanhecke, D., Leclercq, G., Plum, J. & Vandekerckhove, B. Characterization of distinct stages during the differentiation of human CD69+CD3+ thymocytes and identification of thymic emigrants. *Journal of immunology (Baltimore, Md. : 1950)* **155**, 1862-1872 (1995).
23. Res, P., Blom, B., Hori, T., Weijer, K. & Spits, H. Downregulation of CD1 marks acquisition of functional maturation of human thymocytes and defines a control point in late stages of human T cell development. *The Journal of experimental medicine* **185**, 141-151 (1997).
24. Plum, J. *et al.* Human T lymphopoiesis. In vitro and in vivo study models. *Annals of the New York Academy of Sciences* **917**, 724-731 (2000).
25. Plum, J., De Smedt, M., Defresne, M.P., Leclercq, G. & Vandekerckhove, B. Human CD34+ fetal liver stem cells differentiate to T cells in a mouse thymic microenvironment. *Blood* **84**, 1587-1593 (1994).

26. Chung, B. *et al.* Engineering the human thymic microenvironment to support thymopoiesis in vivo. *Stem cells (Dayton, Ohio)* **32**, 2386-2396 (2014).
27. Schmitt, T.M. & Zuniga-Pflucker, J.C. Induction of T cell development from hematopoietic progenitor cells by delta-like-1 in vitro. *Immunity* **17**, 749-756 (2002).
28. Van Coppernelle, S. *et al.* Functionally mature CD4 and CD8 TCRalpha cells are generated in OP9-DL1 cultures from human CD34+ hematopoietic cells. *Journal of immunology (Baltimore, Md. : 1950)* **183**, 4859-4870 (2009).
29. La Motte-Mohs, R.N., Herer, E. & Zuniga-Pflucker, J.C. Induction of T-cell development from human cord blood hematopoietic stem cells by Delta-like 1 in vitro. *Blood* **105**, 1431-1439 (2005).
30. Awong, G., La Motte-Mohs, R.N. & Zuniga-Pflucker, J.C. In vitro human T cell development directed by notch-ligand interactions. *Methods in molecular biology (Clifton, N.J.)* **430**, 135-142 (2008).
31. Awong, G., Herer, E., La Motte-Mohs, R.N. & Zuniga-Pflucker, J.C. Human CD8 T cells generated in vitro from hematopoietic stem cells are functionally mature. *BMC immunology* **12**, 22 (2011).
32. Awong, G. *et al.* Human proT-cells generated in vitro facilitate hematopoietic stem cell-derived T-lymphopoiesis in vivo and restore thymic architecture. *Blood* **122**, 4210-4219 (2013).
33. Snauwaert, S. *et al.* In vitro generation of mature, naive antigen-specific CD8(+) T cells with a single T-cell receptor by agonist selection. *Leukemia* **28**, 830-841 (2014).
34. Schmitt, T.M., Ragnarsson, G.B. & Greenberg, P.D. T cell receptor gene therapy for cancer. *Human gene therapy* **20**, 1240-1248 (2009).
35. Clay, T.M., Custer, M.C., Spiess, P.J. & Nishimura, M.I. Potential use of T cell receptor genes to modify hematopoietic stem cells for the gene therapy of cancer. *Pathology oncology research : POR* **5**, 3-15 (1999).
36. Yang, L. & Baltimore, D. Long-term in vivo provision of antigen-specific T cell immunity by programming hematopoietic stem cells. *Proceedings of the National Academy of Sciences of the United States of America* **102**, 4518-4523 (2005).
37. Ha, S.P. *et al.* Transplantation of mouse HSCs genetically modified to express a CD4-restricted TCR results in long-term immunity that destroys tumors and initiates spontaneous autoimmunity. *The Journal of Clinical Investigation* **120**, 4273-4288 (2010).
38. Vatakis, D.N. *et al.* Introduction of exogenous T-cell receptors into human hematopoietic progenitors results in exclusion of endogenous T-cell receptor

- expression. *Molecular therapy : the journal of the American Society of Gene Therapy* **21**, 1055-1063 (2013).
39. Starck, L., Popp, K., Pircher, H. & Uckert, W. Immunotherapy with TCR-redirected T cells: comparison of TCR-transduced and TCR-engineered hematopoietic stem cell-derived T cells. *Journal of immunology (Baltimore, Md. : 1950)* **192**, 206-213 (2014).
  40. Giannoni, F. *et al.* Allelic exclusion and peripheral reconstitution by TCR transgenic T cells arising from transduced human hematopoietic stem/progenitor cells. *Molecular therapy : the journal of the American Society of Gene Therapy* **21**, 1044-1054 (2013).
  41. Gschweng, E.H. *et al.* HSV-sr39TK positron emission tomography and suicide gene elimination of human hematopoietic stem cells and their progeny in humanized mice. *Cancer research* **74**, 5173-5183 (2014).
  42. Zhao, Y. *et al.* Extrathymic generation of tumor-specific T cells from genetically engineered human hematopoietic stem cells via Notch signaling. *Cancer research* **67**, 2425-2429 (2007).
  43. van Lent, A.U. *et al.* Functional human antigen-specific T cells produced in vitro using retroviral T cell receptor transfer into hematopoietic progenitors. *Journal of immunology (Baltimore, Md. : 1950)* **179**, 4959-4968 (2007).
  44. Rosenberg, S.A. & Restifo, N.P. Adoptive cell transfer as personalized immunotherapy for human cancer. *Science (New York, N.Y.)* **348**, 62-68 (2015).
  45. Gschweng, E., De Oliveira, S. & Kohn, D.B. Hematopoietic stem cells for cancer immunotherapy. *Immunological reviews* **257**, 237-249 (2014).
  46. Hinrichs, C.S. *et al.* Adoptively transferred effector cells derived from naive rather than central memory CD8<sup>+</sup> T cells mediate superior antitumor immunity. *Proceedings of the National Academy of Sciences of the United States of America* **106**, 17469-17474 (2009).
  47. Gattinoni, L. *et al.* Acquisition of full effector function in vitro paradoxically impairs the in vivo antitumor efficacy of adoptively transferred CD8<sup>+</sup> T cells. *J Clin Invest* **115**, 1616-1626 (2005).
  48. Dutertre, C.-A., Wang, L.-F. & Ginhoux, F. Aligning bona fide dendritic cell populations across species. *Cellular Immunology* **291**, 3-10 (2014).
  49. Williams, M. *et al.* Unsupervised High-Dimensional Analysis Aligns Dendritic Cells across Tissues and Species. *Immunity* **45**, 669-684.
  50. Roberts, E.W. *et al.* Critical Role for CD103<sup>+</sup>/CD141<sup>+</sup> Dendritic Cells Bearing CCR7 for Tumor Antigen Trafficking and Priming of T Cell Immunity in Melanoma. *Cancer Cell* **30**, 324-336 (2016).

51. Dzionek, A. *et al.* BDCA-2, BDCA-3, and BDCA-4: Three Markers for Distinct Subsets of Dendritic Cells in Human Peripheral Blood. *The Journal of Immunology* **165**, 6037-6046 (2000).
52. MacDonald, K.P.A. *et al.* Characterization of human blood dendritic cell subsets. *Blood* **100**, 4512-4520 (2002).
53. Villani, A.C. *et al.* Single-cell RNA-seq reveals new types of human blood dendritic cells, monocytes, and progenitors. *Science (New York, N.Y.)* **356** (2017).
54. See, P. *et al.* Mapping the human DC lineage through the integration of high-dimensional techniques. *Science (New York, N.Y.)* **356** (2017).
55. Jongbloed, S.L. *et al.* Human CD141+ (BDCA-3)+ dendritic cells (DCs) represent a unique myeloid DC subset that cross-presents necrotic cell antigens. *The Journal of experimental medicine* **207**, 1247-1260 (2010).
56. Bachem, A. *et al.* Superior antigen cross-presentation and XCR1 expression define human CD11c+CD141+ cells as homologues of mouse CD8+ dendritic cells. *The Journal of experimental medicine* **207**, 1273-1281 (2010).
57. Poulin, L.F. *et al.* Characterization of human DNGR-1+ BDCA3+ leukocytes as putative equivalents of mouse CD8 $\alpha$ + dendritic cells. *The Journal of experimental medicine* **207**, 1261-1271 (2010).
58. Crozat, K. *et al.* The XC chemokine receptor 1 is a conserved selective marker of mammalian cells homologous to mouse CD8 $\alpha$ + dendritic cells. *The Journal of experimental medicine* **207**, 1283-1292 (2010).
59. Radford, K.J. & Caminschi, I. New generation of dendritic cell vaccines. *Human vaccines & immunotherapeutics* **9**, 259-264 (2013).
60. Tullett, K.M., Lahoud, M.H. & Radford, K.J. Harnessing Human Cross-Presenting CLEC9A(+)/XCR1(+) Dendritic Cells for Immunotherapy. *Frontiers in immunology* **5**, 239 (2014).
61. Schraml, Barbara U. *et al.* Genetic Tracing via DNGR-1 Expression History Defines Dendritic Cells as a Hematopoietic Lineage. *Cell* **154**, 843-858 (2013).
62. Lee, J. *et al.* Restricted dendritic cell and monocyte progenitors in human cord blood and bone marrow. *The Journal of experimental medicine* **212**, 385-399 (2015).
63. Lee, J. *et al.* Lineage specification of human dendritic cells is marked by IRF8 expression in hematopoietic stem cells and multipotent progenitors. *Nature immunology* **18**, 877-888 (2017).
64. Puhr, S., Lee, J., Zvezdova, E., Zhou, Y.J. & Liu, K. Dendritic Cell Development – History, Advances, and Open Questions. *Seminars in immunology* **27**, 388-396 (2015).

65. Sallusto, F. & Lanzavecchia, A. Efficient presentation of soluble antigen by cultured human dendritic cells is maintained by granulocyte/macrophage colony-stimulating factor plus interleukin 4 and downregulated by tumor necrosis factor alpha. *The Journal of experimental medicine* **179**, 1109-1118 (1994).
66. Helft, J. *et al.* Dendritic Cell Lineage Potential in Human Early Hematopoietic Progenitors. *Cell reports* **20**, 529-537 (2017).
67. Balan, S. *et al.* Human XCR1+ dendritic cells derived in vitro from CD34+ progenitors closely resemble blood dendritic cells, including their adjuvant responsiveness, contrary to monocyte-derived dendritic cells. *Journal of immunology (Baltimore, Md. : 1950)* **193**, 1622-1635 (2014).
68. Thordardottir, S. *et al.* The aryl hydrocarbon receptor antagonist StemRegenin 1 promotes human plasmacytoid and myeloid dendritic cell development from CD34+ hematopoietic progenitor cells. *Stem cells and development* **23**, 955-967 (2014).
69. Chen, D.S. & Mellman, I. Oncology meets immunology: the cancer-immunity cycle. *Immunity* **39**, 1-10 (2013).
70. Radford, K.J., Tullett, K.M. & Lahoud, M.H. Dendritic cells and cancer immunotherapy. *Current opinion in immunology* **27**, 26-32 (2014).

## CHAPTER 2

### GENERATION OF MATURE T CELLS FROM HUMAN HEMATOPOIETIC STEM/PROGENITOR CELLS IN ARTIFICIAL THYMIC ORGANOIDS

#### Abstract

Studies of human T cell development require robust model systems that recapitulate the full span of thymopoiesis, from hematopoietic stem and progenitor cells (HSPCs) through to mature T cells. Existing *in vitro* models induce T cell commitment from human HSPCs; however, differentiation into mature CD3+TCRab+ single positive (SP) CD8+ or CD4+ cells is limited. We describe here a serum-free, artificial thymic organoid (ATO) system that supports highly efficient and reproducible *in vitro* differentiation and positive selection of conventional human T cells from all sources of HSPCs. ATO-derived T cells exhibited mature naïve phenotypes, a diverse TCR repertoire, and TCR-dependent function. ATOs initiated with TCR-engineered HSPCs produced T cells with antigen specific cytotoxicity and near complete lack of endogenous TCR V $\beta$  expression, consistent with allelic exclusion of V $\beta$  loci. ATOs provide a robust tool for studying human T cell development and stem cell based approaches to engineered T cell therapies.

#### Introduction

Due to the spatiotemporal complexity of T cell development in the thymus, *in vitro* models of T cell differentiation have thus far been unable to fully recapitulate human T

cell development. A major advance was the discovery that murine stromal cell lines expressing a Notch ligand could support *in vitro* T cell differentiation from murine or human HSPCs, as in the classic OP9-DL1 co-culture system<sup>1, 2, 3</sup>. In this and similar monolayer systems, human cord blood (CB) HSPCs undergo T lineage commitment and rapid early T cell differentiation to CD7+ pro-T cells, followed by CD4 “immature single positive” (CD4ISP) precursors around day 20, and CD4+CD8+ double positive (DP) precursors around day 30<sup>3</sup>. Despite this, positive selection of T cell precursors with productively rearranged TCRs is impaired in OP9-DL1 co-culture, and consequently few CD3+CD8+ or CD4+ single positive (SP) T cells develop<sup>2, 3, 4, 5</sup>. By Day 60–70 on OP9-DL1, mature CD8SP represent at most 2–4% of cultured cells<sup>5</sup>. Improved maturation has been reported using CD34+ HSPC isolated from the human postnatal thymus<sup>6</sup> a population largely composed of lineage committed pro-T cells<sup>7</sup>. However, T cell maturation on OP9-DL1 is particularly inefficient using mobilized peripheral blood and bone marrow HSPCs, the latter giving approximately 10% of the DP and CD3+TCR $\alpha\beta$ + cell yields seen with CB cultures<sup>8</sup>.

We and others have shown that three-dimensional (3D) organoid systems using murine<sup>9, 10, 11</sup> or human<sup>12</sup> primary thymic stroma supports improved positive selection and maturation of human T cells *in vitro*. However, these systems are difficult to use given their dependence on primary thymic tissue, and high experimental variability. We therefore sought to develop a system using off-the-shelf, serum-free components able to support efficient and reproducible differentiation and positive selection of human T cells from HSPCs. We report here the development of an artificial thymic organoid (ATO) system based on a *DLL1*-transduced stromal cell line and serum-free, off-the-shelf components that supported robust differentiation, positive selection, and maturation of human CD3+TCR $\alpha\beta$ +CD8SP and CD4SP T cells from CB, bone marrow, and peripheral blood CD34+ HSPCs. Differentiation



was efficient whether initiated with CD34+CD3<sup>-</sup> HSPCs, HSC, or lymphoid progenitors. T cell differentiation in ATOs followed a phenotypic progression that closely recapitulated human thymopoiesis, and was associated with long-term maintenance of CD34<sup>+</sup> T cell progenitors.

Both CD3<sup>+</sup>CD8<sup>SP</sup> and CD3<sup>+</sup>CD4<sup>SP</sup> mature T cells that developed in ATOs exhibited an antigen naïve phenotype, diverse TCR repertoire, and cytokine production and proliferation in response to antigenic stimuli. ATOs also supported highly efficient differentiation of TCR-engineered, antigen-specific T cells from HSPCs transduced with MHC Class I-restricted TCRs specific for the tumor-associated antigens NY-ESO-1 and MART-1. ATO-derived engineered T cells exhibited a naïve phenotype and *in vitro* and *in vivo* antigen-specific cytotoxicity. Moreover, these cells lacked endogenous TCR V $\beta$  expression, consistent with induction of allelic exclusion by the transduced TCR during early T cell differentiation, and suggesting a new approach to generating potentially non-alloreactive engineered T cells for adoptive immunotherapy. ATOs thus are a standardized and highly efficient *in vitro* model of human T cell development that is readily amenable to genetic manipulation and may permit new approaches to the study of human T cell development.

## Results

**Development of an optimized artificial thymic organoid system for *in vitro* human T cell differentiation**

Our goal was to develop a robust system that supports *in vitro* differentiation and positive selection of human T cells from HSPCs from multiple sources. Based on studies using FTOCs and reaggregated organoids, we hypothesized that 3D structure plays a critical role in T cell positive selection. To avoid the use of primary thymic tissue, we tested *DLL1*-transduced stromal cell lines for their ability to support human T cell development in 3D organoid cultures. As we and others have observed that the efficiency of T cell differentiation in the OP9-DL1 system is highly variable between different lots of fetal calf serum<sup>13</sup>, we furthermore sought to identify serum-free conditions capable of supporting T cell differentiation in organoid cultures. To form organoids, we used a simple compaction reaggregation technique<sup>9, 12, 14</sup>, by which stromal cells are aggregated with HSPCs by centrifugation and deployed on a cell culture insert at the air-fluid interface (Fig. 1a). Using this method, we identified the MS5 murine bone marrow stromal cell line<sup>15</sup> transduced with human *DLL1* (MS5-hDLL1, hereafter) as strongly supportive of human T cell differentiation and positive selection (measured by the output of mature CD3+TCR $\alpha$  $\beta$ +CD8SP cells) from T cell-depleted CD34+ cord blood (CB) HSPCs. We also identified RPMI 1640 supplemented with B27, a multi-component additive used in neuronal and embryonic stem cell cultures<sup>16</sup>, and FLT3L, IL-7, and ascorbic acid<sup>17, 18</sup>(“RB27”, hereafter) as a serum-free medium that supported robust human T cell differentiation in MS5-hDLL1 organoid cultures without lot-to-lot variation.

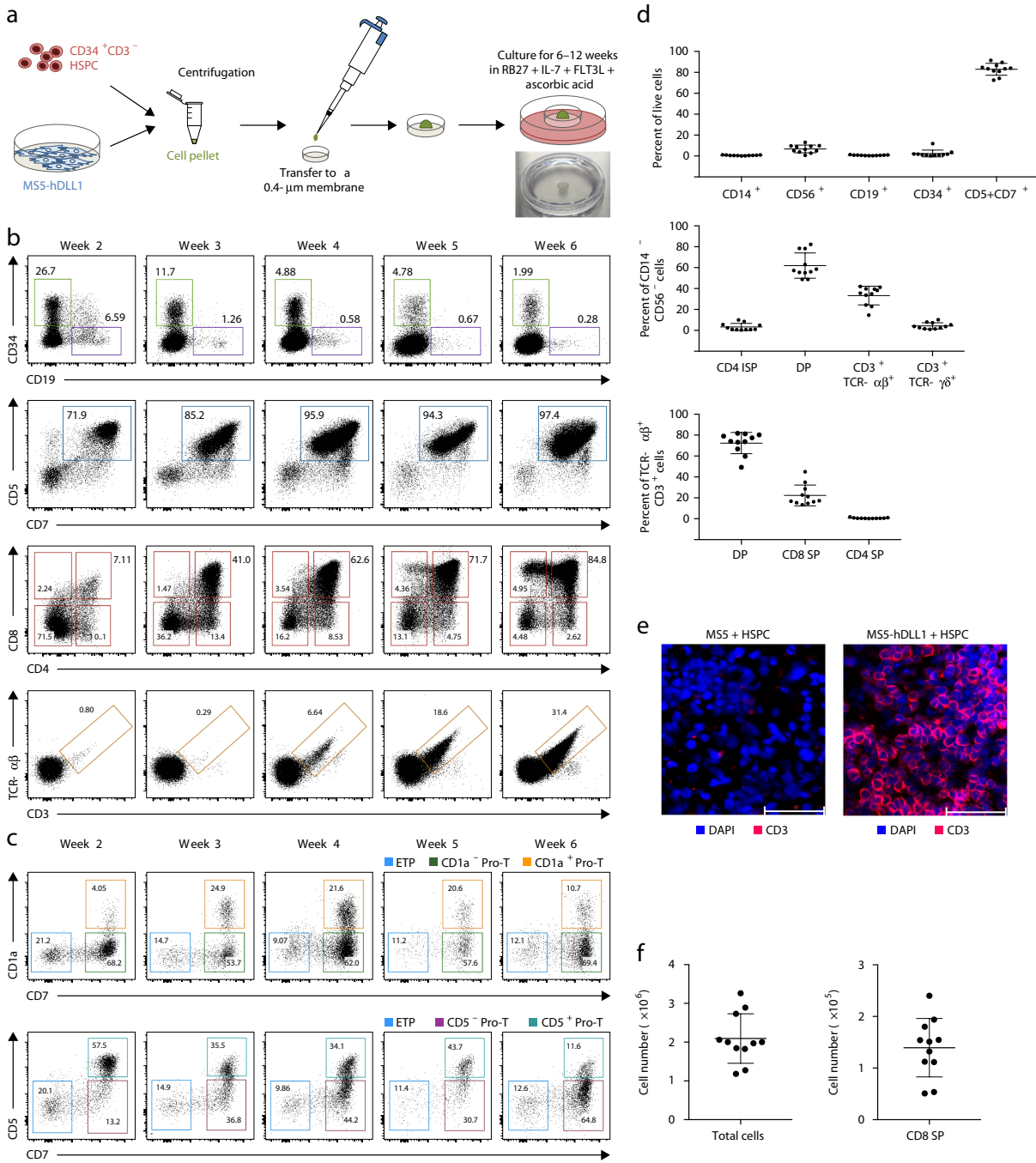


**Fig. 2-1: Human T cell development in the ATO system.** (a) Schematic of the ATO model. Image shows the appearance of a typical ATO attached to cell culture insert at 6 weeks (shown after removal from culture well). (b) Representative kinetic analysis ( $n = 3$ ) of T cell differentiation from CB CD34<sup>+</sup>CD3<sup>-</sup> HSPCs at the indicated time points, gated on CD14<sup>-</sup> and CD56<sup>-</sup> cells to exclude monocytes and NK cells, respectively. (c) Maintenance of early CD34<sup>+</sup> thymic T cell progenitor phenotypes in ATOs based on two classification schemes, both gated on CD34<sup>+</sup> cells as shown

in b (n = 3). (d) Frequencies of cell types in ATOs (n = 11) at 6 weeks. Top, frequencies of monocytes (CD14+), NK cells (CD56+), B cells (CD19+), HSPCs (CD34+) and T lineage cell (CD7+CD5+) (gated on total live cells). Middle, T cell precursor and TCR+ T cell frequencies (gated on CD14-CD56- cells). Bottom, frequency of DP and mature CD8 and CD4 SP T cells (gated on CD3+TCR- $\alpha\beta$ + cells). (e) Representative immunofluorescence analysis (n = 3) for CD3 expression in week 4 organoids generated with CB HSPCs and MS-5 cells (left) or with MS5-hDLL1 cells (i.e., ATOs) (right). Nuclei were stained with DAPI. Scale bars, 50  $\mu\text{m}$ . (f) Numbers of total live cells (left) and CD3+TCR- $\alpha\beta$ + CD8 SP T cells (right) generated per ATO at week 6 from  $7.5 \times 10^3$  to  $22.5 \times 10^3$  CB HSPCs per ATO. Data are shown for 11 independent experiments. In d,f, error bars indicate s.d.

This optimized artificial thymic organoid (ATO) system induced rapid and efficient T lineage commitment from CB CD34+CD3- HSPCs, as shown by a predominance of CD5+CD7+ T-lineage cells and the appearance of CD4+CD3- immature single positive (CD4ISP) and CD4+CD8+ (DP) T cell precursors by week 2 (Fig. 1b). More mature CD3+TCR $\alpha\beta$ + cells emerged as early as week 4 and increased over time, accounting for ~30% of cells at week 6 (Fig. 1b). Long-term maintenance of CD34+ T cell progenitors was also seen in ATOs, and recapitulated the three phenotypic stages of thymic T cell progenitors: multipotent CD34+CD7-CD1a- early thymic progenitors (ETP), and developmentally downstream CD34+CD7+CD1a- and CD34+CD7+CD1a+ pro-T cells (Fig. 1c)<sup>7, 19</sup>. Pro-T1 and pro-T2 progenitor phenotypes, based on an alternative classification scheme using CD5 and CD7<sup>20</sup>, were also readily identified within ATO CD34+ cells (Fig. 1c). Consistent with a T lineage-biased ATO microenvironment, CD19+ B cell frequency was low and decreased over time, and NK and myeloid frequencies remained low throughout (Fig. 1b, d). CD3+TCR $\alpha\beta$ + T cell frequency in ATOs was highly consistent across experiments, and included CD8SP and, to a lesser extent, CD4SP T cells, consistent with positive selection in ATOs (Fig. 1d). A smaller population of CD3+TCR $\gamma\delta$ + T cells was also consistently seen (Fig. 1d). Histological

sections of ATOs demonstrated the formation of dense tissue architecture with abundant lymphoid cells (Supplementary Fig. 1), clusters of which expressed CD3 (Fig. 1e).

Each ATO typically generated  $\sim 2 \times 10^6$  total cells at 6 weeks (Fig. 1f); however, cell yield per HSPC was inversely related to the number of HSPCs seeded and the ratio of HSPCs to stromal cells (Supplementary Fig. 2a). Frequencies of precursor and mature T cells in ATOs was similar across initial HSPC numbers and ratios (Supplemental Fig. 2b), with the exception of ATOs generated with large numbers of stromal cells ( $6 \times 10^5$  per ATO), which showed impaired T cell maturation. Thus, smaller ATOs (typically 7500 HSPCs and  $1.5 \times 10^5$  stromal cells at a 1:20 ratio) were used for further experiments, and showed high reproducibility of cell output and T cell differentiation across technical replicates ( $n=11$ ) and was independent of B27 lot (Supplementary Fig. 3a–d). Of translational relevance, efficient T cell differentiation and cell output was also seen in ATOs cultured with xeno-free B27 (Supplementary Fig. 3e, f) or using irradiated MS5-hDLL1 stromal cells (Supplementary Fig. 3g–j). Recovery of hematopoietic cells generated in ATOs after simple mechanical disruption and filtration resulted in  $>99\%$  CD45+ hematopoietic cells (Supplementary Fig. 3k).

When compared directly to the OP9-DL1 monolayer culture system, ATOs revealed a similar efficiency of T lineage commitment (%CD7+CD5+ cells) but markedly superior generation of both DP and CD3+TCR $\alpha\beta$ + T cells at 4 and 6 weeks (Fig. 2a–d and Supplementary Fig. 4). Improved positive selection was particularly evident in the prevalence of mature CD3+TCR $\alpha\beta$ +CD8SP T cells in ATOs but not OP9-DL1 monolayers (Fig. 2b,c,d and Supplementary Fig. 4). Cross-over experiments testing the impact of culture variables revealed that optimal positive selection and T cell maturation required all three components of the ATO system: 3D structure, MS5-hDLL1 stromal cells, and RB27 medium, as neither monolayer cultures using ATO components, nor OP9-DL1 cells in 3D organoids

supported T cell development (Supplementary Fig. 5). The parental MS5 cell line lacking *DLL1* expression did not support T cell development in either monolayer or 3D cultures, consistent with a requirement for Notch signaling (Supplementary Fig. 5a).

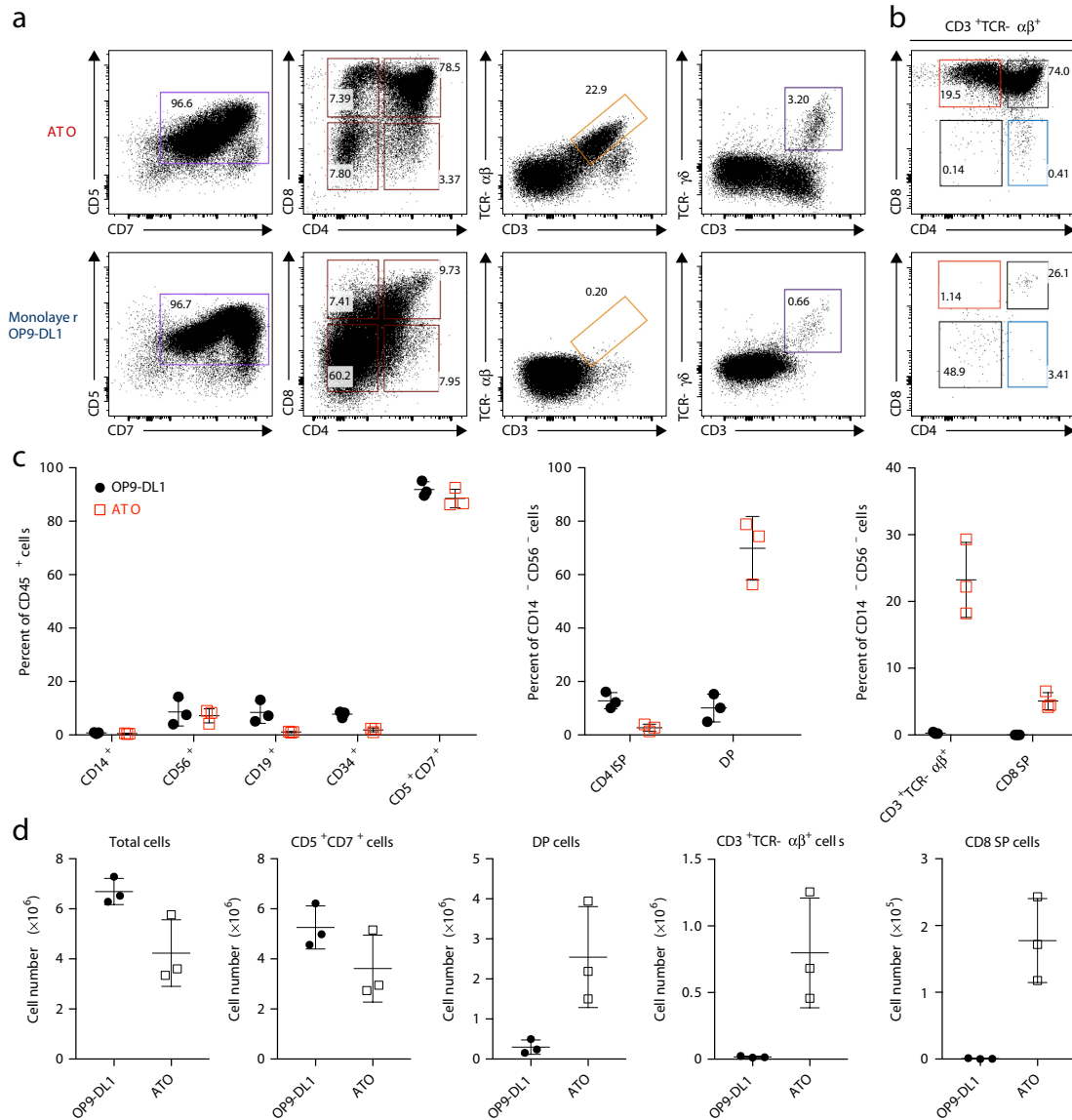


**Fig. 2-2: Comparison of T cell differentiation between the ATO and OP9-DL1 systems.** CD34<sup>+</sup>CD3<sup>-</sup> HSPCs from the same CB donor were used to initiate ATOs or standard OP9-DL1 monolayer cultures (containing 20% FBS) in parallel, followed by analysis using flow cytometry and cell counting. Shown are data from 6-week cultures. (a,b) Representative flow cytometry profiles ( $n = 3$ ) of cells gated on total CD14<sup>-</sup>CD56<sup>+</sup> cells (a) and CD3<sup>+</sup>TCR-αβ<sup>+</sup> cells (b). (c,d) Frequencies of monocytes (CD14<sup>+</sup>), NK cells (CD56<sup>+</sup>), B cells (CD19<sup>+</sup>), HSPCs (CD34<sup>+</sup>) and T lineage cells

(CD7<sup>+</sup>CD5<sup>+</sup>) (gated on total CD45<sup>+</sup> cells), CD4 ISP and DP T cell precursors, and CD3<sup>+</sup>TCR- $\alpha\beta$ <sup>+</sup> and CD3<sup>+</sup>TCR- $\alpha\beta$ <sup>+</sup> CD8 SP mature T cells (gated on CD14<sup>-</sup>CD56<sup>-</sup> cells) in OP9-DL1 monolayer co-cultures versus those in ATOs at 6 weeks of culture (c) and absolute numbers of T cell subsets at week 6 in OP9-DL1 co-cultures versus ATOs using the frequency data shown in c (d). In d, OP9-DL1 cultures were each initiated with  $1.5 \times 10^4$  CD34<sup>+</sup>CD3<sup>-</sup> CB HSPCs cells, and ATOs were each initiated with  $7.5 \times 10^3$  HSPCs from the same CB unit, with technical duplicate ATOs harvested and pooled at 6 weeks for comparison of cell counts. In c,d, bars represent the mean and s.d. of three independent experiments.

### Recapitulation of thymopoiesis and naïve T cell development in ATOs

T cell differentiation in ATOs was next compared to that in the postnatal human thymus. Week 12 CB ATOs showed a similar frequency of CD34<sup>+</sup> pro-T cells and T-lineage committed (CD5<sup>+</sup>CD7<sup>+</sup>) cells to the thymus (Fig. 3a). As in the thymus, most CD3<sup>+</sup> T cells in ATOs were TCR $\alpha\beta$ <sup>+</sup> (Fig. 3a). Mature CD3<sup>+</sup>TCR $\alpha\beta$ <sup>+</sup> CD8SP and CD4SP T cells increased in frequency in ATOs between weeks 6–12 (Fig. 3b and Supplementary Fig. 6a), and exhibited a reversed CD4:CD8 ratio compared to the thymus.

As in the thymus, ATO-derived CD3<sup>+</sup>TCR $\alpha\beta$ <sup>+</sup>CD8SP and CD3<sup>+</sup>TCR $\alpha\beta$ <sup>+</sup>CD4SP T cells transited from a DP-like “immature naïve” (CD45RA<sup>-</sup>CD45RO<sup>+</sup>CD27<sup>+</sup>CCR7<sup>-</sup>CD1A<sup>hi</sup>) to a “mature naïve” (CD45RA<sup>+</sup>CD45RO<sup>-</sup>CD27<sup>+</sup>CCR7<sup>+</sup>CD1A<sup>lo</sup>) phenotype<sup>21, 22</sup> (Fig. 3c and Supplementary Fig. 6a–c). Both immature and mature naïve T cell subsets co-expressed CD62L and CD28, with subset co-expression of CD127 and CD31, the latter associated with recent thymic emigrant T cells in the blood<sup>23</sup> (Supplementary Fig. 6b–c). The activation marker CD25 was not expressed on ATO-derived CD8SP T cells, but was observed on a subset of CD4SP T cells (Supplementary Fig. 6b–c). Taken together, these data show remarkable fidelity of T cell differentiation in ATOs compared to the human thymus,

culminating in the emergence of naïve T cells phenotypically similar to those in the thymus and blood<sup>24, 25</sup>.

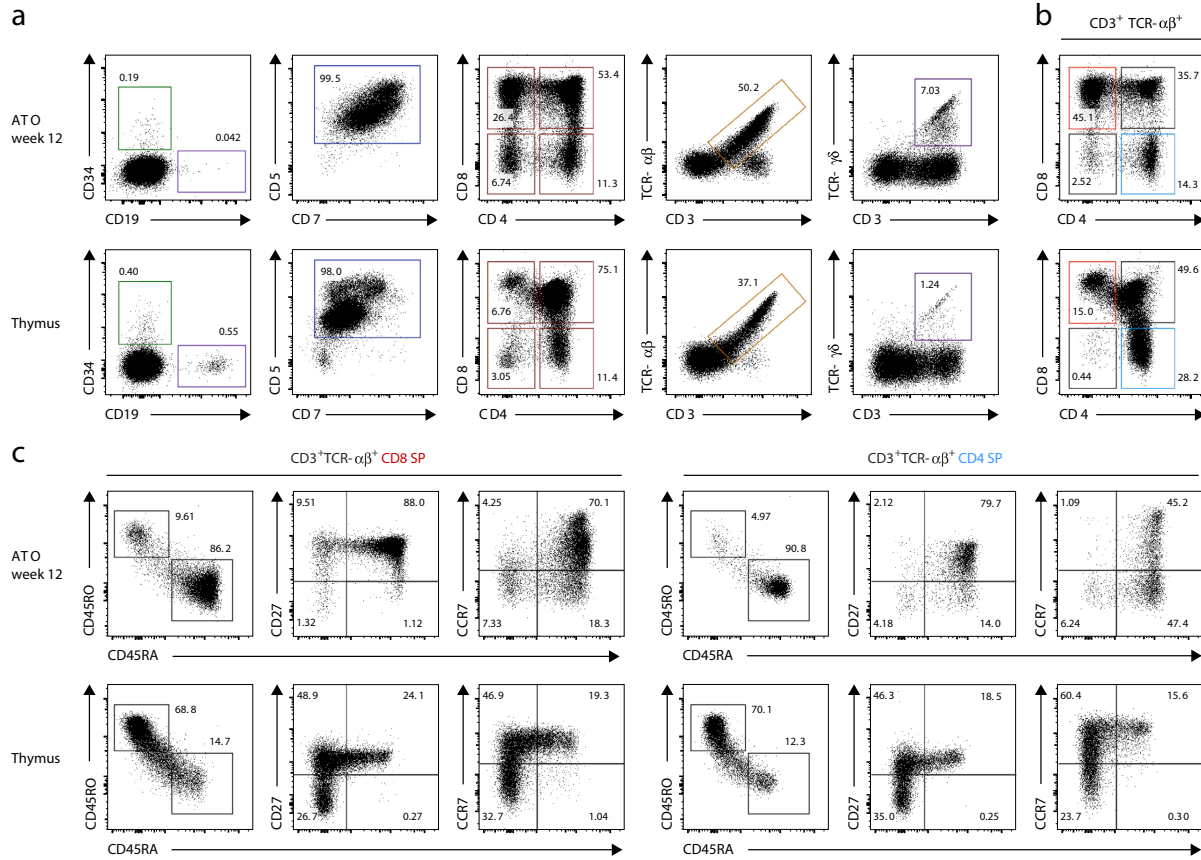


**Fig. 2-3: Comparison of ATO and thymic T cell differentiation and maturation.** (a,b) Representative flow cytometry analysis comparing T cell differentiation in CB ATOs at 12 weeks (top) and human postnatal thymocytes (bottom), gated on total  $CD14^-CD56^-$  (a) and on  $CD3^+TCR-\alpha\beta^+$  (b) cells. (c) Generation of immature ( $CD45RA^-CD45RO^+$ ) and mature ( $CD45RA^+CD45RO^-$ ) naive T cells in ATOs or thymus (gated on  $CD3^+TCR-\alpha\beta^+$  cells, with CD8 SP or CD4 SP subgates indicated). Throughout, data are representative of three independent experiments.

Given the absence of thymic epithelial cells and the late emergence and relatively low frequencies of mature CD4SP T cells, we postulated that MHC class II mediated positive selection may rely on the development of rare dendritic cells in ATOs. Indeed, HLA-DR+ cells were present in ATOs at low frequencies, and included monocytes, B cells, and plasmacytoid,



CLEC9A+, and CD1c+ dendritic cells (Supplementary Fig. 6d), all of which were also present in the thymus, in agreement with previous reports<sup>26, 27</sup> (Supplementary Fig. 6e).

### **T cell differentiation from multiple HSPC sources and subsets**

In addition to CB, efficient T cell differentiation in ATOs was seen from clinically relevant HSPC sources, i.e. adult bone marrow (BM), G-CSF mobilized peripheral blood (MPB), and non-mobilized peripheral blood (PB) (Fig. 4a–d and Supplementary Fig. 7a,b). Kinetics of T cell differentiation varied between sources (Fig. 4c), with thymic CD34+ cells predictably showing the fastest differentiation; however, T cell output was similar across all sources (Fig. 4d). Enriched hematopoietic stem cell (HSC) fractions (lin-CD34+CD38-)<sup>28</sup> from CB, BM, or MPB also demonstrated efficient T cell differentiation in ATOs (Fig. 4e,f and Supplementary Fig. 7c,d).

ATOs also supported T cell differentiation from highly purified lymphoid progenitors isolated from adult BM (Fig. 4g,h). Lymphoid-primed multipotent progenitors (LMPP)<sup>29</sup> and CD24- common lymphoid progenitors<sup>30</sup> (CLP) generated T cells to a greater extent than unfractionated CD34+lin- HSPCs (Fig. 4g, and Supplementary Fig. 7e,f). In contrast, CD24+ CLPs, which possess primarily B and NK cell potential<sup>30, 31</sup> resulted in poor T cell output in ATOs (Fig. 4g,h and Supplementary Fig. 7e). Thus ATOs can serve as a tool for evaluating T lineage potential in human stem and progenitor cell populations.

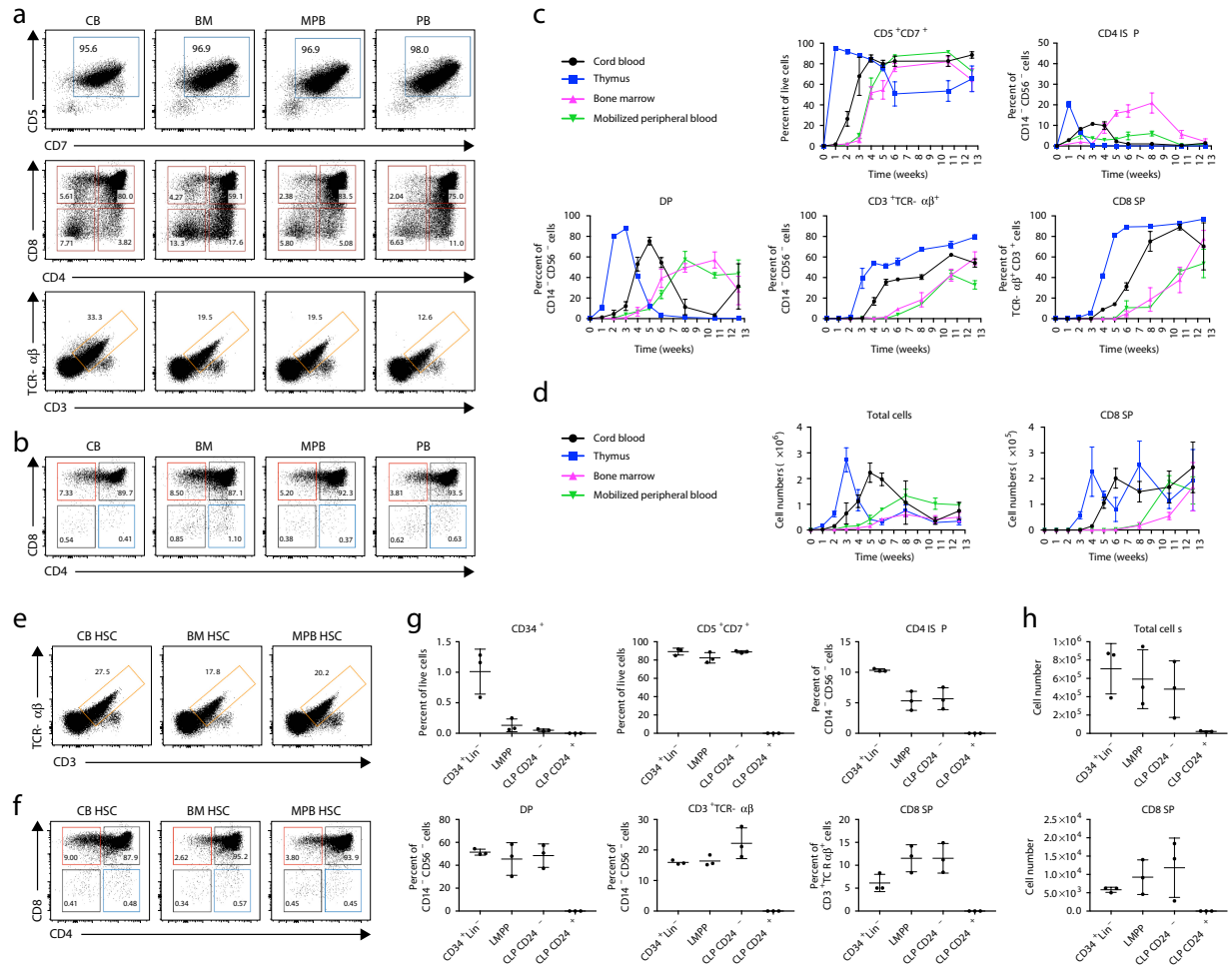


**Fig 2-4: T cell differentiation in ATOs from different HSPC sources and subsets.** (a,b) Representative analysis ( $n = 3$ ) showing efficient T cell development in week 6 ATOs initiated with  $CD34^+CD3^-$  HSPCs from human CB, adult BM, G-CSF-mobilized PB (MPB) or nonmobilized PB (PB). Cells were gated on total  $CD14^-CD56^-$  cells (a) or on  $CD3^+TCR-\alpha\beta^+$  T cells (b). (c) T cell differentiation kinetics over 12 weeks in ATOs generated from 7,500  $CD34^+CD3^-$  cells isolated from CB, neonatal thymi, BM or MPB. Mean and s.d. of T cell precursor and mature T cell frequencies are shown from three technical replicates per tissue. Data are representative of two different experiments. (d) Numbers of total cells and of  $CD3^+TCR-\alpha\beta^+$  CD8 SP T cells from the ATO experiments shown in c. (e,f) T cell differentiation from HSC-enriched ( $Lin^-CD34^+CD38^-$ ) fractions from CB, BM or MPB in week 6 ATOs, gated on  $CD14^-CD56^-$  cells (e) and  $CD3^+TCR-\alpha\beta^+$  T cells (f). Data are representative of independent experiments (CB,  $n = 3$ ; BM,  $n = 2$ ; MPB,  $n = 1$ ). (g) T cell differentiation potential of adult BM total HSPCs ( $CD34^+Lin^-$ ) and purified progenitor (LMPP and CLP) subsets in ATOs at week 6; frequencies of  $CD34^+$  HSPCs, total T lineage cells ( $CD5^+CD7^+$ ) and  $CD34^+TCR-\alpha\beta^+$  CD8 SP T cells.

different T cell subsets are shown. (h) Numbers of total cells and CD3<sup>+</sup>TCR- $\alpha\beta$ <sup>+</sup> CD8 SP T cells from ATOs shown in g. In g,h, mean and s.d. of technical triplicates are shown, and data are representative of three independent experiments.

### **TCR diversity and function of ATO-derived T cells**

Similar to the thymus, *RAG1* and *RAG2* were expressed at the DP stage in ATOs, consistent with TCR gene rearrangement (Supplementary Fig. 8a). Flow cytometric analysis of TCR V $\beta$  frequencies in ATO-derived CD3+TCR $\alpha\beta$ +CD8SP (Fig. 5a) and CD3+TCR $\alpha\beta$ +CD4SP (Supplementary Fig. 8b) T cells revealed strikingly similar diversities to those of corresponding naïve T cells from human thymi. Physiological TCR diversity was confirmed by deep sequencing of TCR V $\alpha$  and V $\beta$  CDR3 regions in ATO-derived CD3+TCR $\alpha\beta$ +CD8SP T cells compared with both thymic and PB naïve CD8SP T cells (Fig. 5b,c). Importantly, skewed V $\alpha$  or V $\beta$  usage was not observed in ATO-derived T cells, arguing against the predominance of unconventional T cell lineages or clonally expanded T cells.

CD8SP T cells isolated from ATOs demonstrated polyfunctional production of IFN $\gamma$ , TNF $\alpha$  and IL-2 in response to PMA/ionomycin (Fig. 5d), and exhibited upregulation of CD25 and 4-1BB and proliferated in response to anti-CD3/CD28 and IL-2 (Fig. 5e,f). CD4SP cells freshly isolated from ATOs produced IFN $\gamma$  and IL-2 in response to PMA/ionomycin, and proliferated in response to anti-CD3/CD28 and IL-2 (Supplementary Fig. 8c,d,e).

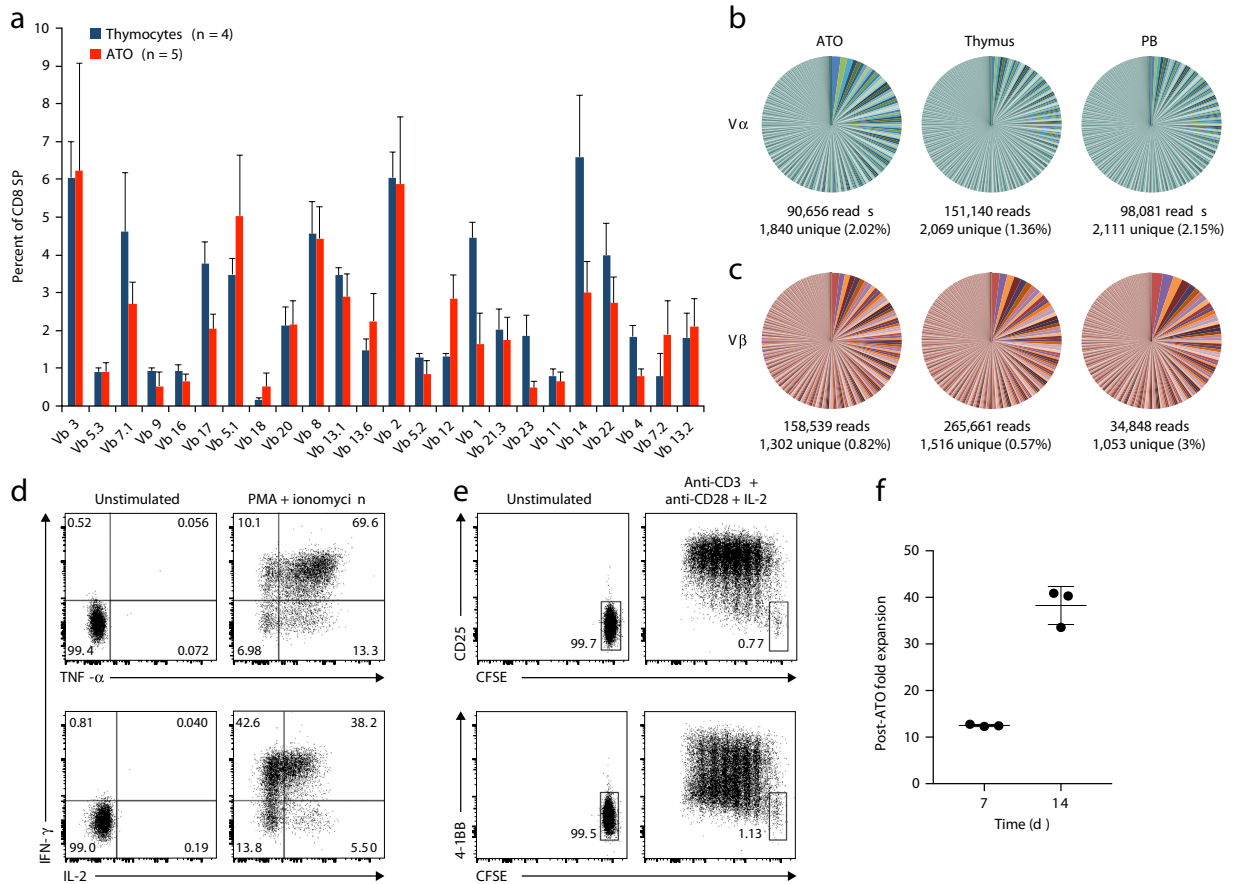


**Fig. 2-5: Generation of TCR diversity and functional T cells in ATOs.** (a) Generation of TCR diversity in CD3<sup>+</sup>TCR- $\alpha\beta$ <sup>+</sup> CD8 SP T cells from week 7 ATOs ( $n = 5$ ) or human thymi ( $n = 4$ ), as shown by flow cytometric analysis of the frequency of TCR V $\beta$  family expression. (b,c) TCR clonotype diversity in CD3<sup>+</sup>TCR- $\alpha\beta$ <sup>+</sup> CD8 SP T cells from ATOs and the thymus, and from naive T cells in the PB, by deep sequencing of the gene encoding the TCR V $\alpha$  (b) or TCR V $\beta$  (c) CDR3 regions. Frequency of individual clonotypes is shown. Data are representative of three independent experiments. (d) Polyfunctional cytokine production by ATO-derived CD3<sup>+</sup>TCR- $\alpha\beta$ <sup>+</sup> CD8 SP T cells after treatment with PMA + ionomycin for 6 h. Data are representative of three individual experiments. (e) Proliferation (as measured by dilution of CFSE, which is a fluorescent dye used to monitor cell division) and activation (upregulation of CD25 and 4-1BB) of ATO-derived CD3<sup>+</sup>TCR- $\alpha\beta$ <sup>+</sup> CD8 SP cells after 5 d of treatment with anti-CD3, anti-CD28 and IL-2. Data are representative of two individual experiments. (f) Post-ATO expansion of ATO-derived CD3<sup>+</sup>TCR- $\alpha\beta$ <sup>+</sup> CD8 SP T cells relative to the starting cell number in response to treatment with anti-CD3, anti-CD28 and IL-2 for 7 d or 14 d. The mean and s.d. of technical triplicates are shown, and data are representative of three independent experiments.

### ***In vitro* generation of naïve TCR-engineered T cells in ATOs**

We next explored if ATOs can be used for the *in vitro* generation of naïve TCR-engineered T cells. CB CD34<sup>+</sup>CD3<sup>-</sup> HSPCs were transduced with a lentiviral vector encoding codon optimized  $\alpha$  and  $\beta$  chains of a HLA-A\*02:01-restricted TCR specific for the NY-ESO-1<sub>157-165</sub>peptide<sup>32</sup>. At 7 weeks, TCR-transduced ATOs showed a similar frequency of CD7<sup>+</sup>CD5<sup>+</sup> T-lineage cells as mock-transduced controls, but markedly increased CD3<sup>+</sup>TCR $\alpha\beta$ <sup>+</sup> T cells, the majority of which expressed the transduced TCR detected by tetramer or an antibody against the transduced V $\beta$ 13.1 chain (Fig. 6a). The frequency of tetramer<sup>+</sup>CD3<sup>+</sup>TCR $\alpha\beta$ <sup>+</sup>CD8SP T cells was similar to that of mock-transduced ATOs, however TCR transduction resulted in accelerated maturation from an immature (CD45RA<sup>-</sup>CD45RO<sup>+</sup>CD27<sup>-</sup>CCR7<sup>-</sup>CD1a<sup>hi</sup>) to a mature (CD45RA<sup>+</sup>CD45RO<sup>-</sup>CD27<sup>+</sup>CCR7<sup>+</sup>CD1a<sup>lo</sup>) naïve T cell phenotype (Fig. 6a). As antigen-specific T cells with an unconventional CD8 $\alpha\alpha$  phenotype have been reported in the OP9-DL1 system<sup>33</sup>, we confirmed that tetramer<sup>+</sup> T cells from ATOs displayed a conventional CD8 $\alpha\beta$  phenotype and lacked expression of CD16 or CD56, markers associated with NK cells and innate-like T cells (Fig. 6b).

TCR transduction also significantly enhanced cell yield from ATOs (average ~500 cells per HSPC) (Fig. 6c), the majority of which were tetramer<sup>+</sup>CD3<sup>+</sup>CD8SP T cells. Thus, by 7 weeks a single ATO initiated with 7,500 TCR-transduced HSPCs generated on average  $\sim 4 \times 10^6$  cells, of which approximately 15% ( $6 \times 10^5$ ) were mature naïve tetramer<sup>+</sup>CD3<sup>+</sup>CD8SPCD45RA<sup>+</sup>CD45RO<sup>-</sup> antigen specific T cells (Fig. 6a,c).

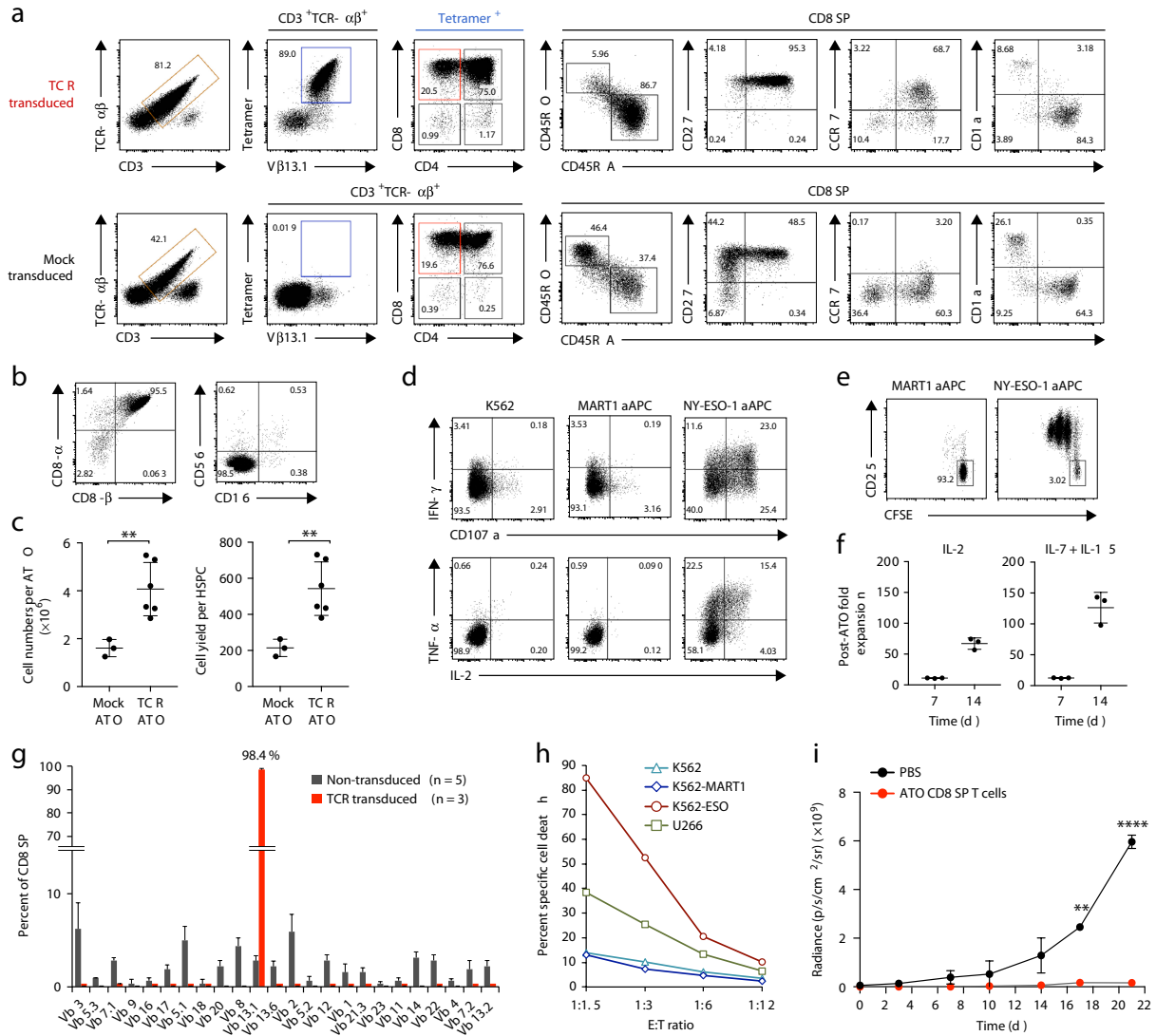


**Fig. 2-6: Generation of antigen-specific T cells from TCR-engineered HSPCs in ATOs.** (a) Representative analysis ( $n = 3$ ) for the generation of HLA-A\*0201–NY-ESO-1<sub>157–165</sub>-specific TCR-engineered (or mock) T cells in week 7 ATOs that were initiated with CB HSPCs. Cells were gated on CD14<sup>-</sup>CD56<sup>-</sup> cells. (b) Conventional T cell phenotype of CD3<sup>+</sup>TCR-αβ<sup>+</sup>tetramer<sup>+</sup> T cells from TCR-transduced CB ATOs. Data are representative of three independent experiments. (c) Cell output from ATOs generated with  $7.5 \times 10^3$  to  $18 \times 10^3$  starting CB HSPCs. Mean and s.d. of independent experiments are shown (mock,  $n = 3$ ; TCR,  $n = 8$ ). \*\* $P = 0.002$  by two-tailed unpaired  $t$ -test). (d) Cytokine production and CD107a membrane mobilization of tetramer<sup>+</sup>CD3<sup>+</sup> CD8 SP T cells in response to K562 cells or to K562 aAPCs expressing an irrelevant (MART-1) or a cognate (NY-ESO-1) SCT. Data are representative of three independent experiments. (e) Proliferation (as measured by CFSE dilution) and activation (as measured by CD25 upregulation) of ATO-derived CD3<sup>+</sup>tetramer<sup>+</sup>CD8 SP T cells in response to irrelevant (MART1) or cognate (NY-ESO-1) aAPCs for 72

h. Data are representative of two independent experiments. (f) Post-ATO expansion of CD3<sup>+</sup>TCR- $\alpha\beta$ <sup>+</sup>CD8 SP T cells (isolated from TCR-transduced ATOs) in response to anti-CD3, anti-CD28 and either IL-2 or IL-7 and IL-15 treatment. Mean and s.d. of technical triplicates are shown; data are representative of three independent experiments. (g) Allelic exclusion by flow cytometry of endogenous TCR V $\beta$  in CD3<sup>+</sup>TCR- $\alpha\beta$ <sup>+</sup>tetramer<sup>+</sup> CD8 SP cells isolated from ATOs of TCR-transduced cells ( $n = 3$ ) versus those from nontransduced cells ( $n = 5$ ). Error bars represent s.d. (h) *In vitro* cytotoxicity assay, in which CD8 SP T cells from HLA-A\*02:01–NY-ESO-1<sub>157–165</sub>-specific TCR-transduced ATOs were activated for 36 h and co-incubated with K562, K562 aAPCs (NY-ESO-1 or MART-1) or the HLA-A\*02:01 U266 cell line which expresses NY-ESO-1 endogenously. Percentage cell death was determined by annexin V staining. Data are representative of two independent experiments. E:T, effector:target. (i) *In vivo* tumor control by ATO-derived TCR-engineered T cells. CD8 SP T cells from TCR-transduced ATOs were activated and expanded for 14 d.  $4.5 \times 10^6$  tetramer<sup>+</sup> T cells or PBS was injected intravenously into NSG mice that had subcutaneously been implanted 3 d earlier with luciferase<sup>+</sup> K562-ESO tumor cells, and serial bioluminescence was recorded. Mean and s.d. for each group is shown (PBS,  $n = 2$ ; TCR-transduced T cells,  $n = 3$ ). \*\* $P = 0.00033$  and \*\*\*\* $P = 0.000066$  by two-tailed unpaired *t*-test.

ATO-derived antigen specific CD8SP T cells exhibited polyfunctional cytokine production (IFN $\gamma$ , TNF $\alpha$  and IL-2), degranulation as assessed by CD107a membrane mobilization, (Fig. 6d) and proliferation (Fig. 6e) in response to artificial antigen presenting cells (aAPCs) expressing CD80 and a cognate HLA-A\*02:01/NY-ESO-1 single chain trimer; but not irrelevant HLA-A\*02:01/MART-1 aAPCs or parental K562 cells. Furthermore, these T cells could be expanded with anti-CD3/CD28 beads and IL-2 or IL-7/IL-15 (Fig. 6f). A previous report of TCR-engineered T cells derived using the OP9-DL1 system reported loss of CD8 $\beta$  expression following repeated *in vitro* stimulation<sup>33</sup>, and while a subpopulation of ATO-derived tetramer<sup>+</sup>CD8SP T cells was CD8 $\beta$ -following re-stimulation with anti-CD3/28 beads, the majority of cells maintained a conventional CD8 $\alpha\beta$  phenotype (Supplementary Fig. 9a).

Flow cytometric analysis of V $\beta$  diversity in ATO-derived TCR-engineered T cells revealed >98% of tetramer+CD3+CD8SP T cells expressed only the transduced V $\beta$ 13.1 segment (Fig. 6g and Supplementary Fig. 9b), suggesting that allelic exclusion of both endogenous V $\beta$  loci occurred during differentiation of TCR-engineered T cells in ATOs.

To test if these findings could be extended beyond the NY-ESO-1 TCR, we generated ATOs using CB HSPCs transduced with an HLA-A\*02:01-restricted TCR specific for MART-1<sup>34</sup>. Tetramer+CD3+CD8SP cells isolated from these ATOs demonstrated a naïve T cell phenotype (Supplemental Fig. 9c) and upregulated IFN $\gamma$  and mobilized CD107a in response to MART-1 but not NY-ESO-1 aAPCs (Supplemental Fig. 9d).

We next tested antigen-specific cytotoxicity of ATO-derived TCR-engineered T cells. Purified NY-ESO-1-specific CD8SP T cells isolated from TCR-transduced ATOs and activated for 36 hours potently induced apoptosis in cell lines expressing cognate pMHC (either K562 cells transduced with an HLA-A\*02:01/NY-ESO-1 SCT; or the HLA-A\*02:01+ U266 multiple myeloma cell line which endogenously expresses NY-ESO-1), but showed little activity against parental K562 cells or K562 cells expressing an irrelevant HLA-A\*02:01/MART-1 SCT (Fig. 6h and Supplementary Fig. 9e). Consistent with their naïve state, prior activation of ATO-derived antigen-specific T cells was required for cytotoxicity. Loss of antigen specificity was not observed following prolonged (14 days) *in vitro* expansion, indicating retention of a conventional T cell phenotype (Supplementary Fig. 9f); furthermore, cytotoxicity was similar to that of TCR-transduced PB CD8+ T cells expanded for the same period (Supplementary Fig. 9f). Consistent with these results, ATO-derived TCR-engineered T cells were able to significantly control disease progression in NSG mice subcutaneously engrafted with antigen-expressing K562 tumors (Fig. 6i).



## Discussion

We present here an *in vitro* system that efficiently initiates and sustains the normal stages of T cell commitment and differentiation from human HSPCs, culminating in the production of mature, naïve CD3+TCR $\alpha\beta$ +CD8SP and CD3+TCR $\alpha\beta$ +CD4SP T cells closely resembling naïve T cells from the thymus and blood.

Compared to existing methods of *in vitro* T cell differentiation, ATOs supported unprecedented levels of positive selection of CD3+TCR $\alpha\beta$ + precursors into mature CD8SP and CD4SP T cell pools—a process impaired in monolayer systems<sup>2, 3, 4, 5</sup>. Enhanced positive selection in ATOs was strictly dependent on both 3D structure and the stromal cell line used, as monolayer cultures set up with ATO components resulted in inefficient T cell maturation, as did 3D organoid cultures using OP9-DL1 cells. We have however observed mature T cell development in ATOs using *DLL1*-transduced immortalized human BM stromal cells, and while efficiency is lower than for MS5-hDLL1, this indicates that neither species-specific nor MS5-specific factors underlie T cell positive selection in ATOs. We also predict that other Notch ligands, such as DLL4, should be effective in driving T cell development in ATOs.

A specific role for 3D structure in T cell positive selection is consistent with the reported ability of FTOCs and reaggregated primary thymic stromal organoids to permit T cell maturation, albeit at low efficiencies<sup>10, 11, 12</sup>. 3D interactions may support positive selection by increasing the valence and/or duration of contact between T cell precursors and selective ligands (such as pMHC); facilitating crosstalk between stromal and hematopoietic cells; or exerting developmental signals on T cell precursors through mechanical forces and/or metabolic gradients not otherwise possible in 2D. The formation of thymic-like spatial niches segregating developing T cells from stromal signals and/or Notch ligands during development

may be another possible mechanism at play in ATOs. In the absence of thymic epithelial cells in ATOs, we hypothesize that selective MHC I ligands for CD8SP positive selection are ubiquitously presented by hematopoietic cells within the ATOs, as has been suggested in the OP9-DL1 system<sup>6</sup>; but that CD4SP positive selection occurs via MHC class II presentation by dendritic cells that develop within ATOs, with their rarity possibly underlying the bias toward CD8+ T cell development in this system. The nature of these and other specific mechanisms of T cell selection can now be readily investigated using the ATO system in conjunction with model TCR/antigen systems.

Another major advance of the ATO system over existing methods is the efficient generation of mature T cells from clinically relevant adult HSPC sources such as bone marrow, and resting or G-CSF mobilized peripheral blood<sup>2, 3, 4, 5</sup>. While several studies have shown improved T cell maturation on OP9-DL1 using thymic CD34+ cells, these primarily consist of committed pro-T cells<sup>7</sup> and have little therapeutic utility.

ATOs can be used as a novel tool to generate naïve, antigen specific engineered T cells from human HSPCs. Differentiation of TCR-engineered T cells from HPSCs has been reported using the OP9-DL1 system however, as with non-transduced HSPCs, positive selection and generation of mature CD3+ T cells was impaired (typically representing only 0–2% of cultures), with the highest efficiencies achieved using thymic CD34+ cells<sup>33, 35, 36</sup>. In comparison, ATOs strongly supported the differentiation and positive selection of mature CD3+ TCR-engineered T cells from CB HSPCs, with similar results observed using MPB HSPCs (not shown). In contrast to TCR-transduced PB T cells, that require activation and prolonged expansion, *in vitro* generation of naïve antigen specific T cells may offer distinct therapeutic advantages for adoptive cell therapy based on studies correlating earlier T cell differentiation state with *in vivo* efficacy<sup>24, 37, 38</sup>. Non-transduced and TCR-transduced ATOs

showed accumulation of naïve CD3+CD8SP T cells over time, with concomitant decrease in DPs, consistent with the absence of T cell egress. Despite this, mature T cells in ATOs retained a naïve phenotype, absence of activation markers, and required activation/priming for effective cytotoxicity. TCR transduction of HSPCs also resulted in near-complete allelic exclusion of endogenous V $\beta$  TCR loci, consistent with findings from *in vivo* studies of TCR-transduced murine and human HSPCs<sup>34, 39, 40</sup>. The expression of potentially alloreactive endogenous TCRs on engineered PB T cells is a major barrier to the development of off-the-shelf adoptive T cell therapies, and current approaches to mitigate donor T cell alloreactivity, such as gene editing<sup>41, 42, 43</sup> or the use of virus-specific T cells<sup>44</sup>, require extensive cell manipulation, potentially compromising function. We illustrate here that ATOs can be used to exploit developmental allelic exclusion of endogenous TCR expression as a novel strategy for generating potentially non-alloreactive antigen specific T cells for immunotherapy. ATOs are thus a new tool for the study and development of stem cell based engineered T cell therapies, given the ease of genetically manipulating both hematopoietic and stromal compartments, and the ability to produce naïve, unperturbed antigen specific T cells.

Finally, the ATO system offers technical simplicity, reproducibility, and potential scalability. The use of serum-free medium avoids the marked variability observed in monolayer systems<sup>13</sup>, and the ability to maintain ATOs intact for the duration of culture (up to 20 weeks) with simple media changes reduces labor through avoiding the frequent transfer of cells onto fresh stromal cells required by monolayer systems<sup>2, 3, 13</sup>. The simplicity of the ATO system permits straightforward adoption of the method in laboratories interested in studying human T cell development and engineered T cell therapies.

\*\*\*

## **Materials and Methods**

### **Isolation of human CD34<sup>+</sup>CD3<sup>-</sup> HSPCs**

Neonatal umbilical cord blood was obtained from discarded cord and placental units from deliveries at UCLA. Bone marrow (BM) was obtained from healthy adult donors (ages 18–51) through discarded material from allogeneic BM donor harvests at UCLA or purchased from AllCells Inc. (Alameda, CA). G-CSF mobilized peripheral blood was obtained from consenting healthy adult donors (ages 44–60) undergoing apheresis for allogeneic stem cell transplant donation at UCLA. Non-mobilized peripheral blood was obtained from healthy adult donors through the UCLA CFAR Virology Core. All tissue samples were obtained under UCLA IRB-approved protocols or exemptions. All samples were enriched for mononuclear cells by Ficoll-Paque (GE Healthcare Life Sciences, Pittsburgh, PA) gradient centrifugation followed by positive selection of CD34<sup>+</sup> cells by magnetic cell sorting (MACS) using the CD34 MicroBead Kit UltraPure (Miltenyi, Auburn CA). CD34<sup>+</sup> cell enriched fractions were cryopreserved after MACS, unless otherwise noted. Prior to use, cells were thawed and residual T cells depleted by FACS by sorting CD34<sup>+</sup>CD3<sup>-</sup> cells, which were immediately seeded into ATOs or transduced as described below. In some experiments, HSCs were enriched by FACS for Lin<sup>-</sup>CD34<sup>+</sup>CD38<sup>-</sup> cells prior to seeding in ATOs. HSPCs used in TCR transduction experiments were from HLA-A\*02:01<sup>+</sup> CB units. High-resolution HLA-A2 typing was performed by the UCLA Immunogenetics Center using sequence-specific oligonucleotide (SSO) beads.

### **Isolation of human bone marrow progenitor subsets**

CD34<sup>+</sup> HSPCs were enriched from fresh BM aspirates, as above, and immediately sorted by FACS for stem/progenitor populations based on positive expression of CD45 and absent expression of lineage markers (CD3, CD14, CD19, CD56, and CD235a; “Lin<sup>-</sup>”) combined with

the following markers: total HSPCs (CD34+), HSC (CD34+CD38-CD45RA-)<sup>28, 45</sup>, LMPP (CD34+CD38+CD45RA+CD10-CD62L<sup>hi</sup>)<sup>29</sup>, CD24- CLP (CD34+CD38+CD45RA+CD10+CD24-)<sup>30</sup>, and CD24+ CLP (CD34+CD38+CD45RA+CD10+CD24+)<sup>30, 31</sup>.

### **Isolation of human thymocytes**

Postnatal human thymi were obtained under IRB exemption as discarded waste from patients undergoing cardiac surgery at Children's Hospital Los Angeles (CHLA). Thymic fragments were finely dissected in RPMI and disrupted by pipetting to release thymocytes into suspension, followed by passage through a 70 µm nylon strainer. Cells were analyzed fresh on the same or following day. Flow cytometry analysis of thymic and ATO-derived T cell progenitors used the following surface phenotypes: Early thymic progenitor (ETP; CD34+CD7-CD1a-), CD1a- pro-T (CD34+CD7+CD1a-), and CD1a+ pro-T (CD34+CD7+CD1a+)<sup>7</sup>; or CD5- pro-T (pro-T1; CD34+CD7+CD5-) and CD5+ pro-T (pro-T2; CD34+CD7+CD5+)<sup>20</sup>. Thymic and ATO-derived T cells and precursors were defined as CD14- CD56- in combination with the following phenotypes: total T lineage cells (CD7+CD5+), double negative (DN; CD4-CD8-), CD4 immature single positive (CD4ISP; CD5+CD4+CD3-), double positive (DP; CD4+CD8+), CD8SP (CD3+TCRαβ+CD8+CD4-), CD4SP (CD3+TCRαβ+CD8-CD4+), immature naïve (CD45RA-CD45RO+ that were CD8SP or CD4SP), mature naïve (CD45RA+CD45RO- that were CD8SP or CD4SP). Immature and mature naïve phenotypes were confirmed by co-staining for CD1a, CD27, CD28, and CCR7.

### **Isolation of primary human T cells**

Thymic T cells were isolated from thymocytes preparations as described above, and peripheral blood and cord blood CD8<sup>+</sup> T cells were isolated from mononuclear cell fractions as described above. CD8<sup>+</sup> T cell isolation from all sources was by magnetic bead enrichment for CD8SP T cells using the CD8<sup>+</sup> T cell Isolation Kit (Miltenyi). In some experiments, thymic T cells were further purified by FACS to deplete CD4ISP or DP precursors, and PB T cells to isolate naïve T cells (CD45RO-CCR7<sup>+</sup>).

### **Cell lines**

The MS5 murine stromal cell line<sup>15</sup> was obtained as a gift. To generate MS5-hDLL1, MS5 cells were transduced with a lentiviral vector encoding human *DLL1* and eGFP. The highest 5% GFP-expressing cells were sorted by FACS and passaged in DMEM/10% FCS. Stable expression was confirmed by flow cytometry for GFP expression after several weeks of culture, and *DLL1* expression confirmed by qRT-PCR and DNA sequencing. The OP9-DL1 cell line<sup>1</sup>(expressing murine *Dll1*) was a gift from Dr. Juan Carlos Zúñiga-Pflücker (University of Toronto) and was passaged in MEMα (ThermoFisher Scientific, Grand Island, NY)/20% FBS in 0.1% gelatin-coated flasks. The K562 cell line was obtained from ATCC and maintained in RPMI/10% FCS. K562 aAPCs were generated by co-transduction of K562 cells with lentiviral vectors encoding full-length human CD80 and HLA-A\*02:01/B2M/NY-ESO-1<sub>157-165</sub> or MART-1<sub>26-35</sub> single chain trimers (SCTs; gifts from Dr. David Baltimore, Caltech). K562 target cells were created by transduction with either SCT without CD80. Luciferase K562 target cells were created by sequential transduction of K562 cells with a firefly luciferase lentiviral vector (gift from Dr. Donald Kohn, UCLA) followed by either SCT vector. K562 transductants were FACS sorted prior to use. The U266 multiple myeloma cell line was a gift from Dr. John Chute (UCLA) and maintained in RPMI/10% FCS.

### **Artificial Thymic Organoid (ATO) cultures**

MS5-hDLL1 (or MS5 or OP9-DL1, as noted) cells were harvested by trypsinization and resuspended in serum free ATO culture medium (“RB27”) composed of RPMI 1640 (Corning, Manassas, VA), 4% B27 supplement (ThermoFisher Scientific, Grand Island, NY), 30  $\mu$ M L-ascorbic acid 2-phosphate sesquimagnesium salt hydrate (Sigma-Aldrich, St. Louis, MO) reconstituted in PBS, 1% penicillin/streptomycin (Gemini Bio-Products, West Sacramento, CA), 1% Glutamax (ThermoFisher Scientific, Grand Island, NY), 5 ng/ml rhFLT3L and 5 ng/ml rhIL-7 (Peprotech, Rocky Hill, NJ). RB27 was made fresh weekly. 4% XenoFree B27 was substituted for B27 in the indicated experiments. Depending on the experiment,  $1.5\text{--}6\times 10^5$  MS5-hDLL1 cells were combined with  $3\times 10^2\text{--}1\times 10^5$  purified CD34<sup>+</sup>CD3<sup>-</sup> cells (or other HSPC populations, as indicated) per ATO in 1.5 ml Eppendorf tubes and centrifuged at 300 g for 5 min. at 4°C in a swinging bucket centrifuge. Supernatants were carefully removed and the cell pellet was resuspended by brief vortexing. For each ATO, a 0.4  $\mu$ m Millicell transwell insert (EMD Millipore, Billerica, MA; Cat. PICM0RG50) was placed in a 6-well plate containing 1 ml RB27 per well. To plate ATOs, inserts were taken out and rested on the edge of plate to drain excess medium. The cell slurry was adjusted to 5  $\mu$ l per ATO, drawn up in with a 20  $\mu$ l pipet tip and plated by forming a drop at the end of the pipet tip which was gently deposited onto the cell insert. The cell insert was placed back in the well containing 1 mL RB27. Medium was changed completely every 3–4 days by aspiration from around the cell insert followed by replacement with 1 ml with fresh RB27/cytokines. ATOs were cultured in this fashion for up to 20 weeks. At the indicated times, ATO cells were harvested by adding FACS buffer (PBS/0.5% bovine serum album/2mM EDTA) to each well and briefly disaggregating the ATO by pipetting with a 1 ml “P1000” pipet, followed by passage through

a 50  $\mu$ m nylon strainer. In some experiments, single cell suspensions of MS5-hDLL1 cells were  $\gamma$ -irradiated at the indicated doses prior to use in ATOs.

### **T cell monolayer co-cultures**

OP9-DL1 monolayer cultures were set up as previously described<sup>1, 3, 13</sup>. Briefly, OP9-DL1 cells were seeded into 0.1% gelatin-coated 12 well plates 1–2 days prior to use to achieve 70–80% confluence. Medium was aspirated from monolayers and  $1.5 \times 10^4$  FACS purified CD34+CD3-HSPCs were plated on stromal monolayers in 2 ml of medium composed of MEM $\alpha$ , 20% FBS, 30  $\mu$ M L-Ascorbic acid, 5 ng/ml rhFLT3L, and 5 ng/ml rhIL-7. In some experiments, MS5 or MS5-hDLL1 was substituted for OP9-DL1, and RB27 was substituted as the culture medium. Cells were transferred to new stromal cell monolayers every 4–5 days by harvesting cells, filtering through a 50  $\mu$ m nylon strainer, and replating in fresh medium. When confluent, cells were split into multiple wells containing fresh stromal layers.

### **Lentiviral vectors and transduction**

The full-length coding sequence of human *DLL1* was cloned by RT-PCR from a human universal reference RNA set (Agilent Technologies, Santa Clara, CA) into the third generation lentiviral vector pCCL-c-MNDU3-X-IRES-eGFP<sup>34</sup> (gift from Dr. Donald Kohn, UCLA). Human *CD80* was similarly cloned into pCCL-c-MNDU3. The third generation lentiviral vector encoding the codon optimized  $\alpha$  and  $\beta$  (Vb13.1) chains of a TCR specific for HLA-A\*02:01/NY-ESO-1<sub>157-165</sub> (derived from the 1G4 TCR clone<sup>46</sup>) is previously described<sup>32</sup>, and was a gift from Dr. Antoni Ribas (UCLA). The codon-optimized HLA-A\*02:01/MART-1<sub>126-35</sub> specific TCR (derived from the F5 TCR clone<sup>47</sup>) was a gift from Dr. Donald Kohn (UCLA). Coding sequences for HLA-A\*02:01/B2M/ NY-ESO-1<sub>157-165</sub> or HLA-A\*02:01/B2M/ MART-1<sub>126-35</sub> single chain trimers were a gift from Dr. David Baltimore (Caltech), and were sub-cloned



into the pCCL-c-MNDU3-X-IRES-mStrawberry lentiviral vector. Packaging and concentration of lentivirus particles was performed as previously described<sup>32</sup>. Briefly, 293T cells (ATCC) were co-transfected with a lentiviral vector plasmid, pCMV-ΔR8.9, and pCAGGS-VSVG using TransIT 293T (Mirus Bio, Madison, WI) for 17 hours followed by treatment with 20 mM sodium butyrate for 8 hours, followed by generation of cell supernatants in serum-free UltraCulture for 48 hours. Supernatants were concentrated by tangential flow filtration using Amicon Ultra-15 100K filters (EMD Millipore, Billerica, MA) at 4000 xg for 40 minutes at 4°C and stored as aliquots at -80°C. For HSPC transduction, 1×10<sup>5</sup>–1×10<sup>6</sup> FACS-sorted CD34+CD3<sup>-</sup> HSPCs were plated in 6-well non-treated plates coated with 20 μg/ml Retronectin (Clontech, Mountain View, CA) in 1 ml X-VIVO-15 (Lonza, Basel, Switzerland) supplemented with 50 ng/ml of recombinant human SCF, FLT3L, and TPO, and 10 ng/ml IL-3 (Peprotech, Rocky Hill, NJ) for 12–18h, after which concentrated lentiviral supernatant was to a final concentration of 1–2×10<sup>7</sup> TU/ml. Mock-transduced cells were cultured in identical conditions without addition of vector. Cells were harvested 24 hours post-transduction, washed, and seeded into ATOs. For transduction of peripheral blood T cells, CD8<sup>+</sup> T cells from healthy donors were isolated by magnetic negative selection using the CD8<sup>+</sup> T cell Isolation Kit (Miltenyi) and activated/expanded in AIM V/5% human AB with anti-CD3/CD28 beads (ThermoFisher Scientific) and 20 ng/ml IL-2 for 4 days prior to transduction, as previously described<sup>32</sup>. Transduced T cells were subsequently expanded in IL-2 (20 ng/ml) prior to use.

## **Immunohistochemistry**

For hematoxylin and eosin (H&E) images, ATOs were embedded in Histogel (ThermoFisher Scientific, Grand Island, NY) and fixed overnight in 10% neutral-buffered formalin (ThermoFisher Scientific, Grand Island, NY). 5  $\mu$ m sections and H&E staining were performed by the UCLA Translational Pathology Core Laboratory (TPCL). For immunofluorescence imaging, ATOs were isolated by cutting the culture insert around each ATO with a scalpel, followed by embedding the membrane and ATO in Tissue-Tek OCT (VWR Radnor, PA) and freezing on dry ice. 5  $\mu$ m frozen sections were fixed in 10% neutral-buffered formalin and stained with anti-CD3 (clone UCHT1; Biolegend, San Diego, CA) at a 1:50 dilution overnight at 4°C followed by incubation with AlexaFluor 594-conjugated anti-mouse IgG (H+L) (Jackson ImmunoResearch, West Grove, PA) at room temperature. H&E and immunofluorescence images were acquired on a Zeiss AxioImager M2 with AxioCam MRM and AxioVision software (Zeiss, Jena, Germany).

### **T cell cytokine assays**

Mature CD8SP or CD4SP cells from ATOs were isolated by magnetic negative selection using the CD8+ or CD4+ Isolation Kits (Miltenyi) and sorted by FACS to further deplete CD45RO+ cells (containing immature naïve T cells and CD4ISP precursors). Purified T cell populations were plated in 96-well U-bottom plates in 200  $\mu$ l AIM V (ThermoFisher Scientific, Grand Island, NY) with 5% human AB serum (Gemini Bio-Products, West Sacramento, CA). PMA/ionomycin/protein transport inhibitor cocktail or control protein transport inhibitor cocktail (eBioscience, San Diego, CA) were added to each well and incubated for 6h. Cells were stained for CD3, CD4, and CD8 (Biolegend, San Diego, CA) and UV455 fixable viability dye (eBioscience, San Diego, CA) prior to fixation and permeabilization with an intracellular

staining buffer kit (eBioscience, San Diego, CA) and intracellular staining with antibodies against IFN $\gamma$ , TNF $\alpha$ , IL-2, IL-4, or IL-17A (Biolegend, San Diego, CA).

### **T cell activation and proliferation assays**

For CFSE proliferation assays, ATO-derived CD8SP or CD4SP T cells were isolated by negative selection MACS as above (with further FACS purification of CD4SP T cells as described above) and labeled with 5  $\mu$ M CFSE (Biolegend, San Diego, CA). Labeled cells were incubated with anti-CD3/CD28 beads (ThermoFisher Scientific, Grand Island, NY) in AIM V/5% human AB serum with 20 ng/ml rhIL-2 (Peprotech, Rocky Hill, NJ), co-stained for CD25 or 4-1BB (Biolegend, San Diego, CA) and analyzed by flow cytometry on day 5. In some experiments CFSE was substituted for CellTrace Violet (CTV; ThermoFisher) with labeling per the manufacturer's protocol. For *in vitro* cell expansion assays,  $5 \times 10^3$ – $1 \times 10^4$  ATO-derived CD8SP or CD4SP T cells isolated as above were plated in 96-well U-bottom plates in 200  $\mu$ l, and activated/expanded with anti-CD3/28 beads and either 20 ng/mL IL-2 or 5 ng/mL IL-7 and 5 ng/mL IL-15 (Peprotech). Beads were removed on day 4, and fresh medium and cytokines were added every 2–3 days with replating into larger wells as needed. Cells were counted weekly with a hemacytometer. In some experiments, cells were restimulated with fresh anti-CD3/CD28 beads on day 14.

### **Artificial APC (aAPC) CTL priming assay**

$1 \times 10^5$  total ATO-derived CD8SP T cells were isolated from week 6 TCR-transduced ATOs by MACS, as above, and co-cultured with K562-derived aAPCs expressing CD80 and single chain trimers of either HLA-A\*02:01/B2M/NY-ESO-1<sub>157-165</sub> or HLA-A\*02:01/B2M/MART-1<sub>26-350</sub> parental K562 cells in 96-well U-bottom plates in 200  $\mu$ l AIM V/5% human AB serum at

a 2:1 T cell:APC ratio for 6h. CD107a-APC antibody (Biolegend, San Diego, CA) was added to wells at a 1:50 final dilution together with a protein transport inhibitor cocktail (eBioscience, San Diego, CA) for the duration of culture. Cells were then stained for surface markers, fixed, permeabilized, and intracellularly stained for cytokines as described above.

### **TCR V $\beta$ phenotypic analysis**

Total cells from pooled week 7 ATOs or postnatal thymi were stained for CD3, CD4, CD8, and TCR $\gamma\delta$ , in conjunction with the IOTest Beta Mark TCR V Kit (Beckman Coulter, Indianapolis, IN). CD3+TCR $\gamma\delta$ -CD8+CD4<sup>-</sup> cells were gated for analysis and V $\beta$  family usage was determined by percent FITC<sup>+</sup>, PE<sup>+</sup>, or FITC+PE<sup>+</sup> cells, representing 3 different V $\beta$  antibodies per tube. For V $\beta$  analysis of TCR-transduced ATOs, total cells from week 6–7 ATOs were additionally labeled with an APC-conjugated HLA-A\*02:01/NY-ESO-1<sub>157-165</sub> tetramer (MBL International, Woburn, MA) for 10 minutes prior to surface antibody staining, and cells were gated on CD3+TCR $\gamma\delta$ -tetramer+CD8+CD4<sup>-</sup> for V $\beta$  analysis.

### **TCR repertoire sequencing**

Total RNA was purified from 40,000–200,000 FACS sorted ATO or thymic CD3+TCR $\alpha\beta$ +CD8<sup>SP</sup>, or PB CD3+TCR $\alpha\beta$ +CD8+CD45<sup>RO</sup>-CCR7<sup>+</sup> naïve CD8<sup>+</sup> T cells using the RNeasy Micro kit (Qiagen) according to manufacturer's instructions. RNA concentration and quality was determined using the Agilent RNA 6000 Nano chip. A targeted cDNA library comprising rearranged TCR variable genes was prepared by 5'-RACE using the SMARTer PCR cDNA Synthesis kit (Clontech) with modifications as follow. First strand cDNA was prepared from 3.5–500 ng total RNA using the manufacturer's protocol but substituting a poly-dT primer (5'-T30VN-3'). Double-stranded TCR $\alpha$  and TCR $\beta$  cDNA libraries were

prepared separately by semi-nested PCR using the Advantage 2 PCR kit (Clontech). Initial amplification of TCR $\alpha$  cDNA used 0.5  $\mu$ L first-strand reaction (= 2.5  $\mu$ L of 1:5 dilution in TE) with the manufacturer's forward Universal Primer Mix and a pair of reverse primers that bound *TRAC* (5'-GCCACAGCACTGTTGCTCTTGAAGTCC-3'). Semi-nested amplification of TCR $\alpha$  cDNA was conducted with manufacturer's forward Primer IIA and barcoded reverse primers that bound *TRAC* (5'-X5GGCAGGGTCAGGGTTCTGGAT-3', where X5 is a 5-nt sample-specific barcode enabling sample pooling prior to deep-sequencing). Amplification of TCR $\beta$  cDNA was similar but initial amplification was performed with a reverse primer that bound *TRBC* (5'-CCACCAGCTCAGCTCCACGTG-3') and semi-nested amplification was conducted with barcoded primers that bound *TRBC* (5'-X5GGGAACACSTTKTTCAGGTCCTC-3'). TCR $\alpha$  and TCR $\beta$  cDNA preparations were cleaned up using the DNA Clean and Concentrator-5 kit (Zymo Research). TCR $\alpha$  and TCR $\beta$  cDNA preparations from up to ten samples were pooled prior to Illumina adaptor ligation and 2  $\times$  150-bp paired-end sequencing on the MiSeq sequencer (Illumina). TCR rearrangements were identified by aligning reads that included the CDR3 to a custom reference sequence library comprising all human TRAV, TRAJ, TRBV, TRBD, and TRBJ sequences contained in the IMGT database<sup>48</sup>. After de-multiplexing using sample-specific barcodes, reads were aligned to a custom reference database comprising all possible combinations of human *TRAV*, *TRAJ*, *TRBV*, *TRBD*, and *TRBJ* sequences downloaded from the IMGT database<sup>48</sup> using BLAT<sup>49</sup>. Best BLAT hits were identified with the pslCDnaFilter utility of the BLAT suite using '-maxAligns=1 -ignoreIntrons' options and clonotype frequencies were calculated using custom Perl scripts (available upon request).

### ***In vitro* cytotoxicity assays**

CD8SP T cells were isolated from pooled ATOs as described above and were activated in 96 well round-bottom plates in AIM V/5% human AB serum with anti-CD3/CD28 beads (ThermoFisher Scientific) and 20 ng/ml IL-2 for 36h. For extended expansions, cells were cultured in IL-2 for up to 14 days. For cytotoxicity assays, 2-fold serial dilutions of T cells were plated in 96 well round bottom plates starting at  $1 \times 10^5$  cells per well in AIM V/5% human AB serum. K562 target cells transduced with HLA-A\*02:01/NY-ESO-1<sub>157-165</sub> or HLA-A\*02:01/MART-1<sub>26-35</sub> single chain trimers, or U266 multiple myeloma cells were plated at  $5 \times 10^4$  cells per well. Apoptotic cell death of target cells was quantified by Annexin V/DAPI staining at 9h. Percent antigen-specific T cells was determined by tetramer staining at the start of assays, and used to retrospectively calculate the effector:target (E:T) ratio of each well. T-cell specific cell death was calculated by subtracting percent Annexin V+ target cells in wells receiving no T cells from wells that received T cells.

### ***In vivo* tumor assays**

All animal experiments were conducted under a protocol approved by the UCLA Chancellor's Animal Research Committee. 4–6 week old male NOD.Cg-Prkdcscid Il2rgtm1Wjl/SzJ (NSG) mice (Jackson Laboratory, Bar Harbor, Maine) were subcutaneously implanted with  $2 \times 10^5$  K562 target cells transduced with a HLA-A\*02:01/NY-ESO-1<sub>157-165</sub> single chain trimer and firefly luciferase (as described above). Mice were imaged for tumor bioluminescence on day 3 by intraperitoneal injection of luciferin. ATO-derived CD8SP T cells were isolated and activated/expanded as above for 14 days.  $5.7 \times 10^6$  T cells (containing  $4.5 \times 10^6$  antigen-specific T cells as determined by tetramer staining on the day of injection) were injected via retro-orbital vein on day 3 post tumor implantation. Injection of PBS into control mice was also

performed. Tumor bioluminescence was repeated every 3–4 days for at least 21 days, after which mice were sacrificed based on disease burden criteria.

### **Flow Cytometry and Antibodies**

All flow cytometry stains were performed in PBS/0.5% BSA/2 mM EDTA for 30 min on ice. FcX (Biolegend, San Diego, CA) was added to all samples for 5 min prior to antibody staining. For tetramer co-staining, PE or APC-conjugated HLA-A\*02:01/NY-ESO-1<sub>157-165</sub> or HLA-A\*02:01/MART-1<sub>26-35</sub> tetramers (MBL International, Woburn, MA) were added to cells at a 1:50 final dilution at room temperature for 10 minutes prior to addition of antibodies for an additional 20 minutes on ice. DAPI was added to all samples prior to analysis. Analysis was performed on an LSRII Fortessa, and FACS on an ARIA or ARIA-H instrument (BD Biosciences, San Jose, CA) at the UCLA Broad Stem Cell Research Center Flow Cytometry Core. For all analyses DAPI+ cells were gated out, and single cells were gated based on FSC-H vs. FSC-W and SSC-H vs. SSC-W. Antibody clones used for surface and intracellular staining were obtained from Biolegend (San Diego, CA): CD1a (HI149), CD3 (UCHT1), CD4 (RPA-T4), CD5 (UCHT2), CD8 (SK1), CD10 (6H6), CD14 (M5E2), CD19 (HIB19), CD24 (ML5), CD25 (BC96), CD27 (O323), CD28 (CD28.2), CD31 (WM59), CD34 (581), CD38 (HIT2), CD45 (HI30), CD45RA (HI100), CD45RO (UCHL1), CD56 (HCD56), CD107a (H4A3), CD127 (A019D5), CD235a (HI264), CCR7 (G043H7), HLA-A2 (BB7.2), interferon  $\gamma$  (4S.B3), IL-2 (MQ1-17H12), IL-4 (MP4-25D2), IL-17A (BL168), TCR $\alpha\beta$  (IP26), TCR $\gamma\delta$  (B1), TNF $\alpha$  (Mab11), V $\beta$ 13.1 (H131), human lineage cocktail (CD3, CD14, CD19, CD20, CD56); and BD Biosciences (San Jose, CA): CD7 (M-T701), and CD62L (DREG-56).

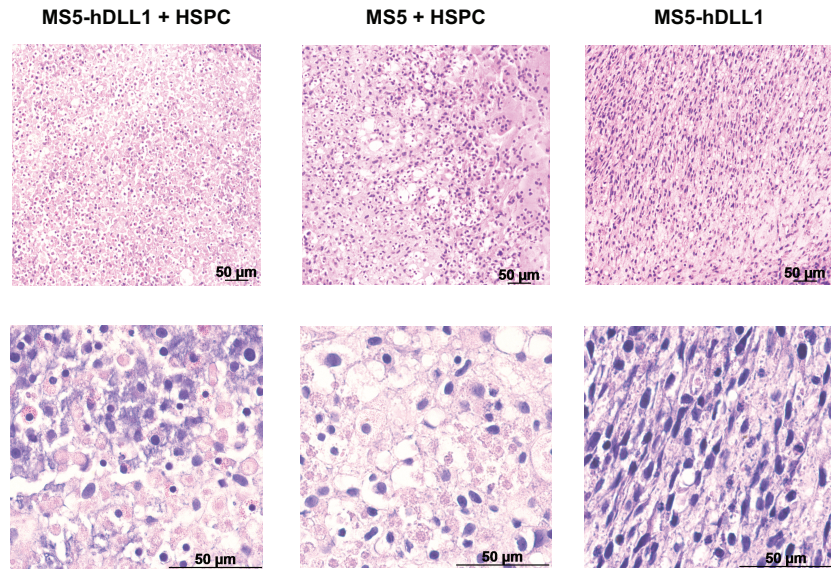
### Statistical Analysis

For Fig. 6c and Fig. 6i, statistics were analyzed using a two-tailed unpaired  $t$  test.

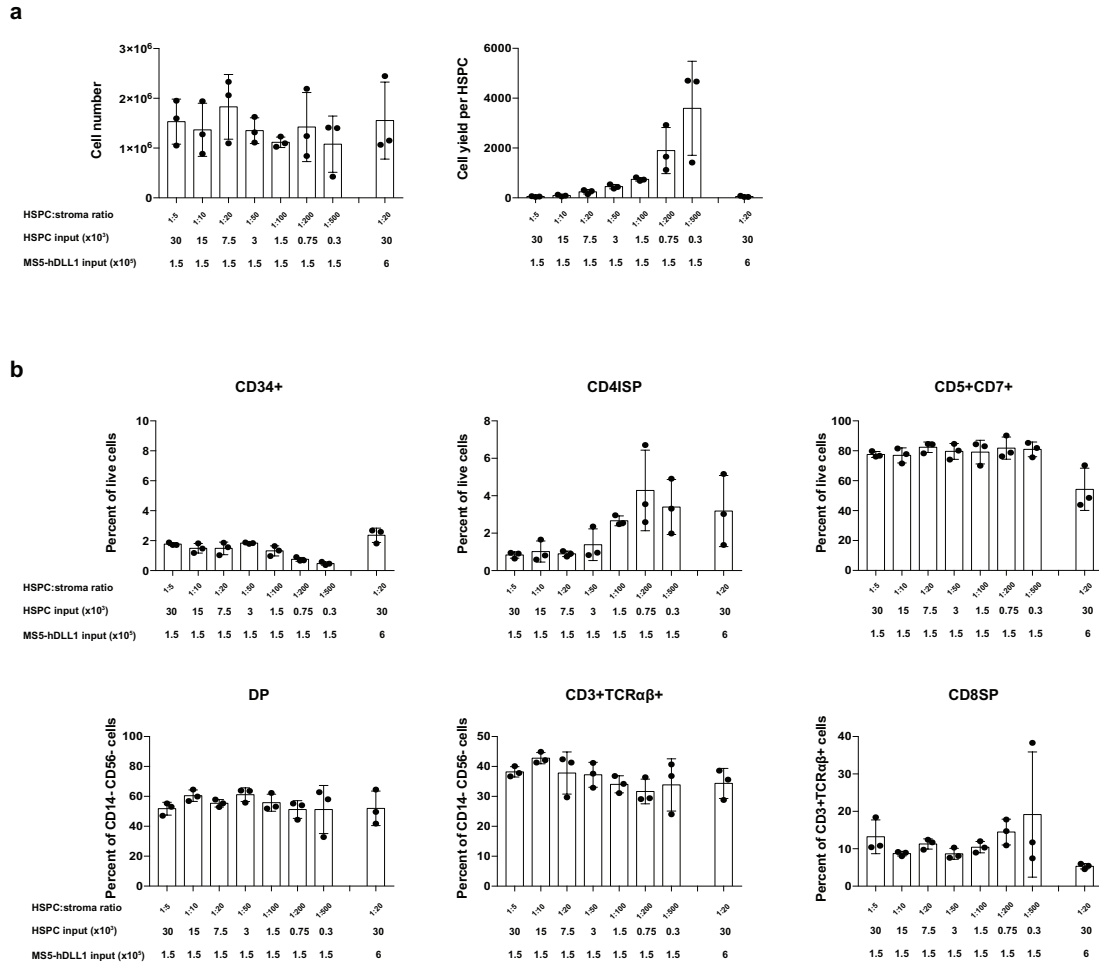
Exact  $n$  values for all experiments are specified in figure legends.



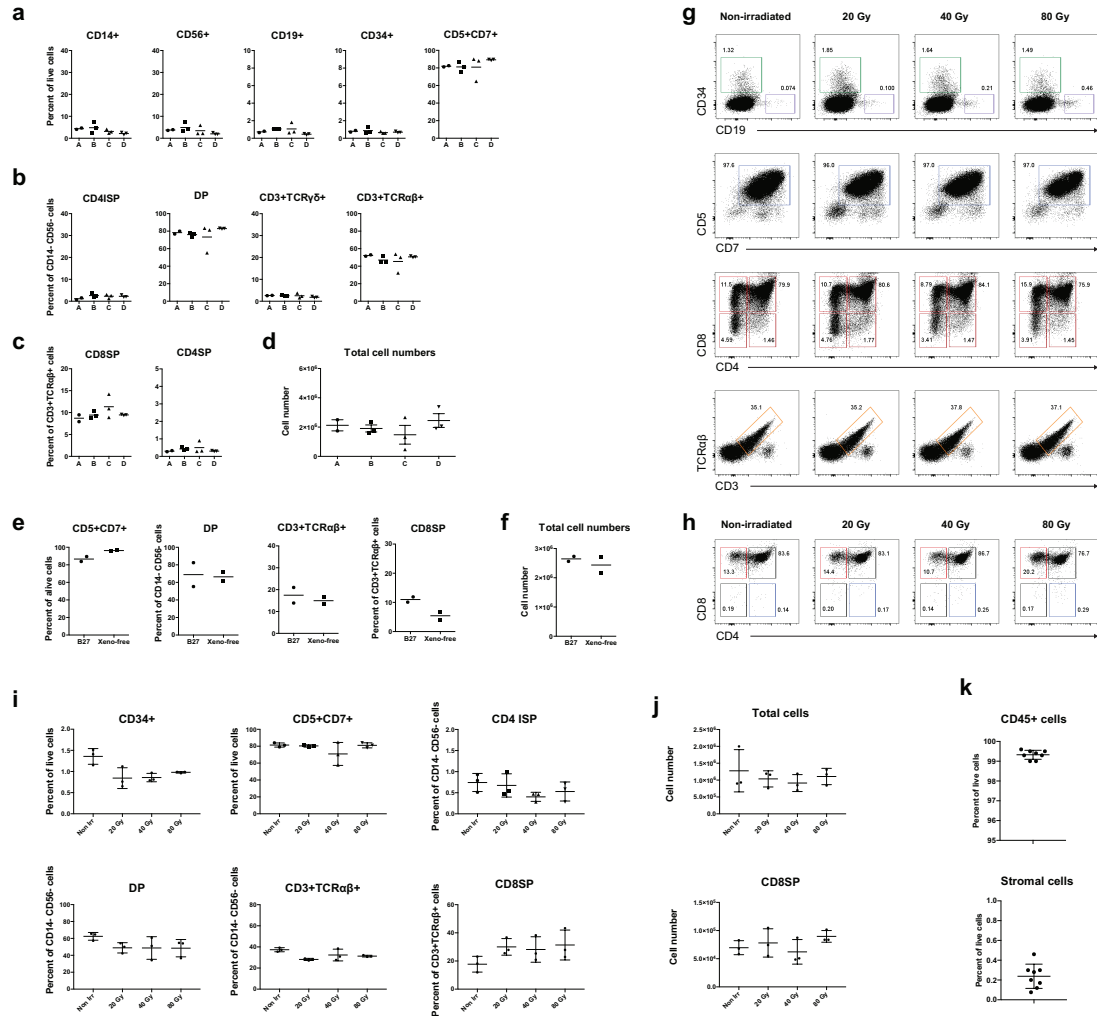
## Supplementary Figures



**Supplementary Figure 2-1: ATOs form solid tissue-like structures.** Hematoxylin and eosin staining showing tissue architecture of week 6 3D cultures generated with CB HSPCs and MS5-hDLL1 (i.e. ATO) (left), parental MS-5 cells (center), or MS5-hDLL1 cells alone (right). Magnification is 100X (top row) or 400X (bottom row).

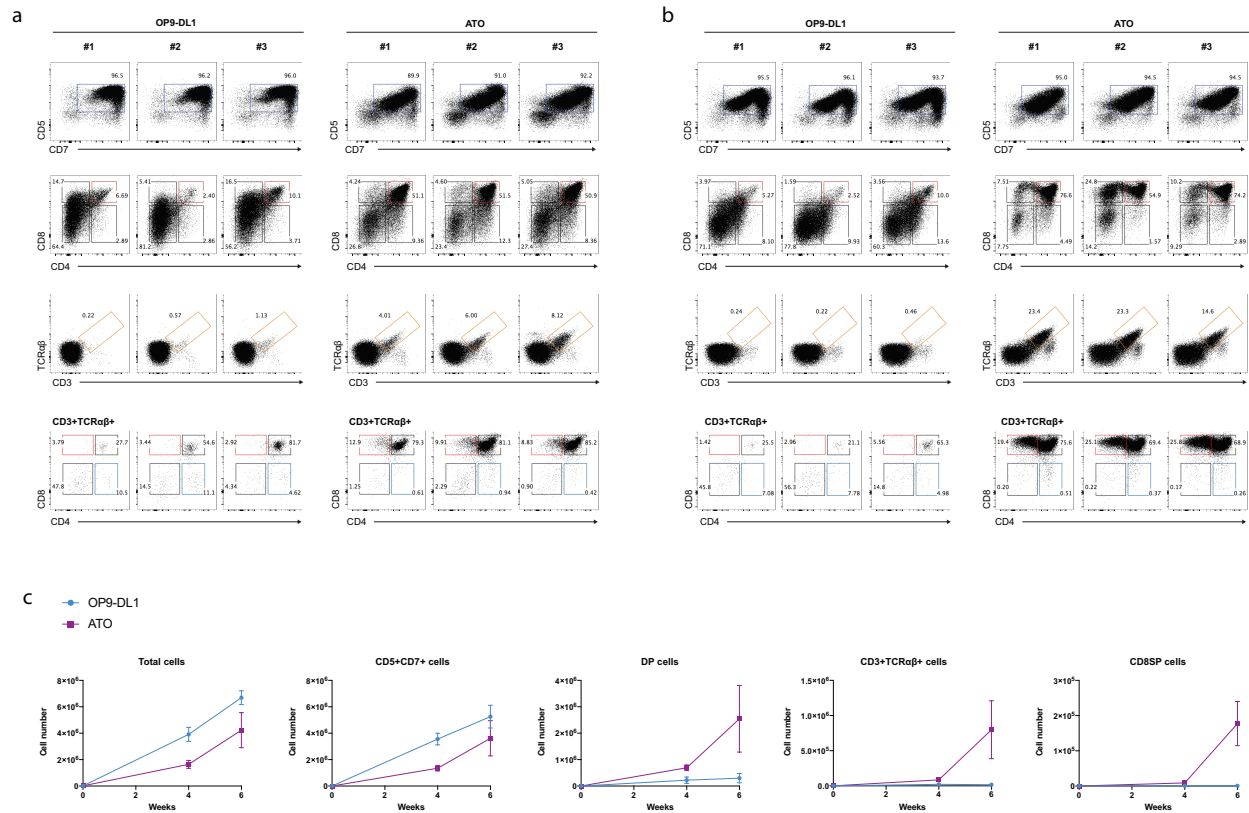


**Supplementary Figure 2-2: The effect of cell number on T cell differentiation in ATOs.** The starting number of HSPCs per ATO affects cell yield per HSPC but not the total cell output or T cell differentiation. (a) Total cell number and yield per input HSPC in week 6 ATOs generated with varying numbers of CD34+CD3- CB HSPCs (0.3- 30x10<sup>3</sup> per ATO) and a constant number of MS5-hDLL1 stromal cells (1.5x10<sup>5</sup> per ATO). Comparison is shown at far right of each graph with larger ATOs (using 30x10<sup>3</sup> HSPC and 6x10<sup>5</sup> stromal cells, at a ratio of 1:20). (b) T cell precursor and mature T cell frequencies in ATOs as described in (a). Mean and SD of triplicate ATOs are shown. Data are representative of two independent experiments.

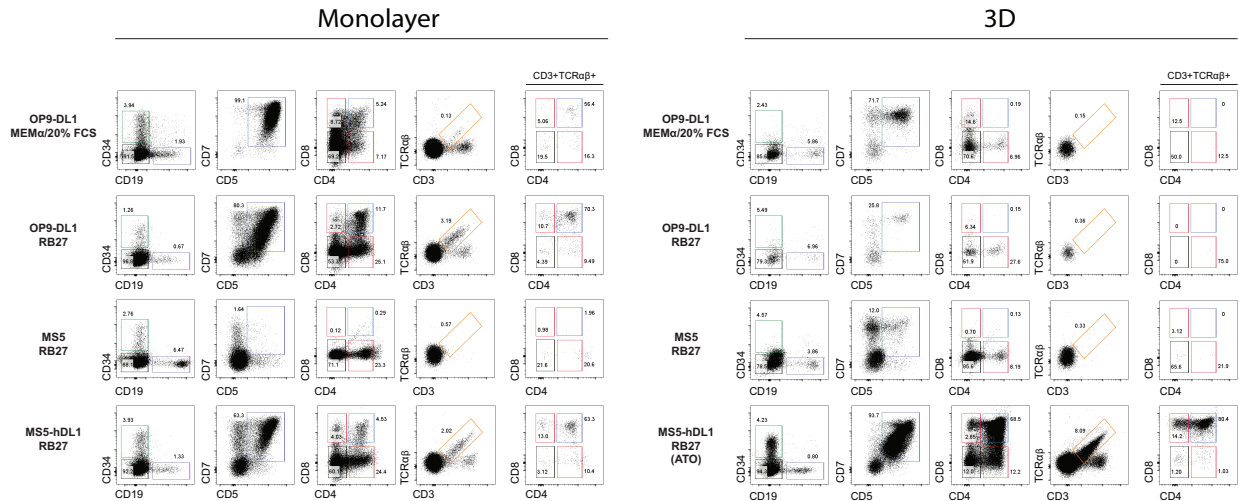


**Supplementary Figure 2-3: T cell differentiation in ATOs is independent of B27 lot and stromal cell irradiation.**

T cell differentiation in ATOs is highly reproducible and not affected by B27 lot variation, xeno-free B27 or stromal irradiation. No significant effect of B27 lot variation on (a) T-lineage commitment, (b-c) T cell differentiation, or (d) total cell numbers in week 6 ATOs generated from a single CB ( $7.5 \times 10^3$  CD34+CD3- HSPCs per ATO) and cultured using 4 different lots of B27 supplement (labeled A-D). Replicate ATOs ( $n=2-3$ ) are shown for each B27 lot. Substitution of standard B27 with xeno-free B27 had no significant impact on (e) T cell differentiation or (f) total cell numbers in week 6 ATOs. Irradiation of MS5-hDLL1 stromal cells with 20-80 Gy prior to ATO generation had little impact on (g-i) T cell differentiation, or (j) numbers of total cells and CD3+TCR $\alpha\beta$ +CD8SP T cells. Mean and SD of triplicate ATOs are shown. Data are representative of two individual experiments. Flow plots in (h) show cells from CD3+TCR $\alpha\beta$ + gate shown in (g). (k) Harvesting cells from ATOs by mechanical disruption at 6 weeks resulted in a suspension of >99% human hematopoietic CD45+ cells (top), and <0.5% GFP+ stromal cells (bottom). Frequencies are shown for 8 independent experiments (error bars represent SD).

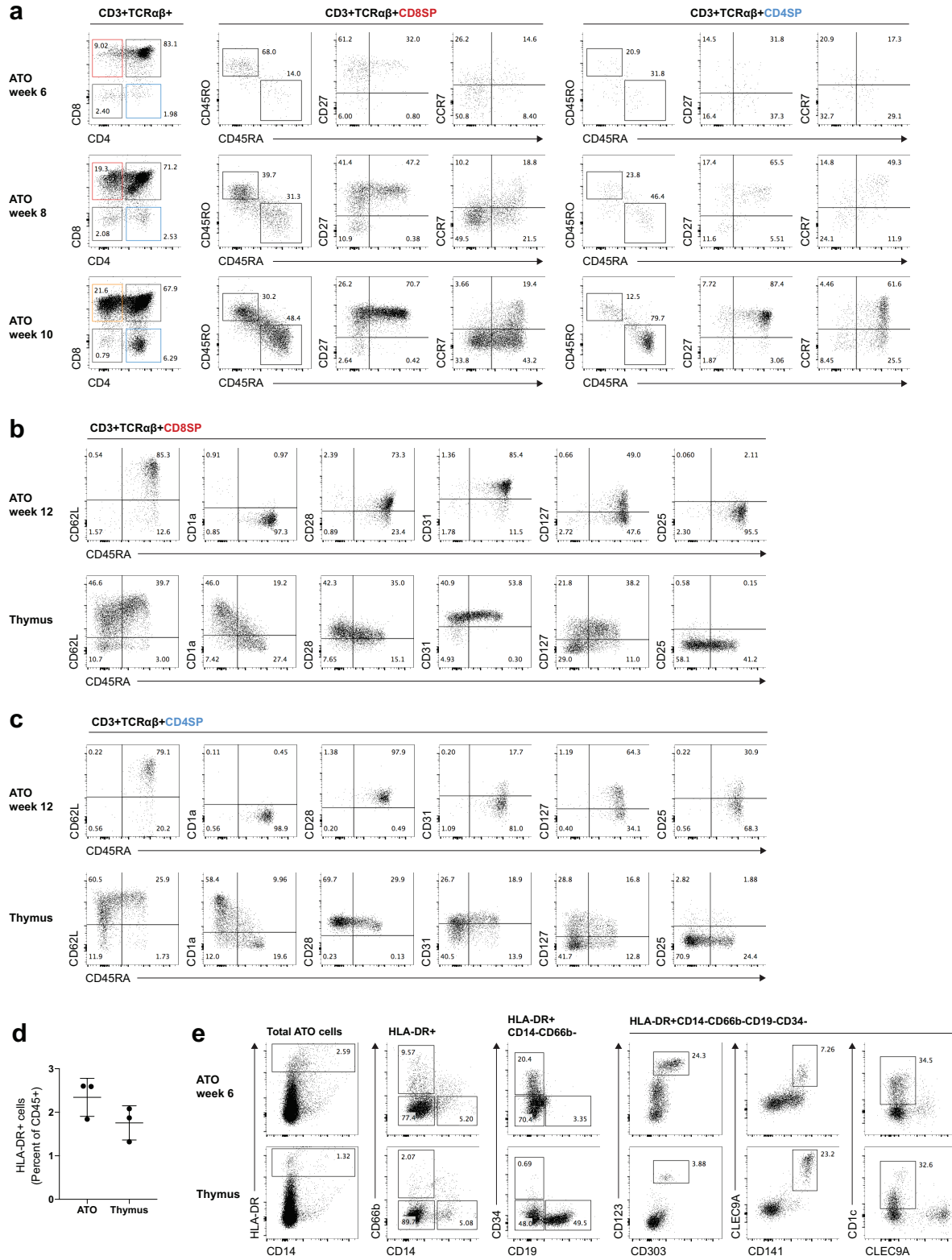


**Supplementary Figure 2-4: Enhanced T cell positive selection and maturation in ATOs compared with OP9-DL1 monolayer co-cultures.** Full flow cytometry data for Fig. 2a is provided, showing T cell differentiation from three different cord blood donors (#1, #2 and #3) at (a) 4 weeks and (b) 6 weeks. ATO and OP9-DL1 cultures were started in parallel with CD34+CD3- HSPCs from the same cord blood units. Cells are gated on total CD14-CD56- cells or CD3+TCRαβ+ T cells as indicated. (c) Absolute cell numbers of T cell subsets at week 4 and 6 in OP9-DL1 co-cultures versus ATOs using the gating strategy shown in (a) and (b). Each OP9-DL1 culture was initiated with  $1.5 \times 10^4$  CD34+CD3- CB HSPCs cells, and each ATO was initiated with  $7.5 \times 10^3$  HSPCs from the same cord blood unit, with technical duplicate ATOs harvested and pooled at the indicated times for comparison of cell counts. Bars represent the mean and SD of three independent experiments.

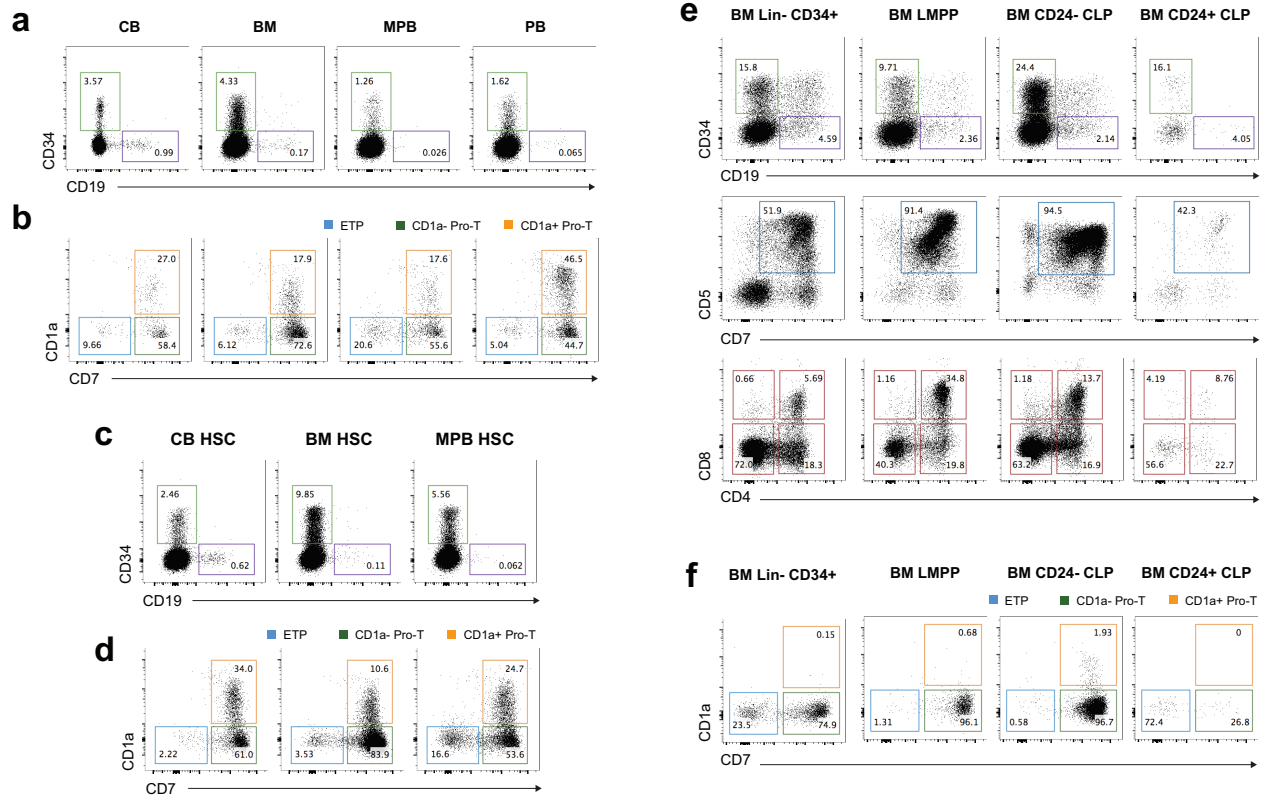


**Supplementary Figure 2-5: Enhanced positive selection in ATOs requires 3D structure and optimal cell line and culture medium.** Enhanced T cell positive selection and maturation in ATOs (defined as MS5-hDLL1 in 3D culture with RB27) compared with monolayer co-cultures. Week 6 monolayer cultures (left) were compared with 3D organoid cultures (right) and included crossover comparisons with either MS5-DL1 or OP9-DL1 cells and RB27 medium or OP9-DL1 standard medium as indicated. Standard medium for OP9-DL1 co-cultures was MEMα/20%FCS with IL-7, FLT3L, and ascorbic acid, and standard medium for ATOs was RB27 with IL-7, FLT3L, and ascorbic acid, as described in Methods. Monolayer or 3D cultures using the parental MS-5 cell line (not transduced with DLL1) are also shown as a negative control. All plots are gated on CD14-CD56- cells or (where indicated) CD3+TCRαβ+ subgates.

**Fig. S6**

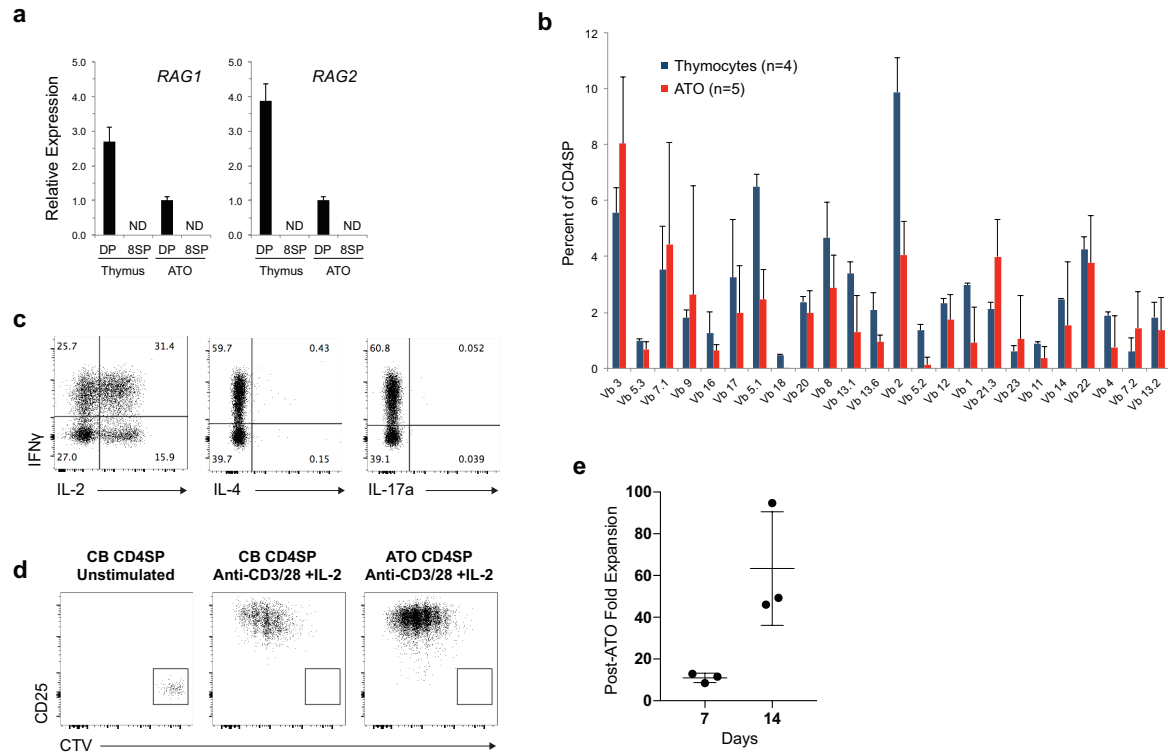


**Supplementary Figure 2-6: Recapitulation of thymopoiesis and naive T cell phenotype in ATOs.** (a) Progressive differentiation of naïve CD3+TCRαβ+CD8SP and CD3+TCRαβ+CD4SP cells in ATOs between weeks 6-10. ATOs were cultured in parallel using CB HSPCs from a single donor and analyzed at the indicated weeks. Cells are gated on CD14-CD56- TCRαβ+CD3+ cells, and sequential sub-gates (CD8SP or CD4SP) are indicated above plots. The corresponding week 12 timepoint is shown in Fig. 2. (b,c) Additional markers characterizing the phenotype of week 12 ATO-derived CD3+TCRαβ+ (b) CD8SP and (c) CD4SP T cells compared with corresponding populations in the human thymus (see also Fig. 2). (d) Frequency of HLA-DR+ cells in CB ATOs compared with postnatal thymi (gated on total CD45+ cells). (e) Multiple HLA-DR+ antigen presenting cell (APC) populations are present in week 6 ATOs. Sequential gates are shown above each plot. HLA-DR+ populations include monocytes (CD14+), granulocytes (CD66b+), B cells (CD19+), HSPCs (CD34+), plasmacytoid DC (CD303+CD123+), CLEC9A+ DC (CD141+CLEC9A+), and CD1c+ DC (CD1c+CLEC9A-). Paired analysis from a postnatal thymus is shown for comparison. Data in (d) and (e) are representative of three independent experiments.

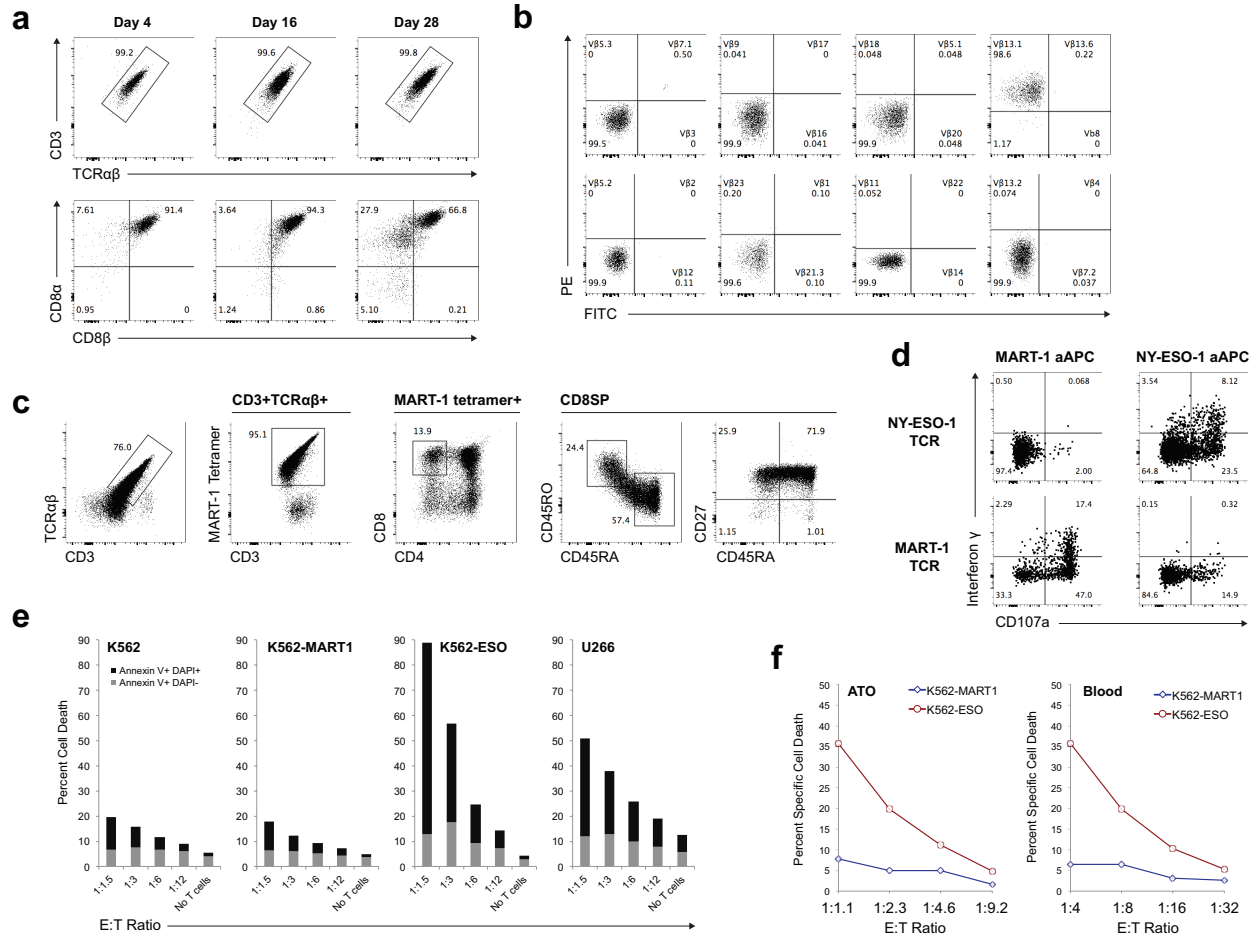


**Supplementary Figure 2-7: Generation of T cells from multiple HSPC sources and subsets.** (a) Persistence of CD34<sup>+</sup> cells in week 6 ATOs initiated with human cord blood (CB), adult bone marrow (BM), G-CSF mobilized peripheral blood (MPB), or non-mobilized peripheral blood (PB) HSPCs. (b) T cell progenitor subsets in ATOs from different HSPC sources, gated on CD34<sup>+</sup> cells as shown in (a). (c) CD34<sup>+</sup> progenitors and (d) CD34<sup>+</sup> progenitor subsets in week 6 ATOs initiated with hematopoietic stem cell (HSC)-enriched (Lin-CD34<sup>+</sup>CD38<sup>-</sup>) fractions from the tissue sources shown. (e, f) Early onset of T cell commitment from LMPP and CD24<sup>-</sup>CLP in 3 week ATOs revealed by (e) early appearance of DP and (f) T cell committed CD34<sup>+</sup>CD7<sup>+</sup> progenitors. Data are representative of two independent experiments.





**Supplementary Figure 2-8: TCR diversity and functional validation of ATO-derived CD4<sup>+</sup> T cells.** (a) Similar to human thymocytes, RAG1 and RAG2 are expressed in ATO-derived CD3<sup>+</sup>CD4<sup>+</sup>CD8<sup>+</sup> (DP) but not mature CD3<sup>+</sup>CD8<sup>+</sup>SP T cells. Quantitative RT-PCR for RAG1 and RAG2 are shown relative to expression of B2M in FACS sorted ATO-derived versus postnatal thymus T cell populations. Mean and SD of triplicate reactions is shown. (b) Generation of TCR diversity in CD3<sup>+</sup>TCR $\alpha\beta$ <sup>+</sup>CD4<sup>+</sup>SP T cells isolated from week 7 ATOs (n=5) or human thymi (n=4), as shown by flow cytometric analysis of the frequency of TCR V $\beta$  family expression. (c) Cytokine production by week 12 ATO-derived CD4<sup>+</sup>SP T cells treated with PMA/ionomycin for 6h. Data are representative of two independent experiments. (d) Proliferation (CTV dilution) and activation (upregulation of CD25) of cord blood (CB) and ATO-derived (week 12) CD4<sup>+</sup>SP T cells after 5 days in response to anti-CD3/CD28 and IL-2. Data are representative of two individual experiments. (e) Post-ATO expansion of ATO-derived CD4<sup>+</sup>SP T cells relative to starting cell number in response to anti-CD3/CD28 and IL-2 after 7 and 14 days. Mean and SD of technical triplicates are shown.



**Supplementary Figure 2-9: Differentiation and allelic exclusion of TCR-engineered T cells in ATOs.** (a) ATO-derived TCR-engineered T cells retain a conventional T cell phenotype despite expansion and re-stimulation. CB HSPCs were transduced with an HLA-A\*0201/NY-ESO-1157-165 specific TCR and then cultured in ATOs. After 6 weeks, CD8SP T cells were isolated from ATOs and activated with anti-CD3/28 beads + IL-2, expanded in IL-2, and re-stimulated with anti-CD3/28 beads on day 14. Preserved surface co-expression of CD8α and CD8β was confirmed by flow cytometry. Data are representative of two independent experiments. (b) Flow cytometric Vβ analysis of CD3+TCRαβ+tetramer+CD8SP T cells from TCR-transduced CB ATOs. Data are representative of 5 independent experiments (shown in graphical form in Fig. 5g). (c) Generation of TCR-engineered T cells from TCR-transduced CB HSPCs in ATOs using an HLA-A\*02:01/MART126-35 specific TCR. Differentiation at week 6 is shown (gated on total CD14-CD56- ATO cells, with sequential gates shown above each plot). Data are representative of two independent experiments. (d) Antigen-specific priming of MART1-specific and NY-ESO-1-specific ATO-derived TCR-engineered T cells by artificial antigen presenting cells (aAPCs) that express CD80 and a HLA-A\*02:01 single chain trimer presenting

either MART126-35 or NY-ESO1156-165 peptide. CD107a membrane mobilization and intracellular IFN  $\gamma$  staining at 6h is shown. (e) In vitro cytotoxicity of ATO-derived TCR-engineered T cells against antigen-positive tumor cells. Frequencies of early (annexin V+ DAPI-) or late (annexin V+ DAPI+) apoptotic tumor cells was determined by flow cytometry at 9h (data are summarized in Fig 6h). (f) Retained antigen specificity following prolonged post-ATO activation/expansion of T cells. CD8SP T cells isolated from TCR-transduced ATOs were expanded for 14 days with anti-CD3/28 and IL-2, and cytotoxicity assays performed as described in panel (f) and Fig. 6h. Assays using TCR-transduced peripheral blood CD8+ donor T cells expanded for 14 days under the same conditions are shown for comparison.

## REFERENCES

1. Schmitt TM, Zúñiga-Pflücker JC. Induction of T Cell Development from Hematopoietic Progenitor Cells by Delta-like-1 In Vitro. *Immunity*. 2002;17:749–756.
2. De Smedt M, Hoebeke I, Plum J. Human bone marrow CD34+ progenitor cells mature to T cells on OP9-DL1 stromal cell line without thymus microenvironment. *Blood Cells Mol Dis*. 2004;33:227–232
3. La Motte-Mohs RN, Herer E, Zuniga-Pflucker JC. Induction of T-cell development from human cord blood hematopoietic stem cells by Delta-like 1 in vitro. *Blood*. 2005;105:1431–1439.
4. de Pooter R, Zúñiga-Pflücker JC. T-cell potential and development in vitro: the OP9-DL1 approach. *Current Opinion in Immunology*. 2007;19:163–168.
5. Awong G, Herer E, La Motte-Mohs RN, Zuniga-Pflucker JC. Human CD8 T cells generated in vitro from hematopoietic stem cells are functionally mature. *BMC Immunol*. 2011;12:22.
6. Van Coppenolle S, et al. Functionally mature CD4 and CD8 TCRalpha/beta cells are generated in OP9-DL1 cultures from human CD34+ hematopoietic cells. *Journal of immunology (Baltimore, Md : 1950)* 2009;183:4859–4870.
7. Hao QL, et al. Human intrathymic lineage commitment is marked by differential CD7 expression: identification of CD7- lympho-myeloid thymic progenitors. *Blood*. 2008;111:1318–1326.
8. De Smedt M, et al. T-lymphoid differentiation potential measured in vitro is higher in CD34+CD38-/lo hematopoietic stem cells from umbilical cord blood than from bone marrow and is an intrinsic property of the cells. *Haematologica*. 2011;96:646.

9. Anderson G, Jenkinson EJ, Moore NC, Owen JJT. MHC class II-positive epithelium and mesenchyme cells are both required for T-cell development in the thymus. *Nature*. 1993;362:70–73.
10. Plum J, De Smedt M, Defresne M, Leclercq G, Vandekerckhove B. Human CD34+ fetal liver stem cells differentiate to T cells in a mouse thymic microenvironment. *Blood*. 1994;84:1587–1593.
11. Poznansky MC, et al. Efficient generation of human T cells from a tissue-engineered thymic organoid. *Nat Biotech*. 2000;18:729–734.
12. Chung B, et al. Engineering the human thymic microenvironment to support thymopoiesis in vivo. *Stem Cells*. 2014;32:2386–2396.
13. Awong G, Motte-Mohs RNL, Zúñiga-Pflücker JC. In Vitro Human T Cell Development Directed by Notch–Ligand Interactions. In: Bunting KD, editor. *Hematopoietic Stem Cell Protocols*. Humana Press; Totowa, NJ: 2008. pp. 135–142.
14. Sheridan JM, Taoudi S, Medvinsky A, Blackburn CC. A novel method for the generation of reaggregated organotypic cultures that permits juxtaposition of defined cell populations. *genesis*. 2009;47:346–351.
15. Itoh K, et al. Reproducible establishment of hemopoietic supportive stromal cell lines from murine bone marrow. *Experimental hematology*. 1989;17:145–153.
16. Brewer GJ, Torricelli JR, Evege EK, Price PJ. Optimized survival of hippocampal neurons in B27-supplemented Neurobasal, a new serum-free medium combination. *Journal of neuroscience research*. 1993;35:567–576.
17. Huijskens MJAJ, et al. Technical Advance: Ascorbic acid induces development of double-positive T cells from human hematopoietic stem cells in the absence of stromal cells. *Journal of Leukocyte Biology*. 2014;96:1165–1175.

18. Manning J, et al. Vitamin C promotes maturation of T-cells. *Antioxidants & redox signaling*. 2013;19:2054–2067.
19. Casero D, et al. Long non-coding RNA profiling of human lymphoid progenitor cells reveals transcriptional divergence of B cell and T cell lineages. *Nature immunology*. 2015;16:1282–1291.
20. Awong G, et al. Characterization in vitro and engraftment potential in vivo of human progenitor T cells generated from hematopoietic stem cells. *Blood*. 2009;114:972–982.
21. Vanhecke D, Leclercq G, Plum J, Vandekerckhove B. Characterization of distinct stages during the differentiation of human CD69+CD3+ thymocytes and identification of thymic emigrants. *Journal of immunology (Baltimore, Md : 1950)* 1995;155:1862–1872.
22. Res P, Blom B, Hori T, Weijer K, Spits H. Downregulation of CD1 marks acquisition of functional maturation of human thymocytes and defines a control point in late stages of human T cell development. *The Journal of experimental medicine*. 1997;185:141–151.
23. Kimmig S, et al. Two subsets of naive T helper cells with distinct T cell receptor excision circle content in human adult peripheral blood. *The Journal of experimental medicine*. 2002;195:789–794.
24. Hinrichs CS, et al. Adoptively transferred effector cells derived from naive rather than central memory CD8+ T cells mediate superior antitumor immunity. *Proceedings of the National Academy of Sciences of the United States of America*. 2009;106:17469–17474.
25. Restifo NP, Dudley ME, Rosenberg SA. Adoptive immunotherapy for cancer: harnessing the T cell response. *Nat Rev Immunol*. 2012;12:269–281.

26. Gurka S, Dirks S, Photiadis J, Kroczeck RA. Expression analysis of surface molecules on human thymic dendritic cells with the 10th HLDA Workshop antibody panel. *Clinical & Translational Immunology*. 2015;4:e47.
27. Martinez VG, et al. A discrete population of IFN [lambda]-expressing BDCA3hi dendritic cells is present in human thymus. *Immunol Cell Biol*. 2015;93:673–678.
28. Hao QL, Shah AJ, Thiemann FT, Smogorzewska EM, Crooks GM. A functional comparison of CD34 + CD38<sup>-</sup> cells in cord blood and bone marrow. *Blood*. 1995;86:3745–3753.
29. Kohn LA, et al. Lymphoid priming in human bone marrow begins before expression of CD10 with upregulation of L-selectin. *Nature immunology*. 2012;13:963–971.
30. Six EM, et al. A human postnatal lymphoid progenitor capable of circulating and seeding the thymus. *The Journal of experimental medicine*. 2007;204:3085–3093.
31. Galy A, Travis M, Cen D, Chen B. Human T, B, natural killer, and dendritic cells arise from a common bone marrow progenitor cell subset. *Immunity*. 1995;3:459–473.
32. Gschweng EH, et al. HSV-sr39TK positron emission tomography and suicide gene elimination of human hematopoietic stem cells and their progeny in humanized mice. *Cancer research*. 2014;74:5173–5183.
33. Snauwaert S, et al. In vitro generation of mature, naive antigen-specific CD8(+) T cells with a single T-cell receptor by agonist selection. *Leukemia*. 2014;28:830–841.
34. Giannoni F, et al. Allelic exclusion and peripheral reconstitution by TCR transgenic T cells arising from transduced human hematopoietic stem/progenitor cells. *Mol Ther*. 2013;21:1044–1054.

35. Zhao Y, et al. Extrathymic generation of tumor-specific T cells from genetically engineered human hematopoietic stem cells via Notch signaling. *Cancer research*. 2007;67:2425–2429.
36. van Lent AU, et al. Functional human antigen-specific T cells produced in vitro using retroviral T cell receptor transfer into hematopoietic progenitors. *Journal of immunology (Baltimore, Md : 1950)* 2007;179:4959–4968.
37. Gattinoni L, et al. Acquisition of full effector function in vitro paradoxically impairs the in vivo antitumor efficacy of adoptively transferred CD8+ T cells. *The Journal of clinical investigation*. 2005;115:1616–1626.
38. Hinrichs CS, Rosenberg SA. Exploiting the curative potential of adoptive T-cell therapy for cancer. *Immunological Reviews*. 2014;257:56–71. [PMC free article] [PubMed]
39. Vatakis DN, et al. Introduction of exogenous T-cell receptors into human hematopoietic progenitors results in exclusion of endogenous T-cell receptor expression. *Mol Ther*. 2013;21:1055–1063.
40. Starck L, Popp K, Pircher H, Uckert W. Immunotherapy with TCR-redirection T cells: comparison of TCR-transduced and TCR-engineered hematopoietic stem cell-derived T cells. *Journal of immunology (Baltimore, Md : 1950)* 2014;192:206–213.
41. Torikai H, et al. A foundation for universal T-cell based immunotherapy: T cells engineered to express a CD19-specific chimeric-antigen-receptor and eliminate expression of endogenous TCR. *Blood*. 2012;119:5697–5705.
42. Berdien B, Mock U, Atanackovic D, Fehse B. TALEN-mediated editing of endogenous T-cell receptors facilitates efficient reprogramming of T lymphocytes by lentiviral gene transfer. *Gene therapy*. 2014;21:539–548.



43. Poirot L, et al. Multiplex Genome-Edited T-cell Manufacturing Platform for “Off-the-Shelf” Adoptive T-cell Immunotherapies. *Cancer research*. 2015;75:3853–3864. [PubMed]
44. Themeli M, Riviere I, Sadelain M. New cell sources for T cell engineering and adoptive immunotherapy. *Cell stem cell*. 2015;16:357–366.
45. Majeti R, Park CY, Weissman IL. Identification of a hierarchy of multipotent hematopoietic progenitors in human cord blood. *Cell stem cell*. 2007;1:635–645.
46. Robbins PF, et al. Single and dual amino acid substitutions in TCR CDRs can enhance antigen-specific T cell functions. *Journal of immunology (Baltimore, Md : 1950)* 2008;180:6116–6131.
47. Johnson LA, et al. Gene Transfer of Tumor-Reactive TCR Confers Both High Avidity and Tumor Reactivity to Nonreactive Peripheral Blood Mononuclear Cells and Tumor-Infiltrating Lymphocytes. *The Journal of Immunology*. 2006;177:6548–6559. [PMC free article] [PubMed]
48. Giudicelli V, Chaume D, Lefranc MP. IMGT/GENE-DB: a comprehensive database for human and mouse immunoglobulin and T cell receptor genes. *Nucleic Acids Research*. 2005;33:D256–D261.
49. Kent WJ. BLAT—The BLAST-Like Alignment Tool. *Genome Research*. 2002;12:656–664.

## CHAPTER 3

### REGULATION OF HUMAN cDC1 (CLEC9A+) DENDRITIC CELL DIFFERENTIATION BY NOTCH SIGNALING

#### Abstract

Human cDC1 dendritic cells (DC), also known as CLEC9A+ DC, CD141+ (BDCA3+) DC, and XCR1+ DC, are a steady-state endogenous DC subset with constitutive ability to traffic to secondary lymphoid tissues, efficiently cross-present cellular antigens to T cells, and prime CD4+ and CD8+ antiviral and antitumor T cell responses. As such, cDC1 have been proposed as ideal candidates for adoptive immunotherapy, however their rarity *in vivo* and a lack of knowledge regarding their development have thus far precluded their therapeutic use.

We used *in vitro* differentiation approaches to identify a novel role for Notch signaling in positively regulating the differentiation of human cDC1 from CD34+ hematopoietic stem and progenitor cells (HSPCs) at the expense of monocyte, cDC2, and pDC differentiation. This effect of Notch signaling was cell-intrinsic and conserved across HSPCs from cord blood, bone marrow, and G-CSF mobilized peripheral blood. Mechanistically, Notch signaling skewed highly purified monocyte/dendritic cell progenitors (MDP) and common dendritic cell progenitors (CDP) to the cDC1 lineage via rapid induction of a cDC1 transcriptional program in MDPs that included upregulation of *IRF8*, *BATF3*, and *MYCL*.

Notch-induced cDC1 were similar to primary blood cDC1 based on surface marker and global gene expression profiles. They expressed *CCR7* and underwent chemotaxis in response

to CCL21, and upregulated T cell costimulatory molecules in response to TLR3 and TLR8 agonists. Functionally, Notch-induced cDC1 activated autologous T cells in an antigen-specific manner and were adept at cross-presenting necrotic cell antigens and priming naïve CD8<sup>+</sup> T cell responses.

Our data reveal a key role for Notch signaling in regulating human cDC1 differentiation, providing insight into the development of this important DC lineage in humans. Furthermore, we propose that Notch ligands may be used for the directed differentiation of large numbers of functional cDC1 from HSPCs, permitting the preclinical development of next-generation cDC1-based cellular vaccines.

## Introduction

Dendritic cells (DC) are the critical link between the innate sensing of pathogens and danger signals and the priming of adaptive T cell immunity. Due to the scarcity of DCs in the tissue and blood, the majority of both mouse and human studies investigating DC function have relied on monocyte-derived DCs (MoDC)<sup>1</sup>, which are impaired in key physiological DC traits including cross-presentation and lymph node homing<sup>2</sup>. Recent studies have revealed the identity of three main classes of bona fide endogenous DCs in humans which closely correspond to those in mice by gene and surface marker expression<sup>3, 4, 5, 6, 7</sup>. In humans, these are contained within the lineage negative (lin<sup>-</sup>) HLA-DR<sup>+</sup> mononuclear cell fraction and may be defined by specific surface markers as cDC1 (CLEC9A<sup>+</sup>CD141<sup>+</sup>), cDC2 (CLEC9a<sup>-</sup>CD141<sup>-</sup>CD1c<sup>+</sup>), and plasmacytoid DC (pDC; CD123<sup>hi</sup>CD303<sup>+</sup>)<sup>8</sup>. Of these, the cDC1 population (corresponding to CD8α<sup>+</sup> and CD103<sup>+</sup> DCs in mice<sup>5, 8, 9</sup>) has been shown to be critical for cross-presenting cellular antigens and priming anti-viral and anti-tumor T cell responses<sup>9, 10</sup>.

<sup>11, 12, 13</sup>. Subsequently, there has been great interest in using human cDC1s for adoptive immunotherapy to prime anti-tumor immunity<sup>14, 15</sup>, however their scarcity in the blood (approximately 0.03% of peripheral blood mononuclear cells; PBMCs)<sup>10</sup> has thus far precluded pre-clinical or clinical testing.

Human cDC1 develop from DC lineage-committed precursors contained within the bone marrow CD34+ hematopoietic stem and progenitor (HSPC) compartment<sup>16</sup>. While cDC1 specification may occur as early as the hematopoietic stem cell and lymphoid-primed multipotent progenitor stages<sup>17, 18</sup>, terminal differentiation appears to progress from a granulocyte-monocyte progenitor (GMP) through step-wise lineage restriction to a monocyte-DC progenitor (MDP) and finally a common DC progenitor (CDP) capable of generating cDC1, cDC2, and pDCs<sup>16</sup>. This and other studies further identified FLT3L and GM-CSF as critical cytokines supportive of human DC differentiation, however specific molecular cues regulating the development of cDC1 from HSPCs are unknown.

We report here that Notch signaling, in the presence of FLT3L and GM-CSF, induces cDC1 differentiation from HSPCs with concomitant decreases in monocyte, cDC2, and pDC differentiation. This effect was conserved across alternative Notch ligands, and across HSPCs from different tissue sources and developmental stages. Differentiation of purified DC progenitors exhibited marked skewing to cDC1 fate in the presence of a Notch ligand, and even a brief exposure was sufficient to induce in multipotent MDPs a transcriptional program consistent with cDC1 specification. HSPC-derived Notch-induced cDC1 were strikingly similar to endogenous cDC1 both transcriptionally and functionally. The identification of a role for Notch signaling in human cDC1 differentiation sheds light on factors directly regulating human cDC1 commitment, and presents a path forward for the directed differentiation of cDC1 for adoptive immunotherapy.

## Results

### **Notch signaling promotes the differentiation of human cDC1 from hematopoietic stem and progenitor cells**

Due to the expression of Notch receptors on human bone marrow DC progenitors (unpublished data), we adapted a stromal cell-based *in vitro* DC differentiation assay to examine the effect of Notch signaling on DC differentiation. The MS5 mouse stromal cell line<sup>19</sup>, which in the presence of FLT3L and GM-CSF supports the differentiation of cDC1, cDC2, and pDC<sup>16, 18</sup> was transduced with a lentiviral vector encoding the Notch ligand Delta-like ligand 1 (MS5-hDLL1, hereafter)<sup>20</sup>. DC-depleted human cord blood (CB) CD34+ HSPCs co-cultured on MS5 in the presence of SCF, TPO, FLT3L, and GM-CSF (SFTGM) for 19-21 days showed a broad distribution of monocytes, cDC1, cDC2, and pDC (Fig 1a); however co-culture on MS5-hDLL1 cells revealed striking enrichment of cDC1 (on average 66% of total CD45+ cells, compared with 6% in control MS5 cultures,  $p < 0.0001$ ), identified by co-expression of HLA-DR, CD141, and CLEC9A (Fig 1a-b). While CD66b+ granulocytes were seen in both culture conditions at similar frequencies, statistically significant decreases in the frequency of CD14+ monocytes, cDC2 (CD1c+ DC), and pDCs were observed in MS5-hDLL1 cultures, with the latter being virtually absent (Fig. 1a-b). Both increased cDC1 and decreased monocyte, cDC2, and pDC frequencies were reflected in absolute cell numbers at the end of the culture period (Fig. 1c). Kinetic analysis of hematopoietic differentiation in MS5-hDLL1 co-cultures revealed a rapid rise in cDC1 frequency starting around day 8 of culture and plateauing around day 17 (Fig. 1d), which was not observed in control MS5 cultures.

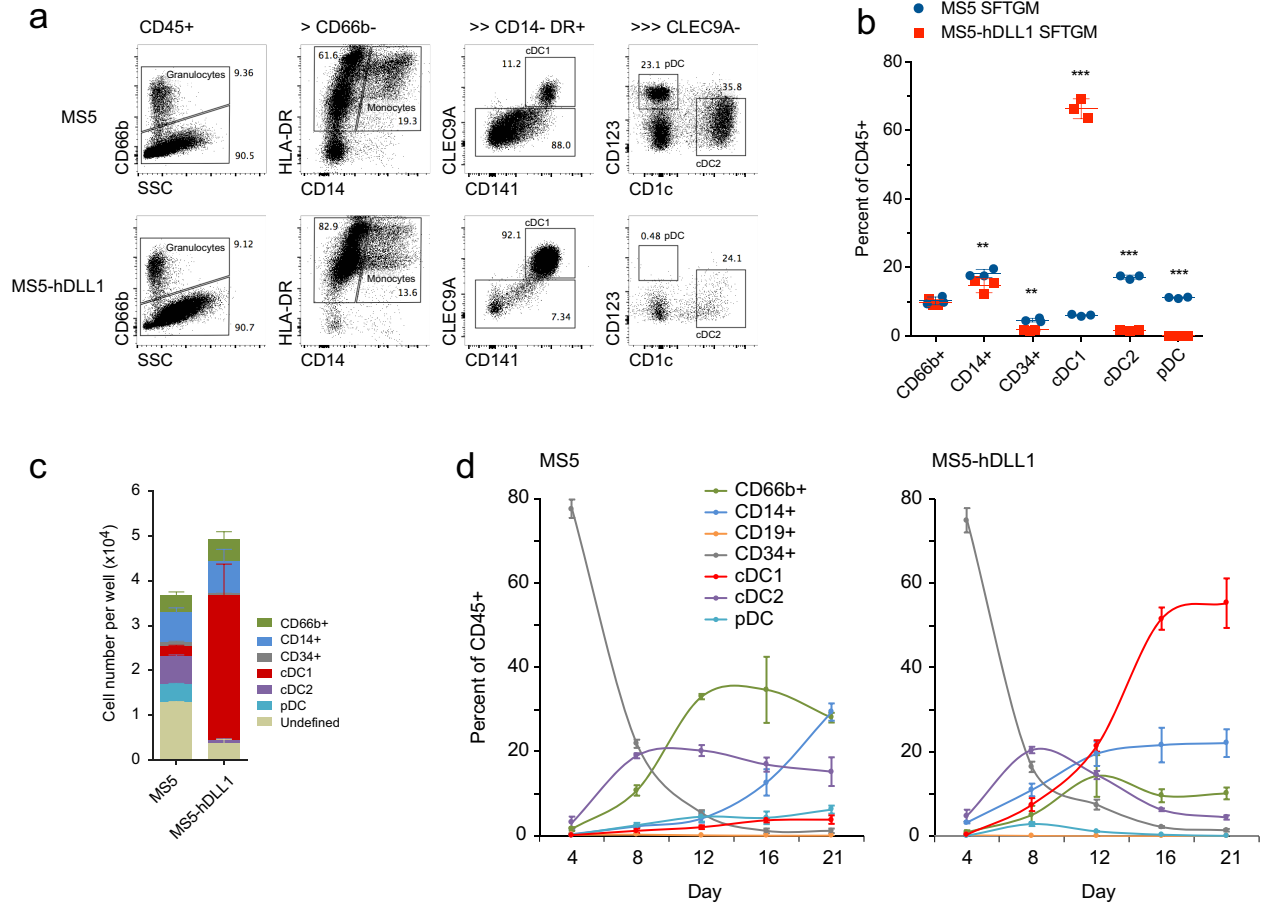


**Fig. 3-1: Notch ligands promote cDC1 output from HSPCs at the expense of monocyte, cDC2, and pDC output.**

(a) Flow cytometry showing differentiation of cord blood (CB) CD34+ HSPCs for 20 days on MS5 or MS5-hDLL1 stromal cells in optimized DC culture conditions. (b) Frequencies and (c) cell numbers of granulocyte (CD66b+), monocyte (CD14+), or DC populations in day 20 cultures. (d) Kinetics of multilineage hematopoietic differentiation in DC conditions on MS5 or MS5-hDLL1 over 21 days. For all panels, error bars indicate the standard deviation of technical triplicate samples. Panels shown are representative of three independent experiments.

The effect of stromal Notch ligand expression on enhancing cDC1 frequency was conserved across alternative Notch ligands (DLL1, DLL4, and JAG1) (Fig. 2a), and also across HSPCs isolated from human CB, bone marrow (BM), and G-CSF mobilized peripheral blood (MPB), with relative differences in cDC1 output possibly reflecting differences in the progenitor composition of each source (Fig. 2b).

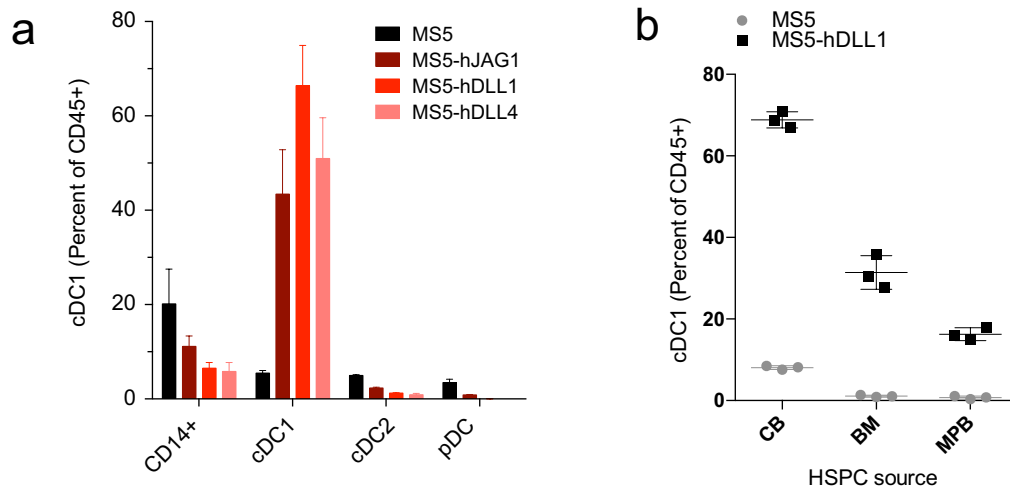


**Fig. 3-2: Notch ligand induced cDC1 differentiation is conserved across alternative Notch ligands and different HSPC sources.** (a) Different Notch ligands have similar effects on cDC1 differentiation. HSPCs were cultures on MS5 cells, or MS5 transduced with human *JAG1*, *DLL1*, or *DLL4* in DC culture conditions, and cDC1 frequencies were analyzed on day 20. (b) Notch signaling promotes cDC1 differentiation from CD34+ HSPCs from cord blood (CB), bone marrow (BM), or G-CSF mobilized-peripheral blood (MPB). For all panels, error bars indicate the standard deviation of technical triplicate samples. Panels are representative of two independent experiments.

We next confirmed that the effect of stromal DLL1 was occurring through Notch receptor signaling on hematopoietic cells. Treatment of CB HSPC MS5-hDLL1 co-cultures with the gamma-secretase inhibitor RO4929097<sup>21</sup> resulted in abrogation of increased cDC1 frequency and restoration of monocyte, cDC2, and pDC differentiation (Fig. 3a). Conversely, lentiviral transduction of HSPCs with a constitutively activated intracellular Notch1 domain (ICN1)<sup>22</sup> in MS5 co-cultures lacking DLL1 recapitulated the effect of stromal DLL1 on increasing cDC1 and decreasing monocyte, cDC2, and pDC frequencies (Fig 3b).

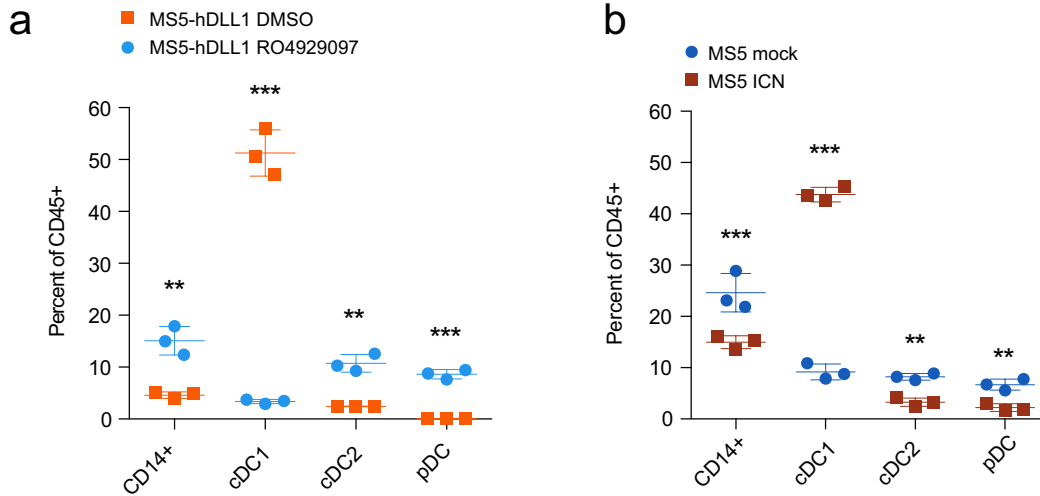


**Fig. 3-3: The effect of DLL1 on cDC1 differentiation is Notch-dependent and cell intrinsic.** (a) Abrogation of the effect of DLL1 on CLEC9A+ DC differentiation by the gamma-secretase inhibitor RO4929097, which was added to MS5-hDLL1 DC cultures and analyzed on day 15. (b) Transduction of HSPCs with intracellular Notch1 (ICN) recapitulates the effect of a Notch ligand in the absence of exogenous stromal cell DLL1. For all panels, error bars indicate the standard deviation of technical triplicate samples. Panels are representative of two independent experiments.

### Notch signaling acts on multipotent DC progenitors to induce cDC1 transcriptional priming

We hypothesized that Notch signaling was exerting its effect on multipotent DC progenitors to direct commitment to the cDC1 lineage. To test this, we sorted human multipotent GMPs<sup>23</sup>, monocyte-DC-restricted MDPs, and DC-committed CDPs<sup>16</sup> from healthy donor bone marrow and evaluated the effect of stromal DLL1 on hematopoietic differentiation. We found that Notch-induced cDC1 differentiation and suppression of monocytic, cDC2, and pDC differentiation was evident at the GMP stage, but most prominent at the MDP and CDP stages (Fig. 4a), suggesting that Notch signaling may be most relevant to cDC1 fate decisions in DC-specific progenitors (Fig. 4b).



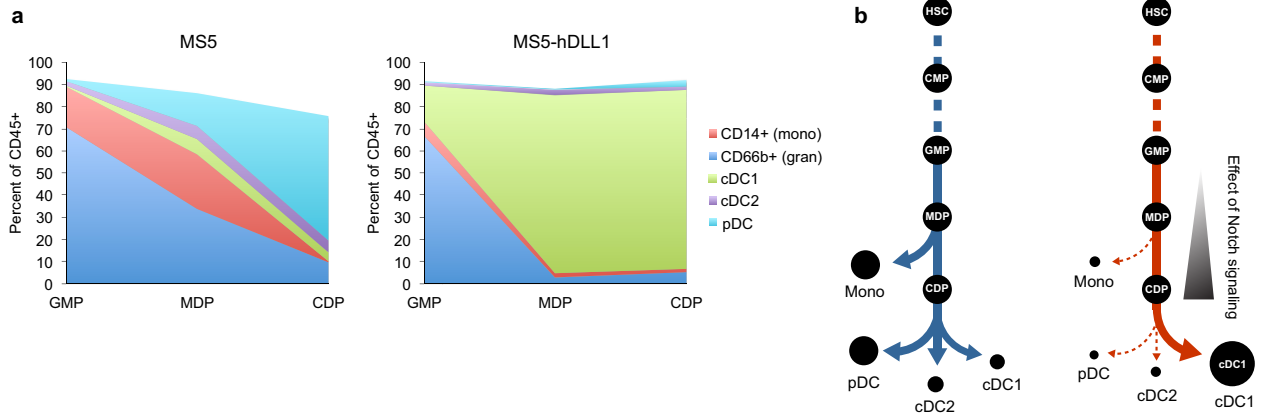


**Fig. 3-4: Notch signaling acts on DC-specific progenitors to direct cDC1 differentiation and suppress alternative lineage fates.** (a) Human BM myeloid/DC progenitors were isolated by FACS based on validated phenotypes and differentiated on MS5 or MS5-hDLL4 for 20 days. Frequencies of monocytes, granulocytes, or DCs generated from each progenitor type are shown. Results are representative of two independent experiments. GMP: granulocyte/monocyte progenitor; MDP: monocyte-DC progenitor; CDP: common dendritic cell progenitor. (b) Schematic summarizing the effect of Notch on DC on monocytic and DC lineage commitment. Left panel: weak or no Notch signaling (e.g. MS5); Right panel: strong Notch signaling (e.g. MS5-hDLL1).

We next tested the hypothesis that Notch signaling induces cDC1 transcriptional priming in multipotent DC progenitors. We isolated fresh BM MDPs and co-cultured them on MS5 or MS5-hDLL1 in DC-supportive conditions for 48h. CD34+ progenitor cells (negative for DC markers) were re-sorted from these cultures, and global gene expression analyzed by RNA-seq. RNA from pre-culture, freshly isolated MDPs was used as a baseline comparison. Of the genes specifically upregulated in MS5-hDLL1 co-cultures, the Notch targets *HES1*, *HES4*, and *DTX1* were identified, consistent with Notch activation; however, we also found clear upregulation of the transcription factors *IRF8*, *BATF3*, and *MYCL*, three factors shown to be critical for cDC1 DC development and function in mice and humans<sup>17, 24, 25, 26, 27</sup> (Fig. 5a). Interestingly, transcription of the cDC1-specific markers *CLEC9A* and *THBD* (encoding CD141) were also upregulated in DLL1-exposed MDPs despite absence of their

surface expression, suggesting very early onset of a Notch-induced cDC1 transcriptional program (Fig. 5a). Indeed, clustering of freshly isolated, MS5<sup>-</sup> and MS5-hDLL1-exposed MDPs based on a validated mature cDC1 transcriptional profile derived from single-cell RNAseq data of primary human cDC1<sup>6</sup> revealed DLL1-specific upregulation in MDPs of a large subset of mature cDC1-specific genes (Fig. 5b).

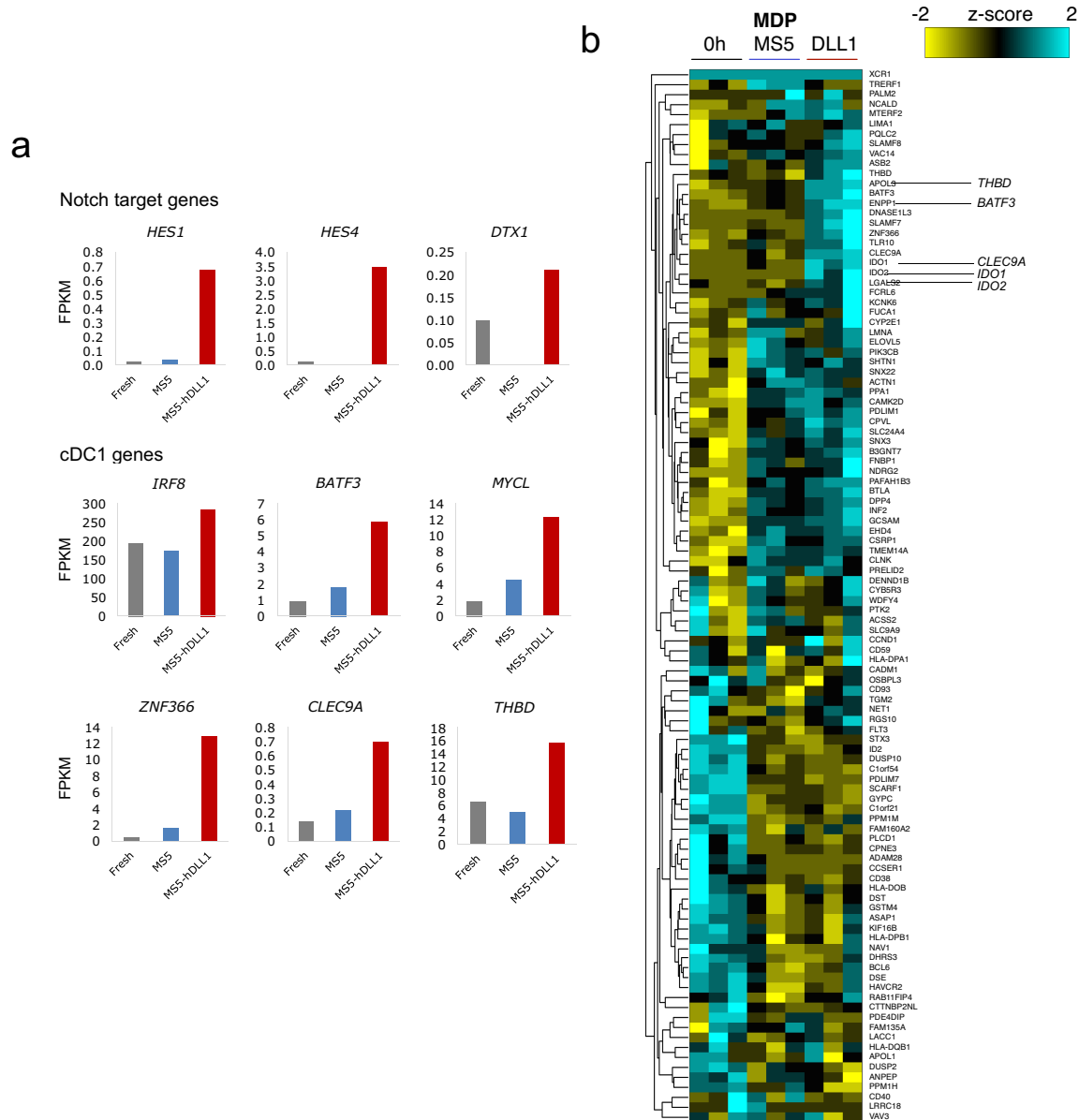


**Fig. 3-5: Notch signaling induces a cDC1 transcriptional program in multipotent MDPs prior to cDC1 differentiation.** (a) Purified BM monocyte-DC progenitors (MDP) were isolated by FACS and cultured on MS5 or MS5-

hDLL1 cells for 48h. CD34+ cells were resorted from these cultures and RNA-seq performed. Freshly sorted MDP (0h) are shown as a pre-culture control. Biological triplicate MDP samples from three different BM donors were run in parallel. Relative expression of selected genes is expressed as fragments per kilobase of transcript per million mapped reads (FPKM) (the average of triplicate samples is shown). (b) Samples were clustered based on relative expression of a cDC1 gene signature derived from single cell RNA-seq of peripheral blood DC populations<sup>6</sup>. Each column represents an independent donor source.

### **Notch-induced cDC1 are phenotypically and transcriptionally similar to blood cDC1**

We next turned to validating the identify and function of Notch-induced cDC1. cDC1 derived from CB CD34+ HSPCs on MS5-hDLL1 showed surface expression of pan-DC markers including CD205, CD1a, CD135 (FLT3), Dectin-1, ILT1, and ILT3; but importantly, in addition to CLEC9A and CD141, also expressed the cDC1-specific markers CADM1 and TLR3 (Fig. 6). As reported for blood cDC1, Notch-induced cDC1 had low expression of the monocytic/cDC2 markers CD11b, CD11c, CD115 (M-CSFR), CD172a (SIRPa), and CD206 relative to CD14+ monocytes contained within the same culture, and furthermore completely lacked expression of the MoDC-specific marker CD209 (DC-SIGN) (Fig 6).

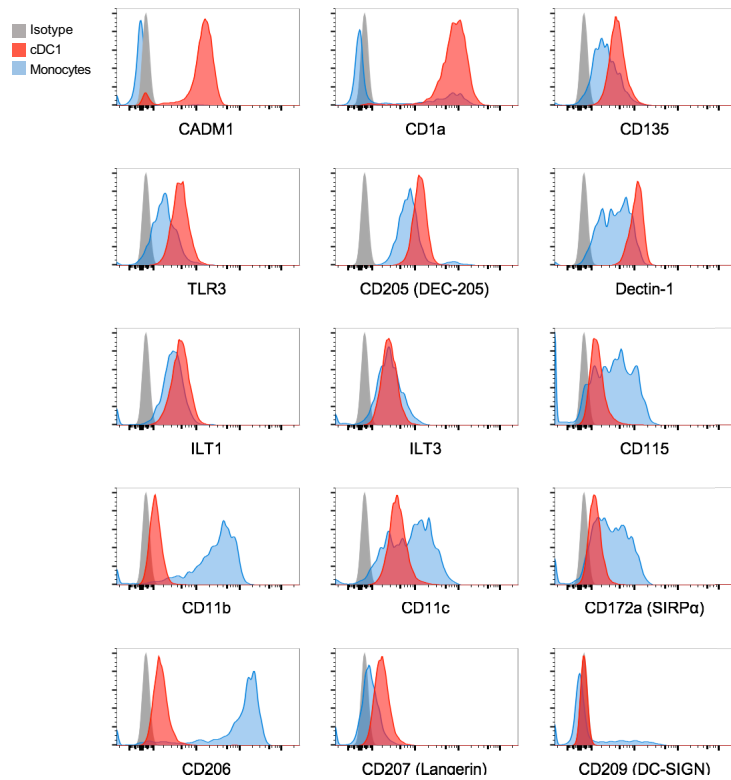


**Fig. 3-6: Notch-induced cDC1 express surface markers consistent with cDC1 identity.** Flow cytometry showing surface phenotype of cDC1 (red) or CD14+ monocytes (blue) from day 20 MS5-hDLL1 cultures demonstrating expression by cDC1 of DC-associated markers (e.g. CADM1, CD135, TLR3, DEC-205) and low expression of monocytic/MoDC markers (e.g. CD11b, SIRPa, DC-SIGN).

To further validate cDC1 identity, we sorted CB and MPB Notch-induced cDC1 from MS5-hDLL1 co-cultures and compared them to primary blood cDC1 by RNA-seq. For comparison, we isolated cDC2 generated *in vitro* in MS5 co-cultures initiated with HSPCs from the same donors, as well as primary cDC2 from the blood. As a distantly related comparison, we isolated RNA from MoDC derived from blood CD14+ monocytes (Fig. 7a). Clustering of these seven populations to a validated blood cDC1 gene signature identified from single-cell RNA-seq of blood DC populations<sup>6</sup> revealed a very high concordance in expression of this signature between Notch-induced cDC1 (regardless of HSPC source) and primary blood cDC1, strongly supporting their identity as cDC1 (Fig. 7b). Conversely, *in vitro* derived and primary cDC2 and MoDC did not exhibit specific expression of cDC1 signature genes (Fig. 7b).

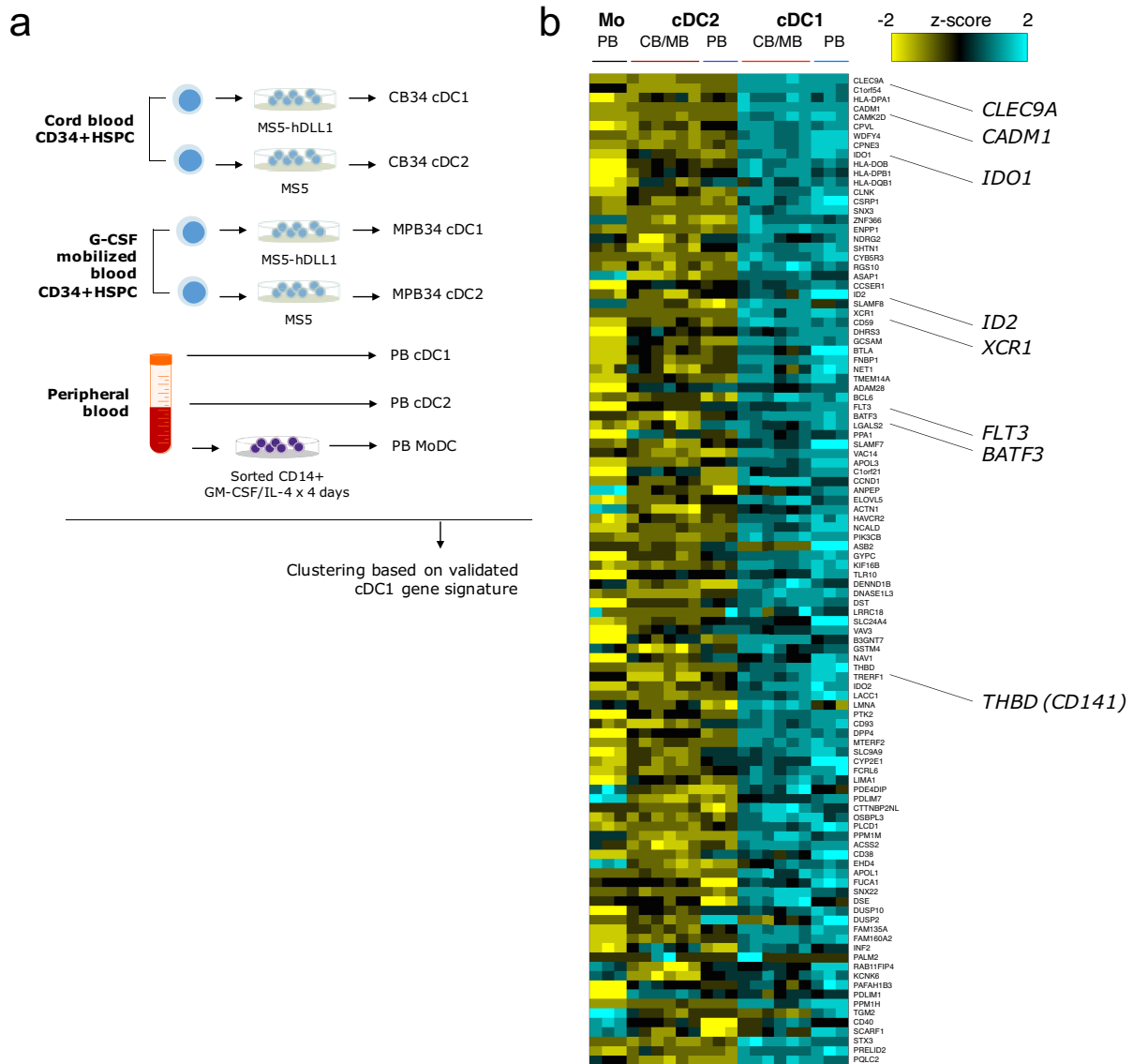


**Fig. 3-7: Notch-induced cDC1 express a gene signature of endogenous cDC1 regardless of HSPC origin.** (a) Schematic showing the culture and sorting strategy used for gene expression profiling of Notch-induced and primary DCs by RNA-seq. (b) Gene expression profiling by RNA-seq of CB and MPB HSPC-derived, Notch-induced cDC1 compared with primary cDC1s from the peripheral blood (PB). cDC2 generated on MS5 co-cultures from the same CB and MPB HSPC samples were run for comparison, as were PB cDC2s, and monocyte-derived DCs (Mo) generated from healthy donor PB CD14<sup>+</sup> monocytes. Samples were clustered based on relative expression of a cDC1 gene signature derived from single cell RNA-seq of peripheral blood DC populations<sup>6</sup>. Each column represents an independent cell donor source.

## Notch-induced cDC1 exhibit lymph node homing and T cell activation potential

We next examined the phenotype and functional properties of Notch-induced DCs with regard to lymph node homing and T cell activation potential. By Wright-Giemsa staining, Notch-induced cDC1 derived from CB CD34<sup>+</sup> HSPCs in MS5-hDLL1 co-cultures were large granular lymphocyte-like cells with occasional cytoplasmic projections; however, in response to poly(I:C) and R848 (agonists of TLR3 and TLR8, respectively, which are known to induce cDC1 maturation<sup>28</sup>) underwent morphologic change and exhibited large cytoplasmic folds and hair-like projections, consistent with an activated DC state (Fig 8a). Flow cytometric analysis of cDC1 freshly isolated from MS5-hDLL1 co-cultures showed surface expression of the T cell costimulatory molecule CD80, but low expression levels of CD83, CD86, HLA-DR and the activation-induced co-inhibitory ligand PD-L1, all of which were strongly upregulated by treatment with poly(I:C) and R484 (Fig. 8b). Interestingly, these markers were also upregulated (albeit to a lesser degree) when cultured off stroma for 24h even in the absence of poly(I:C)/R848, a phenomenon also reported for primary blood cDC1<sup>10</sup>. Expression of the lymph node-homing receptors CCR7 and CD62L followed a similar pattern, with moderate basal expression which was maximally upregulated in the presence of poly(I:C) and R848 (Fig. 8b). Activation-induced expression of CCR7 was consistent with robust *in vitro* chemotaxis to CCL21 in transwell assays (Fig 8c), suggesting lymph node homing potential, a critical property of functional cDC1<sup>13</sup>.

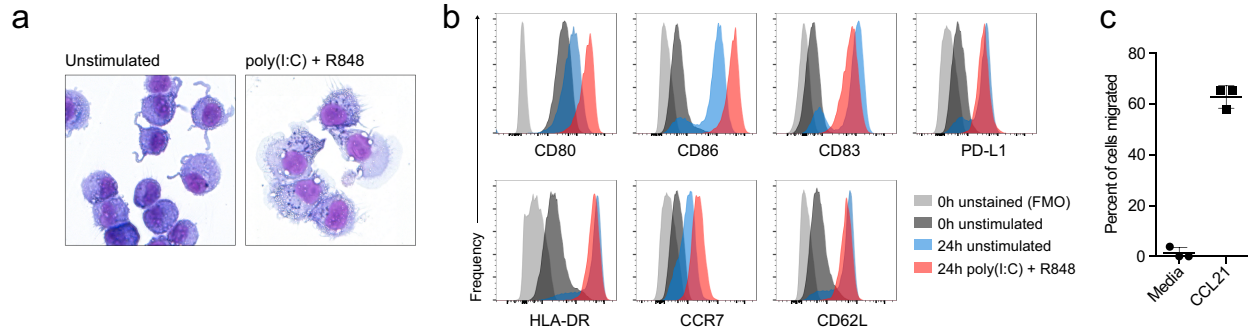


**Fig. 3-8: Notch-induced cDC1 respond to TLR 3/8 agonists, express costimulatory and lymph node homing molecules, and undergo chemotaxis in response to CCL21.** (a) Wright-Giemsa staining of Notch-induced CB HSPC-derived cDC1 showing activation-associated morphological changes in response to stimulation with poly(I:C) (TLR3 agonist) and R848 (TLR8 agonist). (b) Expression and upregulation of T cell costimulatory and co-inhibitory molecules on Notch-induced cDC1, as well as CCR7 and CD62L, involved in lymph-node homing. (c) Transwell migration of Notch-induced cDC1 in response to CCL21, indicating functional chemotaxis via CCR7, and lymph node homing potential. All panel results are representative of two independent experiments.

### Notch-induced cDC1 are adept at T cell activation

We tested the ability of Notch-induced cDC1 to activate T cells. Notch-induced cDC1 derived from CB HSPCs potently activated allogeneic CD4<sup>+</sup> and CD8<sup>+</sup> naïve T cells in mixed lymphocyte reactions (Fig 9a), and indeed could do so even without maturation with poly(I:C) and R848, consistent with a spontaneous maturation state when removed from stromal co-culture (Fig 8b). To examine antigen-specific T cell activation, we generated Notch-induced cDC1 from MPB HSPCs from HLA-A\*02:01 (A2)-positive donors and tested their ability to activate autologous T cells transduced with an A2-restricted TCR specific for the tumor-associated epitope NY-ESO-1<sub>157-165</sub> (1G4)<sup>20, 29</sup> in an antigen-specific manner (Fig. 7b). MPB-derived cDC1 pulsed with cognate (NY-ESO-1<sub>157-165</sub>) but not irrelevant (MART-1<sub>26-35</sub>) peptide strongly activated 1G4 TCR-transduced T cells (Fig. 9b). The ability to introduce

full-length proteins into DCs for unbiased epitope presentation is a potentially useful option for immunotherapeutic applications. We confirmed that transduction of MPB CD34+ HSPCs with a full-length cDNA encoding NY-ESO-1 prior to cDC1-induction on MS5-hDLL1 generated cDC1 capable of potently activating autologous 1G4-transduced T cells (Fig 9b).

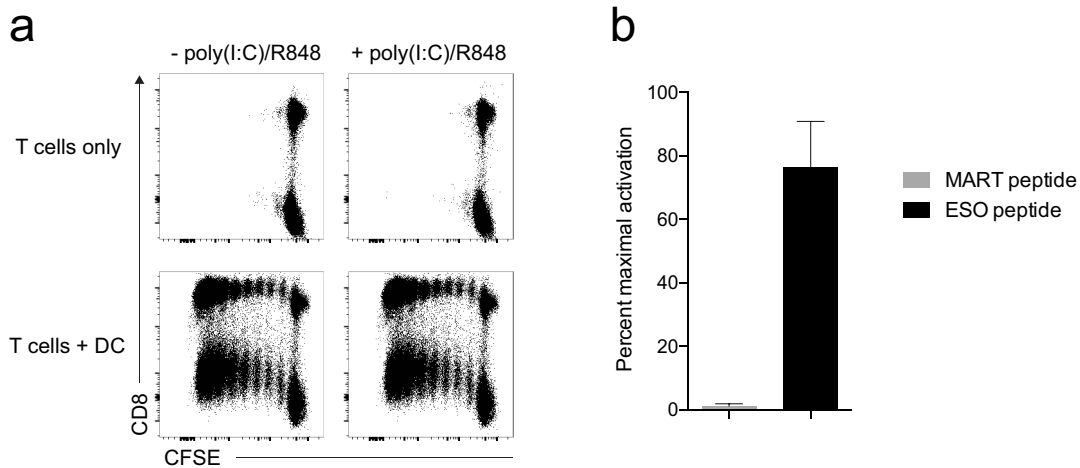


**Fig. 3-9: Notch-induced cDC1 potently activate naïve allogeneic T cells and autologous antigen-specific T cells.**

(a) Mixed lymphocyte reactions (MLR) between Notch-induced cDC1 with or without maturation in poly(I:C)/R848, and allogeneic PB naïve CD4+ and CD8+ T cells. T cell proliferation at 5 days is shown by CFSE dilution. (b) Activation of antigen-specific T cells by Notch-induced cDC1. Notch-induced MPB HPSC-derived HLA-A\*02:01+ cDC1 were pulsed with non-specific (MART-1) or specific (NY-ESO-1) peptides and co-cultured with autologous 1G4 TCR-transduced T cells for 8 hours. T cell activation was measured by intracellular staining for IFN-gamma and expressed as a percent of maximal activation by PMA/ionomycin.

### Notch-induced cDC1 cross-present cellular antigens to T cells

Cross-presentation is the ability to present T cell epitopes derived from environmentally acquired antigens, such as necrotic cells or cellular debris, and is thought to be a critical process in the initiation of anti-tumor T cell immunity. As physiological cross-presentation is a trait largely associated with cDC1 in humans and mice<sup>9, 10, 11, 13</sup> in part



through the capture of necrotic cells by CLEC9A (DNGR1)<sup>30, 31, 32</sup>, we tested the ability of Notch-induced cDC1 to capture and cross-present antigens from tumor cell debris. Notch-induced cDC1 derived from MPB HSPCs were pulsed overnight with necrotic K562 cells which had been transduced with either a control vector or full-length NY-ESO-1, and killed by gamma-irradiation and freeze/thaw. cDC1 exposed to killed NY-ESO-1-transduced but not control K562 cells competently cross-presented the NY-ESO-1<sub>157-165</sub> epitope to activate autologous 1G4 TCR-transduced T cells (Fig. 10).

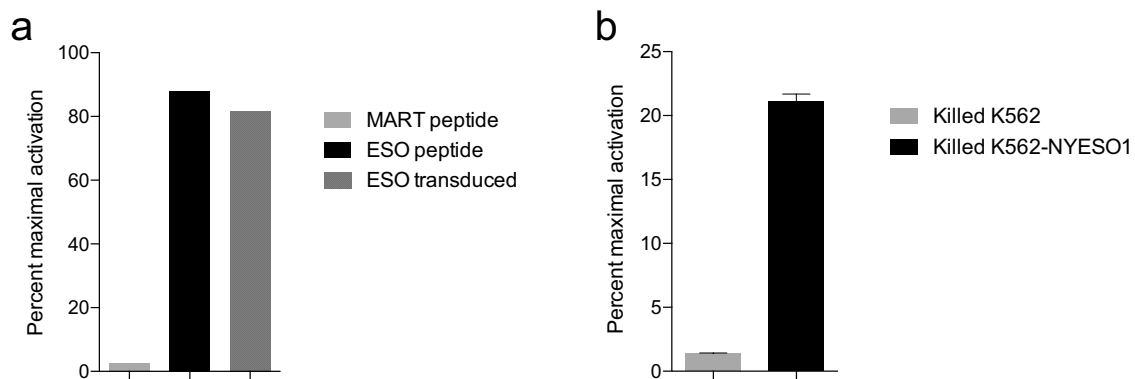


**Fig. 3-10: Notch-induced cDC1 cross-present antigen from necrotic cells to activate autologous antigen-specific T cells.** (a) Presentation of endogenous antigen transduced at the HSPC stage. MPB HSPCs were transduced with full-length NY-ESO-1 cDNA prior to cDC1 induction, and progeny Notch-induced cDC1 co-cultured with autologous 1G4 TCR-transduced T cells. cDC1 derived from non-transduced HSPCs and pulsed with non-specific (MART-1) or specific (NY-ESO-1) peptides were used as negative and positive controls, respectively. T cell activation was measured by intracellular staining for IFN-gamma and expressed as a percent of maximal activation by PMA/ionomycin. (b) Cross-presentation of cellular antigens by Notch-induced CLEC9A+ DCs. MPB-derived Notch-induced cDC1 were pulsed overnight with killed cell preparations of either control (K562-mStrawberry) or full-length NY-ESO-1-transduced (K562-NYESO1-mStrawberry) cell lines and co-cultured with autologous 1G4 TCR-transduced T cells for 8 hours. T cell activation was measured by intracellular staining for IFN-gamma and expressed as a percent of maximal activation by PMA/ionomycin.

## Notch-induced cDC1 prime *de novo* antigen-specific T cell immune responses

As the overall goal of DC adoptive immunotherapy is to prime *de novo* antigen-specific T cell responses, we tested the ability of Notch-induced cDC1 to prime and expand naïve T cells reactive to either NY-ESO-1 or the model melanoma-associated antigen MART-1<sup>33, 34</sup>. Indeed, Notch-induced cDC1 derived from MPB CD34+ HPSCs pulsed with A2-restricted MART-1<sub>26-35</sub> or NY-ESO-1<sub>157-165</sub> peptides elicited antigen-specific clonal expansion of T cells from among pools of naïve, autologous T cells, as determined by tetramer staining (Fig 11a-b). Both basal and post-expansion frequencies of T cells reactive to MART-1 were higher than those of NY-ESO-1, consistent with the reported high-frequency of MART-1<sub>26-35</sub> reactive T cells in healthy donor blood<sup>35</sup>.

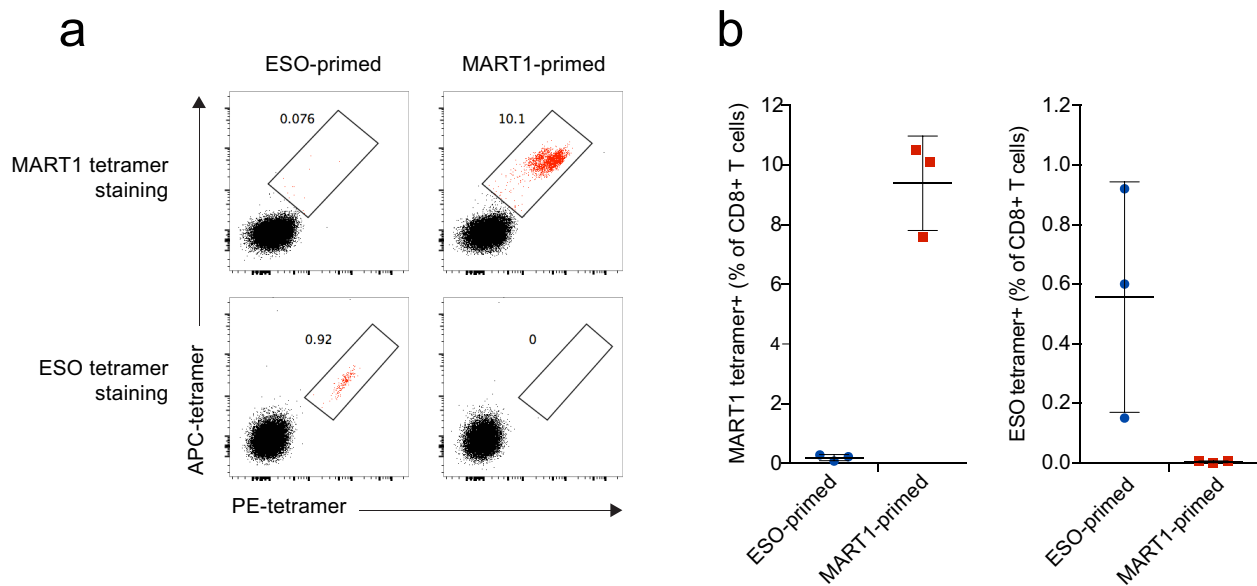


**Fig 3-11. Notch-induced cDC1 prime *de novo* CD8+ T cell responses to tumor-associated antigens.** MPB HSPC-derived cDC1 were peptide-pulsed with MART-1<sub>25-36</sub> or NY-ESO-1<sub>157-165</sub> peptides and co-cultured with autologous polyclonal naïve T cells for 7 days. The frequency of A\*02:01/MART1<sub>25-36</sub> or A\*02:01/NY-ESO-1<sub>157-165</sub>

tetramer-positive T cells (gated on CD3+CD8+) from each DC/peptide condition are shown in (a) representative flow cytometry analysis and (b) data from triplicate T cell wells.

## Discussion

We have shown here a specific and novel role for Notch signaling in inducing the differentiation of human cDC1 from HSPCs. This role for Notch was conserved in HSPCs from across different tissue and developmental sources, including neonatal, and steady-state adult HSPCs, suggesting a generalizable role in human cDC1 differentiation throughout life.

Our data suggest that Notch signaling acts on multipotent DC-specific progenitors to rapidly induce cDC1-associated transcriptional regulators including *IRF8*, *BATF3*, and *MYCL*, resulting in cDC1 specification and differentiation at the expense of monocyte, cDC2, and pDC lineage fates. From an ontological point of view this is relevant as multipotent human myeloid progenitors and indeed the DC-specified MDP and CDP progenitors are present as circulating progenitors in the blood (unpublished data). We postulate that Notch-ligand rich tissue microenvironments, notably in the thymus and skin, may play a role in the programming of circulating DC-progenitors into tissue-resident cDC1, however further investigation is needed to test this hypothesis. Indeed, cDC1 are present in the human thymus<sup>36</sup>, where they likely have implication for thymocytes positive and negative selection, however their origin is unclear. Recently, it was shown that human CD34+ thymic-resident early thymic progenitors (ETPs) preferentially generated CDP-like DC progenitors in response to JAG1 but not DLL1 in an OP9-based stromal co-culture system<sup>37</sup>, however in contrast to our studies, found that differentiation of cDC was suppressed by DLL1. These disparate findings may be due to differences in parental stromal cell line used (OP9 versus MS5), cytokine conditions (we found that cDC1 differentiation from human HSPC is critically

dependent on either GM-CSF or IL-3; data not shown), and cDC phenotypic definition (the study did not specifically examine the cDC1 phenotype, instead grouping cDC populations together with CD33+CD13+ myeloid-lineage cells).

Another group also recently observed that cDC1 lineage priming may occur as early as the hematopoietic stem cell stage in human bone marrow through induction of *IRF8*<sup>17</sup>. As *IRF8* and its cDC1-associated targets *BATF3*<sup>24</sup> and *MYCL*<sup>27</sup> were induced in bone marrow MDPs within 48 hours of co-culture in a DLL1-specific manner, it would be of interest to see whether Notch ligand-rich niches within the bone marrow microenvironment may physiologically bias HSPCs to the cDC1 lineage in a fashion analogous to Notch-induced T-lineage priming of pre-thymic bone marrow emigrants<sup>38</sup>.

Importantly, the effect of Notch signaling on promoting cDC1 differentiation was observed only in the presence of the DC-supporting cytokines FLT3L and GM-CSF, and stromal cell support. Further work delineating the molecular integration of Notch, cytokine receptor, and stromal cell signals will lead to a clearer understanding of cDC1 differentiation.

Previous studies investigating the role of Notch signaling in human DC differentiation took place prior to the identification of cDC subsets and their respective surface markers, and are thus unclear with respect to cDC1 differentiation. For example, Ohishi et. al.<sup>39</sup> reported that human CD34+ HSPCs cultured in the presence of GM-CSF and TNF- $\alpha$  could generate CD14+ monocytes, and that secondary culture of these cells in the presence of GM-CSF, TNF- $\alpha$ , and immobilized DLL1 increased the output of CD14- CD1a+ DCs; however, based on the starting population this most likely represented the conversion of monocytes to MoDC. Olivier et. al.<sup>40</sup> reported that co-culture of human CB CD34+ HSPCs on OP9 stromal cells expressing DLL1 in the presence of FLT3L and IL-7 resulted in preferential generation of

pDC; this opposite finding to ours may in part be explained by the lack of GM-CSF/IL-3 or the alternative stromal cell line, as discussed above.

As endogenous cDC1 play critical, non-redundant roles in initiating anti-tumor and antiviral T cell immunity, their application to adoptive immunotherapy is tantalizing but has not yet been possible due to their scarcity in the blood<sup>14, 15</sup>. Our data suggest that Notch signaling can be applied to the directed differentiation of human HSPCs to cDC1s that bear the transcriptional and functional hallmarks of their endogenous counterparts. Indeed, the observed lymph node homing potential, cross-presentation, and T cell priming activities suggest that as an accessible source of *in vitro* derived DCs, Notch-induced cDC1 may be superior to MoDC for both the study of DC function, and potentially clinical application.

Previous groups have demonstrated methods for the *in vitro* differentiation of cDC1-like cells from HSPCs, which have been instrumental for determining cytokine requirements and progenitor identities in human DC differentiation<sup>16, 18</sup>. However, these methods generate mixed populations of myeloid cells, cDC1, cDC2, and pDC; with cDC1 typically present at low frequencies. With regard to cDC1 generation specifically, a protocol incorporating stroma-free culture of CD34+ cells in SCF, FLT3L, TPO, IL-6 with the aryl hydrocarbon receptor antagonist StemRegenin 1 generated all three DC subsets, however cDC1 (identified by CD141 expression) represented <1.5% of total cultured cells, yielding around 1x10<sup>5</sup> cDC1 per 1x10<sup>5</sup> input HSPC<sup>41</sup>. A two-step protocol incorporating culture with FLT3L, SCF, IL-3 and TPO, followed by FLT3L, SCF, GM-CSF, and IL-4 (FST3\*) yielded 1.8x10<sup>6</sup> +/- 1.5x10<sup>6</sup> cDC1 (defined as XCR1+) per 1x10<sup>5</sup> CB CD34+ HSPCs and resulted in cDC1 purity of around 12% of cultured cells<sup>42, 43</sup>. In comparison, the use of Notch-ligand expressing stromal cells resulted in a cDC1 purity of 60-70% of cultured cells, and a calculated yield of around 2x10<sup>6</sup> cDC1 per 1x10<sup>5</sup> input CB HSPCs, with slightly lower numbers seen using mobilized peripheral blood

(a clinically relevant source for autologous HSPCs). While optimizations are likely to further improve yields, the identification of Notch signaling as a regulator of cDC1 differentiation, and the ability as demonstrated to generate cDC1 *in vitro* in a scalable fashion using a Notch ligand may permit the preclinical development of next generation cDC1-based immunotherapies.

\*\*\*

## Materials and Methods

### Isolation of human CD34+ HSPCs

Neonatal umbilical cord blood was obtained from discarded cord and placental units from deliveries at UCLA. Bone marrow (BM) was obtained from healthy adult donors (ages 18–51) through discarded material from allogeneic BM donor harvests at UCLA, or purchased from AllCells Inc. (Alameda, CA). G-CSF mobilized peripheral blood was obtained from consenting healthy adult donors undergoing apheresis for allogeneic stem cell transplant donation at UCLA. All tissue samples were obtained under UCLA IRB-approved protocols or exemptions. All samples were enriched for mononuclear cells by Ficoll-Paque (GE Healthcare Life Sciences, Pittsburgh, PA) gradient centrifugation followed by positive selection of CD34+ cells by magnetic cell sorting (MACS) using the CD34 MicroBead Kit UltraPure (Miltenyi, Auburn CA). CD34+ cell enriched fractions were cryopreserved after MACS, unless otherwise noted. Prior to use, cells were thawed and further purified by FACS as described below. These cells were then immediately added to cultures, or transduced as described below. HSPCs used for antigen specific functional assays were from HLA-A\*02:01+ CB or MPB donors. HLA-A2 typing was performed by the UCLA Immunogenetics Center using sequence-specific oligonucleotide (SSO) beads.

### Isolation of human bone marrow progenitor subsets

CD34+ HSPCs were enriched from fresh BM aspirates, as above, and sorted by FACS for stem/progenitor populations based on positive expression of CD45 and absent expression of lineage markers (CD3, CD14, CD16, CD19, CD56, and CD235a; “Lin<sup>-</sup>”) combined with the following markers: GMP (CD34+CD38+CD45RA+CD10-CD123<sup>int</sup>CD115<sup>-</sup>), MDP

(CD34+CD38+CD45RA+CD10-CD123<sup>int</sup>CD115+), and CDP (CD34+CD38+CD45RA+CD10-CD123<sup>hi</sup>)<sup>16, 23</sup>.

### **Isolation of primary human T cells**

Peripheral blood (PB) and MPB T cells were isolated from mononuclear cell fractions as described above. T cells were isolated by magnetic bead enrichment using the Pan-T Cell Isolation Kit (Miltenyi) or, for naïve T cell priming experiments, the Naïve Pan-T Cell Isolation Kit (Miltenyi).

### **Cell lines**

To generate the MS5-hDLL1, MS5-hDLL4, and MS5-hJAG1 cell lines, the murine MS-5 bone marrow stromal cell line was transduced with a lentiviral vector encoding human *DLL1*, *DLL4*, or *JAG1* (and eGFP), respectively, as previously described<sup>20</sup>. The highest 5% GFP-expressing cells were sorted by FACS and passaged in DMEM/10% FCS. Stable expression was confirmed by flow cytometry for GFP expression after several weeks of culture, and Notch ligand expression confirmed by flow cytometry, qRT-PCR, and DNA sequencing. The K562 cell line was obtained from ATCC and maintained in RPMI/10% FCS. NY-ESO-1 expressing K562 cells were generated by transduction of K562 cells with a lentiviral vector encoding full-length human NY-ESO-1 and mStrawberry.

### **Dendritic cell differentiation cultures**

MS5-hDLL1 (or MS5 control cells) cells were harvested by trypsinization and resuspended in MEMalpha with 20% HyClone FBS (both from ThermoFisher Scientific, Grand Island, NY). Cells were seeded into 0.1% gelatin-coated 96-well plates at a density of  $\sim 1 \times 10^5$  cells/mL in



100uL per well the day prior to use to achieve ~90% confluence on the day of use. Medium was aspirated from monolayers and  $5 \times 10^3$  FACS-purified DC-depleted HSPCs (CD34+ cells negative for the lineage/DC markers CD3, CD14, CD19, CD56, CD66b, CD235a, CD1c, and CLEC9A) were plated on stromal monolayers in 200ul of media consisting of MEMa, 20% FBS, 5 ng/ml rhSCF, 5 ng/ml rhFLT3L, 50 ng/ml rhTPO, and 10 ng/ml rhGM-CSF (all from Peprotech, Rocky Hill, NJ), abbreviated to MEMa/20/SFTGM hereafter. A half-media change was performed every 3-4 days by gently aspirating half the well volume with a 200ul pipet or vacuum aspirator on low power, followed by replacement with an equal volume of fresh, pre-warmed medium containing 2X final cytokine concentration. Cultures were harvested at the indicated timepoints (typically day 17-21 for optimal cDC1 differentiation) by gently pipetting up and down with a 200ul multichannel pipette to create a single cell suspension followed by collection in a reservoir; wells were washed twice with cold MACS buffer and all washes were pooled and filtered through a 70 um nylon cell strainer to remove debris. In some experiments, the gamma-secretase inhibitor RO4929097<sup>21</sup> or DMSO vehicle control was added and refreshed with each half-media change. In some experiments, the stromal cell line was substituted for MS5-hDLL4 or MS5-hJAG1. For DC functional experiments, cDC1 were further purified from MS5-hDLL1 cultures by FACS sorting for CD14-CD66b-SIRPa<sup>int</sup>CD141+ DCs, based on the ability to discriminate cDC1 from cDC2 by SIRPa<sup>8</sup>. Antibody staining for CLEC9A was not used as a positive sorting marker for cDC1 to avoid blocking its function in downstream assays.

### **Lentiviral vectors and transduction**

The full-length coding sequences of human *DLL1* and *JAG1* were cloned by RT-PCR from a human universal reference RNA set (Agilent Technologies, Santa Clara, CA) into the third

generation lentiviral vector pCCL-c-MNDU3-X-IRES-eGFP (gift from Dr. Donald Kohn, UCLA). The coding sequence of human *DLL4* was synthesized and cloned into the same vector. The third generation lentiviral vector encoding the codon optimized  $\alpha$  and  $\beta$  (V $\beta$ 13.1) chains of a TCR specific for HLA-A\*02:01/NY-ESO-1<sub>157-165</sub> (derived from the 1G4 TCR clone<sup>29</sup>) is previously described<sup>20, 44</sup>, and was a gift from Dr. Antoni Ribas (UCLA). The lentiviral construct encoding the human Notch1 intracellular domain (EF.hICN1.Ubc.GFP) was a gift from Linzhao Cheng (Addgene plasmid 17626)<sup>22</sup>. The NY-ESO-1 coding sequence was a gift from Dr. Owen Witte (UCLA) and was sub-cloned into the pCCL-c-MNDU3-X-IRES-mStrawberry lentiviral vector. Packaging and concentration of lentivirus particles was performed as previously described<sup>20</sup>. Briefly, 293T cells (ATCC) were co-transfected with a lentiviral vector plasmid, pCMV- $\Delta$ R8.9, and pCAGGS-VSVG using TransIT 293T (Mirus Bio, Madison, WI) for 17 hours followed by treatment with 20 mM sodium butyrate for 8 hours, followed by generation of cell supernatants in serum-free UltraCulture for 48 hours. Supernatants were concentrated by tangential flow filtration using Amicon Ultra-15 100K filters (EMD Millipore, Billerica, MA) at 4000 xg for 40 minutes at 4°C and stored as aliquots at -80°C. For HSPC transduction,  $1 \times 10^5$ – $1 \times 10^6$  FACS-sorted CD34+ HSPCs were plated in 6-well non-treated plates coated with 20  $\mu$ g/ml Retronectin (Clontech, Mountain View, CA) in 1 ml X-VIVO-15 (Lonza, Basel, Switzerland) supplemented with 50 ng/ml of recombinant human SCF, FLT3L, and TPO, and 10 ng/ml IL-3 (Peprotech, Rocky Hill, NJ) for 12–18h, concentrated lentiviral supernatant was then added to a final concentration of  $1$ – $2 \times 10^7$  TU/ml. Cells were harvested 24 hours post-transduction, washed, and seeded into DC cultures. For transduction of peripheral blood T cells, CD8+ T cells were isolated by magnetic negative selection using the CD8+ T cell Isolation Kit (Miltenyi) and activated/expanded in AIM V/5% human AB with anti-CD3/CD28 beads (ThermoFisher Scientific) and 20 ng/ml IL-

2 for 4 days prior to transduction, as previously described<sup>20</sup>. Transduced T cells were subsequently expanded in IL-2 (20 ng/ml) prior to use.

### **Mixed lymphocyte reactions**

cDC1 were generated from CB CD34<sup>+</sup> HSPCs on MS5-hDLL1 cultures and were isolated by FACS as described above. cDC1 were matured overnight in MEMa/20/SFTGM with or without 10 ug/ml polyinosinic–polycytidylic acid potassium salt (polyI:C) and 10 ug/ml resiquimod (R848) (both from Sigma Aldrich, St. Louis, MO) overnight. Naïve peripheral blood T cells were isolated from HLA-A2-mismatched allogeneic peripheral blood mononuclear cells (PBMCs) as described above, and labeled with 5 µM CFSE (Biolegend, San Diego, CA) per manufacturer’s protocol. cDC1 and naïve T cells were mixed 1:4 in 200ul per well in a 96-well round-bottom plate in AIM V (ThermoFisher Scientific, Grand Island, NY) with 5% human AB serum (Gemini Bio-Products, West Sacramento, CA) with SFTGM to support DC function and analyzed by flow cytometry on day 5.

### **Antigen-specific T cell activation assays**

To model antigen specific T cell activation, cDC1 were generated as described above on MS5-hDLL1 from cryopreserved HLA-A\*02:01<sup>+</sup> (A2) mobilized peripheral blood (MPB) CD34<sup>+</sup> HSPCs. Autologous T cells from the cryopreserved CD34<sup>-</sup> MACS fraction were isolated, activated, and transduced with the A2-restricted 1G4 TCR as described above. Transduced cells were expanded in 20 ng/mL IL-2, which was changed to 0.2 ng/mL IL-2 24h prior to activation experiments. cDC1 were purified from MS5-hDLL1 monolayers as described above, and cultured overnight in MEMa/20/SFTGM with 10 ug/ml NY-ESO-1<sub>157-165</sub> or MART-1<sub>26-35</sub> peptide in the presence of poly(I:C) and R848, washed, and mixed 1:4 with TCR-

transduced T cells in AIM V/5%AB serum with poly(I:C)/R848 and SFTGM to support DC function. A protein transport inhibitor cocktail (eBioscience, San Diego, CA) was added to each well and incubated for 6h. Cells were stained for CD3, CD4, and CD8 (Biolegend, San Diego, CA) prior to fixation and permeabilization with an intracellular staining buffer kit (eBioscience, San Diego, CA) and intracellular staining with an antibody against IFN $\gamma$  (Biolegend, San Diego, CA). In some experiments, HSPCs were transduced with full-length NY-ESO-1 as described above prior to cDC1 differentiation.

### **Cross-presentation assays**

cDC1 were generated as described above from cryopreserved A2<sup>+</sup> MPB CD34<sup>+</sup> HSPCs. Autologous T cells were isolated and transduced with the 1G4 TCR as described above. Purified cDC1 were pulsed for 12-16h in MEMa/20/SFTGM with killed K562 cells. These were generated by irradiating either K562-mStrawberry or K562-NY-ESO-1-mStrawberry cells at 200 Gy followed by culture for 24h, followed by one freeze/thaw cycle in liquid nitrogen, resulting in a mix containing intact killed cells and cell debris. Killed cell preparations were added to DCs in a 2:1 (input K562 cell:DC) ratio together with poly(I:C) and R848. DCs were washed and co-cultured with 1G4-transduced autologous T cells in AIM V/5%AB serum (with poly(I:C)/R848/SFTGM to support DC function) for 2h, followed by addition of a PTI cocktail and CD107a-APC antibody (final dilution 1:100) (Biolegend) for 6h, followed by fixation and intracellular staining for IFN $\gamma$  as described above.

### **T cell priming assays**

Priming of naïve T cells by cDC1 was adapted from a published protocol<sup>45</sup>. cDC1 were generated as described above from cryopreserved A2<sup>+</sup> MPB CD34<sup>+</sup> HSPCs. Total naïve

autologous T cells were isolated as described above and cultured overnight in AIM V/5%AB serum with 5 ng/ml rhIL-7. Purified cDC1 were pulsed overnight in MEMa/20/SFTGM with 10 ug/ml NY-ESO-1<sub>157-165</sub> or MART-1<sub>26-35</sub> peptide in the presence of poly(I:C) and R848. T cells and cDC1 were washed and co-cultured at a 1:4 ratio in AIM V/5%AB with poly(I:C)/R848, 10 ng/ml GM-CSF, and 30 ng/ml IL-21 in 96-well round bottom plates, with replicate wells containing  $1 \times 10^5$  T cells/well. After 72h, a half-media change was done using AIM V/5% AB containing only rhIL-7 and rhIL-15 (5 ng/ml each, final concentration). After 5 days, the cells were transferred to a 48-well plate with addition of an equal volume of AIM V/5%AM/IL-7/IL-15. On day 7, cells were collected and stained with PE and APC tetramers for the NY-ESO-1 or MART-1 A2-restricted epitopes (MBL International Corp., Woburn, MA) per manufacturer's protocol, and surface antibodies, followed by flow cytometric analysis. Antigen-specific T cells were defined as CD3+CD8+ T cells that were double-positive for PE and APC tetramers.

### **Flow Cytometry and Antibodies**

All flow cytometry stains were performed in PBS/0.5% BSA/2 mM EDTA for 30 min on ice. FcX (Biolegend, San Diego, CA) was added to all samples for 5 min prior to antibody staining. For tetramer co-staining, PE or APC-conjugated HLA-A\*02:01/NY-ESO-1<sub>157-165</sub> or HLA-A\*02:01/MART-1<sub>26-35</sub> tetramers (MBL International, Woburn, MA) were added to cells at a 1:20 final dilution at room temperature for 30 minutes prior to addition of antibodies for an additional 15 minutes on ice. DAPI was added to all samples prior to analysis. Analysis was performed on an LSRIIFortessa, and FACS sorting on an ARIA or ARIA-H instrument (BD Biosciences, San Jose, CA) at the UCLA Broad Stem Cell Research Center Flow Cytometry Core. For all analyses DAPI+ cells were gated out, and single cells were gated based on FSC-

H vs. FSC-W and SSC-H vs. SSC-W. Antibody clones used for surface and intracellular staining were obtained from Biolegend (San Diego, CA): CD1a (HI149), CD1c (L161), CD3 (UCHT1), CD4 (RPA-T4), CD8 (SK1), CD10 (HI10a), CD11b (ICRF44), CD11c (3.9), CD14 (M5E2), CD19 (HIB19), CD34 (581), CD38 (HIT2), CD45 (HI30), CD45RA (HI100), CD62L (DREG-56), CD66b (G10F5), CD107a (H4A3), CD115 (9-4D2-1E4), CD123 (6H6), CD135 (BV10A4H2), CD141 (M80), CD205 (HD30), CD206 (15-2), CD207 (10E2), CD209 (9E9A8), CD235a (HI264), CLEC9a (8F9), CCR7 (G043H7), Dectin-1 (15E2), HLA-A2 (BB7.2), ILT1 (24), ILT3 (ZM4.1), interferon  $\gamma$  (4S.B3), TLR3 (TLR-104), human lineage cocktail (CD3, CD14, CD16, CD19, CD20, CD56), and mouse CD29 (HM $\beta$ 1-1); or R&D systems: CADM1, SIRPa (602411).

#### **RNA-seq**

cDC1 derived from biological triplicate CB and MPB CD34<sup>+</sup> HSPC samples were generated in MEMa/20/SFTGM MS5-hDLL1 co-cultures and isolated by FACS as mCD29<sup>-</sup> (MS5 marker), HLA-DR<sup>+</sup>CD14<sup>-</sup>CD66b<sup>-</sup>CD141<sup>+</sup>CLEC9A<sup>+</sup> DCs. Cultures using the same starting HSPCs but on MS5 were used as a source for *in vitro* derived cDC2, sorted by FACS as mCD29<sup>-</sup>HLA-DR<sup>+</sup>CD14<sup>-</sup>CD66b<sup>-</sup>CLEC9A<sup>-</sup>CD1c<sup>+</sup> DCs. Primary DCs were isolated from PBMCs from healthy donors by magnetic enrichment with the Myeloid Dendritic Cell Isolation Kit (Miltenyi), followed by FACS sorting as above.  $5 \times 10^4$ - $1 \times 10^5$  Cells were sorted directly into RLT buffer (Qiagen) and total RNA isolated using the RNeasy Micro kit (Qiagen). RNA concentration and quality was determined using Agilent RNA 6000 Nano chip, and sequencing libraries were prepared using the SMARTer Stranded Total RNA-Seq Kit, Pico Input Mammalian (Clontech) by the UCLA Genomics & Bioinformatics Core, and 2x150 paired-end sequencing was performed on an Illumina HiSeq3000 instrument with 6 samples

multiplexed per lane. For DC progenitor RNA-seq, freshly isolated MDP were sorted from biological triplicate adult bone marrow aspirates as described above and cultured in MEMa/20/SFTGM on either MS5 or MS5-hDLL1 for 48 hours. Cells were harvested and CD141-CLEC9A-CD11c-CD34<sup>+</sup> MPDs were re-sorted from cultures into RLT, and RNA-seq ran as above.

### **RNA-seq Data Analysis**

RNA-seq reads were aligned using STAR v2.5.2b<sup>46</sup>. The GRCh38 assembly of the human genome and the corresponding junction database from Ensemble's gene annotation were used as reference for STAR. The count matrix for genes in the Ensembl genome annotation was generated by STAR using strand-aware gene-level summaries. DESeq v1.14.1<sup>47</sup> was used for normalization (using the geometric mean across samples), differential expression (to classify genes as differentially expressed, Benjamini-Hochberg adjusted p-value < 0.01) and to compute moderate expression estimates by means of variance-stabilized data. Heatmaps were built with Matlab using variance-stabilized data and euclidean distance on per-gene z-scores. Single-cell expression signatures for specific cell types were retrieved from Villani et al<sup>6</sup>, Supplementary Table 2.

### **Statistical Analysis**

Statistical significance in relevant figures was analyzed using a two-tailed unpaired *t* test. Exact *n* values for all experiments are specified in figure legends.

## REFERENCES

1. Sallusto, F. & Lanzavecchia, A. Efficient presentation of soluble antigen by cultured human dendritic cells is maintained by granulocyte/macrophage colony-stimulating factor plus interleukin 4 and downregulated by tumor necrosis factor alpha. *The Journal of experimental medicine* **179**, 1109-1118 (1994).
2. Radford, K.J., Tullett, K.M. & Lahoud, M.H. Dendritic cells and cancer immunotherapy. *Current opinion in immunology* **27**, 26-32 (2014).
3. Dzionek, A. *et al.* BDCA-2, BDCA-3, and BDCA-4: Three Markers for Distinct Subsets of Dendritic Cells in Human Peripheral Blood. *The Journal of Immunology* **165**, 6037-6046 (2000).
4. MacDonald, K.P.A. *et al.* Characterization of human blood dendritic cell subsets. *Blood* **100**, 4512-4520 (2002).
5. Guilliams, M. *et al.* Unsupervised High-Dimensional Analysis Aligns Dendritic Cells across Tissues and Species. *Immunity* **45**, 669-684.
6. Villani, A.C. *et al.* Single-cell RNA-seq reveals new types of human blood dendritic cells, monocytes, and progenitors. *Science (New York, N.Y.)* **356** (2017).
7. See, P. *et al.* Mapping the human DC lineage through the integration of high-dimensional techniques. *Science (New York, N.Y.)* **356** (2017).
8. Dutertre, C.-A., Wang, L.-F. & Ginhoux, F. Aligning bona fide dendritic cell populations across species. *Cellular Immunology* **291**, 3-10 (2014).
9. Bachem, A. *et al.* Superior antigen cross-presentation and XCR1 expression define human CD11c<sup>+</sup>CD141<sup>+</sup> cells as homologues of mouse CD8<sup>+</sup> dendritic cells. *The Journal of experimental medicine* **207**, 1273-1281 (2010).
10. Jongbloed, S.L. *et al.* Human CD141<sup>+</sup> (BDCA-3)<sup>+</sup> dendritic cells (DCs) represent a unique myeloid DC subset that cross-presents necrotic cell antigens. *The Journal of experimental medicine* **207**, 1247-1260 (2010).
11. Poulin, L.F. *et al.* Characterization of human DNGR-1<sup>+</sup> BDCA3<sup>+</sup> leukocytes as putative equivalents of mouse CD8α<sup>+</sup> dendritic cells. *The Journal of experimental medicine* **207**, 1261-1271 (2010).
12. van der Aa, E., van Montfoort, N. & Woltman, A.M. BDCA3<sup>+</sup>CLEC9A<sup>+</sup> human dendritic cell function and development. *Seminars in Cell & Developmental Biology* **41**, 39-48 (2015).



13. Roberts, E.W. *et al.* Critical Role for CD103+/CD141+ Dendritic Cells Bearing CCR7 for Tumor Antigen Trafficking and Priming of T Cell Immunity in Melanoma. *Cancer Cell* **30**, 324-336 (2016).
14. Radford, K.J. & Caminschi, I. New generation of dendritic cell vaccines. *Human vaccines & immunotherapeutics* **9**, 259-264 (2013).
15. Tullett, K.M., Lahoud, M.H. & Radford, K.J. Harnessing Human Cross-Presenting CLEC9A(+)XCR1(+) Dendritic Cells for Immunotherapy. *Frontiers in immunology* **5**, 239 (2014).
16. Lee, J. *et al.* Restricted dendritic cell and monocyte progenitors in human cord blood and bone marrow. *The Journal of experimental medicine* **212**, 385-399 (2015).
17. Lee, J. *et al.* Lineage specification of human dendritic cells is marked by IRF8 expression in hematopoietic stem cells and multipotent progenitors. *Nature immunology* **18**, 877-888 (2017).
18. Helft, J. *et al.* Dendritic Cell Lineage Potential in Human Early Hematopoietic Progenitors. *Cell reports* **20**, 529-537 (2017).
19. Itoh, K. *et al.* Reproducible establishment of hemopoietic supportive stromal cell lines from murine bone marrow. *Experimental hematology* **17**, 145-153 (1989).
20. Seet, C.S. *et al.* Generation of mature T cells from human hematopoietic stem and progenitor cells in artificial thymic organoids. *Nature methods* **14**, 521-530 (2017).
21. Luistro, L. *et al.* Preclinical profile of a potent gamma-secretase inhibitor targeting notch signaling with in vivo efficacy and pharmacodynamic properties. *Cancer research* **69**, 7672-7680 (2009).
22. Yu, X. *et al.* HES1 inhibits cycling of hematopoietic progenitor cells via DNA binding. *Stem cells (Dayton, Ohio)* **24**, 876-888 (2006).
23. Manz, M.G., Miyamoto, T., Akashi, K. & Weissman, I.L. Prospective isolation of human clonogenic common myeloid progenitors. *Proceedings of the National Academy of Sciences of the United States of America* **99**, 11872-11877 (2002).
24. Jaiswal, H. *et al.* Batf3 and Id2 have a synergistic effect on Irf8-directed classical CD8alpha+ dendritic cell development. *Journal of immunology (Baltimore, Md. : 1950)* **191**, 5993-6001 (2013).
25. Grajales-Reyes, G.E. *et al.* Batf3 maintains autoactivation of Irf8 for commitment of a CD8alpha(+) conventional DC clonogenic progenitor. *Nature immunology* **16**, 708-717 (2015).

26. Chandra, J., Kuo, P.T., Hahn, A.M., Belz, G.T. & Frazer, I.H. Batf3 selectively determines acquisition of CD8(+) dendritic cell phenotype and function. *Immunology and cell biology* **95**, 215-223 (2017).
27. Kc, W. *et al.* L-Myc expression by dendritic cells is required for optimal T-cell priming. *Nature* **507**, 243-247 (2014).
28. Minoda, Y. *et al.* Human CD141(+) Dendritic Cell and CD1c(+) Dendritic Cell Undergo Concordant Early Genetic Programming after Activation in Humanized Mice In Vivo. *Frontiers in immunology* **8**, 1419 (2017).
29. Robbins, P.F. *et al.* Single and dual amino acid substitutions in TCR CDRs can enhance antigen-specific T cell functions. *Journal of immunology (Baltimore, Md. : 1950)* **180**, 6116-6131 (2008).
30. Schreiber, G. *et al.* The C-type lectin receptor CLEC9A mediates antigen uptake and (cross-)presentation by human blood BDCA3+ myeloid dendritic cells. *Blood* **119**, 2284-2292 (2012).
31. Sancho, D. *et al.* Identification of a dendritic cell receptor that couples sensing of necrosis to immunity. *Nature* **458**, 899-903 (2009).
32. Zhang, J.-G. *et al.* The Dendritic Cell Receptor Clec9A Binds Damaged Cells via Exposed Actin Filaments. *Immunity* **36**, 646-657 (2012).
33. Rivoltini, L. *et al.* Induction of tumor-reactive CTL from peripheral blood and tumor-infiltrating lymphocytes of melanoma patients by in vitro stimulation with an immunodominant peptide of the human melanoma antigen MART-1. *Journal of immunology (Baltimore, Md. : 1950)* **154**, 2257-2265 (1995).
34. Kawakami, Y. *et al.* Identification of the immunodominant peptides of the MART-1 human melanoma antigen recognized by the majority of HLA-A2-restricted tumor infiltrating lymphocytes. *The Journal of experimental medicine* **180**, 347-352 (1994).
35. Dietrich, P.Y. *et al.* Prevalent role of TCR alpha-chain in the selection of the preimmune repertoire specific for a human tumor-associated self-antigen. *Journal of immunology (Baltimore, Md. : 1950)* **170**, 5103-5109 (2003).
36. Martinez, V.G. *et al.* A discrete population of IFN lambda-expressing BDCA3hi dendritic cells is present in human thymus. *Immunology and cell biology* **93**, 673-678 (2015).
37. Martín-Gayo, E. *et al.* Spatially restricted JAG1-Notch signaling in human thymus provides suitable DC developmental niches. *The Journal of experimental medicine* **214**, 3361-3379 (2017).

38. Yu, V.W.C. *et al.* Specific bone cells produce DLL4 to generate thymus-seeding progenitors from bone marrow. *The Journal of experimental medicine* **212**, 759-774 (2015).
39. Ohishi, K., Varnum-Finney, B., Serda, R.E., Anasetti, C. & Bernstein, I.D. The Notch ligand, Delta-1, inhibits the differentiation of monocytes into macrophages but permits their differentiation into dendritic cells. *Blood* **98**, 1402-1407 (2001).
40. Olivier, A., Lauret, E., Gonin, P. & Galy, A. The Notch ligand delta-1 is a hematopoietic development cofactor for plasmacytoid dendritic cells. *Blood* **107**, 2694-2701 (2006).
41. Thordardottir, S. *et al.* The aryl hydrocarbon receptor antagonist StemRegenin 1 promotes human plasmacytoid and myeloid dendritic cell development from CD34+ hematopoietic progenitor cells. *Stem cells and development* **23**, 955-967 (2014).
42. Balan, S. *et al.* Human XCR1+ dendritic cells derived in vitro from CD34+ progenitors closely resemble blood dendritic cells, including their adjuvant responsiveness, contrary to monocyte-derived dendritic cells. *Journal of immunology (Baltimore, Md. : 1950)* **193**, 1622-1635 (2014).
43. Balan, S. & Dalod, M. In Vitro Generation of Human XCR1(+) Dendritic Cells from CD34(+) Hematopoietic Progenitors. *Methods in molecular biology (Clifton, N.J.)* **1423**, 19-37 (2016).
44. Gschweng, E.H. *et al.* HSV-sr39TK positron emission tomography and suicide gene elimination of human hematopoietic stem cells and their progeny in humanized mice. *Cancer research* **74**, 5173-5183 (2014).
45. Wölfl, M. & Greenberg, P.D. Antigen-specific activation and cytokine-facilitated expansion of naive, human CD8+ T cells. *Nature Protocols* **9**, 950 (2014).
46. Dobin, A. *et al.* STAR: ultrafast universal RNA-seq aligner. *Bioinformatics (Oxford, England)* **29**, 15-21 (2013).
47. Anders, S. & Huber, W. Differential expression analysis for sequence count data. *Genome biology* **11**, R106 (2010).